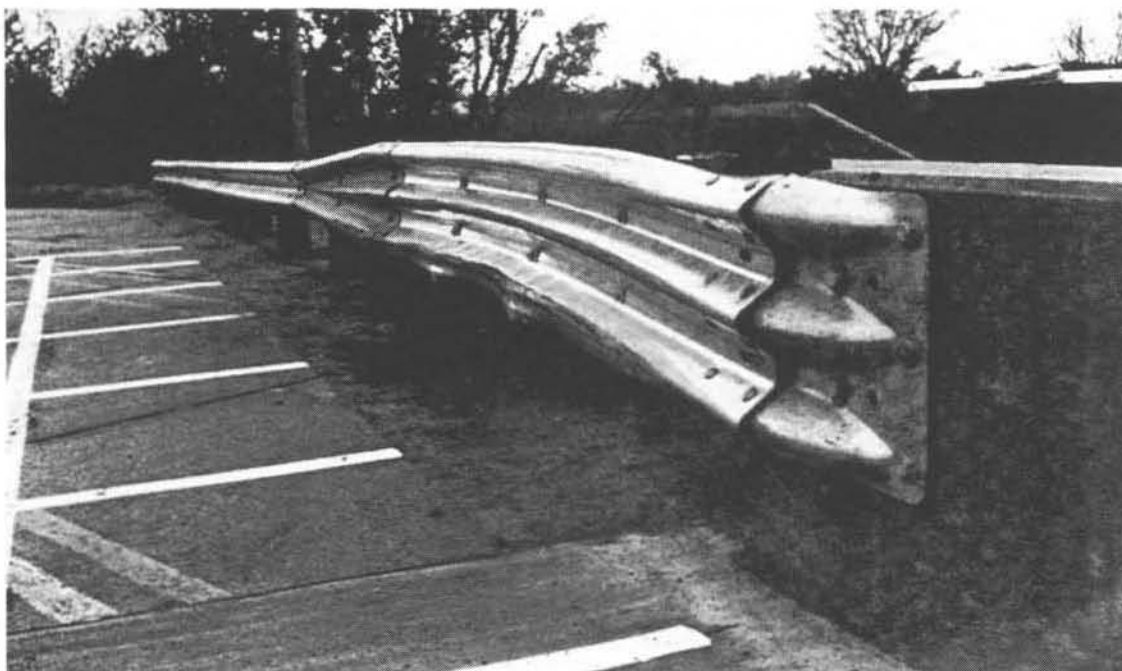


**FULL-SCALE VEHICLE CRASH TESTS**  
**on**  
**GUARDRAIL-BRIDGERAIL TRANSITION DESIGNS**  
**with**  
**SPECIAL POST SPACING**



by  
Dr. Edward R. Post, P.E.  
Professor of Civil Engineering

*Sponsored by*  
Nebraska Department of Roads  
HP&R 86-2

*in cooperation with*  
U.S. Department of Transportation  
Federal Highway Administration

TRANSPORTATION RESEARCH REPORT TRP-03-008-87

Civil Engineering Department  
W348 Nebraska Hall  
University of Nebraska-Lincoln  
Lincoln, Nebraska  
68588-0531

May 1987

1. Report No. NE-DOR-R87-2	2. Government Accession No.	3. Recipient's Catalog No.	
4. Title and Subtitle Full-Scale Vehicle Crash Tests on Guardrail-Bridgerail Transition Design With Special Post Spacing		5. Report Date May 1987	
		6. Performing Organization Code	
7. Author(s) Dr. Edward R. Post, P.E.		8. Performing Organization Report No. TRP-03-008-87	
9. Performing Organization Name and Address Civil Engineering Department W348 Nebraska Hall University of Nebraska-Lincoln Lincoln, NE 68588-0531		10. Work Unit No.	
		11. Contract or Grant No. HPR 86-2	
12. Sponsoring Agency Name and Address Roadway Design Division Nebraska Department of Roads P.O. Box 94759 Lincoln, NE 68509		13. Type of Report and Period Covered Final Report	
		14. Sponsoring Agency Code	
15. Supplementary Notes Prepared in cooperation with U.S. Department of Transportation, Federal Highway Administration			
16. Abstract Full-scale 4,500 lb. vehicle impact tests at 60 mph and 25 deg. were conducted on four new guardrail-bridgerail "transition" designs for use in Nebraska in which the first wood post from the bridge end was left out. The post was left out to represent a common field problem in which a concrete footing prevents the installation of the post. To compensate for the post left out, a stronger beam member and heavier wood posts were used in addition to a 4:1 tapered-end on the end of the concrete bridgerail. The tapered-end was used to (1) reduce the unsupported span length, and (2) provide a smooth guardrail deflection curve during vehicle re-direction. All of the transition designs were identical except for the transition beam member. The designs consisted of 2 heavy 10 in. x 10 in. posts followed by 4 heavy 8 in. x 8 in. posts. The remaining posts were standard 6 in. x 8 in. posts. Over a guardrail length of 18 ft.-9 in., the posts were spaced 3 ft.-1 1/2 in. centers, whereas, over the remaining length, a standard post spacing of 6 ft.-3 in. was used. The posts were installed in a "native" silty-clay (type CL) soil. In terms of the evaluation guidelines in NCHRP 230, the overall performance of the transition designs were:  <ul style="list-style-type: none"> <li>* Single Thrie Beam Transition . . . . . Unsatisfactory</li> <li>* Double Thrie Beam Transition . . . . . Satisfactory</li> <li>* Tubular Thrie Beam Transition . . . . . Satisfactory</li> <li>* Double W-Beam Transition . . . . . Unsatisfactory</li> </ul>			
17. Key Words Guardrail Transitions, Crash Tests, Roadside Safety		18. Distribution Statement	
19. Security Classif. (of this report) Unclassified	20. Security Classif. (of this page) Unclassified	21. No. of Pages 140	22. Price

## TABLE OF CONTENTS

	<u>Page</u>
LIST OF FIGURES . . . . .	iv
LIST OF TABLES . . . . .	vi
NOMENCLATURE . . . . .	vii
ACKNOWLEDGEMENTS . . . . .	viii
I. INTRODUCTION . . . . .	1
A. PROBLEM STATEMENT . . . . .	2
B. OBJECTIVES OF RESEARCH STUDY . . . . .	4
II. TECHNICAL DISCUSSION . . . . .	6
A. TEST CONDITIONS . . . . .	7
A.1. Test Facility . . . . .	7
Location . . . . .	7
Cable Tow System . . . . .	7
Cable Guidance System . . . . .	10
A.2. Design and Construction of Test Article . . . . .	12
Simulated Bridge Deck and Railing . . . . .	12
Approach Guardrail . . . . .	16
Soil . . . . .	19
A.3. Test Vehicles . . . . .	22
A.4. Data Acquisition Systems . . . . .	24
High-Speed Photography System . . . . .	24
Electronic Speed Trap System . . . . .	24
Metraplex Accelerometer System . . . . .	25

# TABLE OF CONTENTS (continued)

	A.5. Test Parameters and Evaluation Criteria . . .	<u>Page</u> 25
B.	TEST RESULTS . . . . .	29
	B.1. TEST NO. 1. TUBULAR THRIE BEAM TRANSITION. .	30
	B.2. TEST NO. 2. SINGLE THRIE BEAM TRANSITION . .	40
	B.3. TEST NO. 3. SINGLE THRIE BEAM TRANSITION . .	48
	B.4. TEST NO. 4. DOUBLE THRIE BEAM TRANSITION . .	57
	B.5. TEST NO. 5. DOUBLE THRIE BEAM TRANSITION . .	65
	B.6. TEST NO. 6. DOUBLE W-BEAM TRANSITION . . . .	74
III.	SUMMARY AND CONCLUSIONS . . . . .	83
IV.	REFERENCES . . . . .	91
	APPENDICIES . . . . .	93
	APPENDIX A - SOIL TESTS . . . . .	94
	APPENDIX B - DESIGN DETAILS OF SIMULATED BRIDGE DECK AND RAILING . . . . .	98
	APPENDIX C - BARRIER VII COMPUTER MODEL SIMULATIONS . . . . .	101
	APPENDIX D - METHOD TO DETERMINE OCCUPANT RISK . .	131
	APPENDIX E - INJURY ACCIDENT PROBABILITY . . . . .	136



## LIST OF FIGURES

	<u>Page</u>
1. AASHTO Approved Guardrail-Bridgerail	
Transition Design . . . . .	3
2. Transition Designs . . . . .	5
3. Photographs of Cable Tow System . . . . .	8
4. Detailed Sketch of Cable Tow System . . . . .	9
5. Photographs of Cable Guidance System . . . . .	11
6. Design Details of Simulated Bridge	
Deck and Railing . . . . .	13
7. Photographs of Bridge Deck and	
Railing Construction . . . . .	14
8. Design Details of Approach Guardrail . . . . .	17
9. Photographs of Approach Guardrail Installation . . . . .	18
10. Photographs of Wood Post Installation . . . . .	21
11. Photographs of Dummy and Electronic Equipment . . . . .	26
12. Electronic Data Acquisiton System . . . . .	27
13. Sequential Photographs of Test No. 1 . . . . .	33
14. Photographs of Test No. 1 Guardrail Damage . . . . .	34
15. Test No. 1...Guardrail Permanent Set . . . . .	35
16. Photographs of Test Vehicle Before and	
After Test No. 1 . . . . .	37
17. Sequential photographs of Test No. 2 . . . . .	43
18. Photographs of Test No. 2 Guardrail Damage . . . . .	44
19. Test No. 2...Guardrail Permanent Set . . . . .	45

# LIST OF FIGURES (continued)

	<u>Page</u>
20. Photographs of Test Vehicle Before and After Test No. 2 . . . . .	46
21. Sequential Photographs of Test No. 3 . . . . .	51
22. Photographs of Test No. 3 Guardrail Damage . . . . .	52
23. Test No. 3...Guardrail Permanent Set . . . . .	54
24. Photographs of Test Vehicle Before and After Test No. 3 . . . . .	56
25. Sequential Photographs of Test No. 4 . . . . .	60
26. Photographs of Test No. 4 Guardrail Damage . . . . .	61
27. Test No. 4...Guardrail Permanent Set . . . . .	62
28. Photographs of Test Vehicle Before and After Impact Test No. 4 . . . . .	64
29. Sequential Photographs of Test No. 5 . . . . .	68
30. Photographs of Test No. 5 Guardrail Damage . . . . .	69
31. Test No. 5...Guardrail Permanent Set . . . . .	71
32. Photographs of Test Vehicle Before and After Impact Test No. 5 . . . . .	73
33. Sequential Photographs of Test No. 6 . . . . .	77
34. Photographs of Test No. 6 Guardrail Damage . . . . .	78
35. Test No. 6...Guardrail Permanent Set . . . . .	80
36. Photographs of Test Vehicle Before and After Test No. 6 . . . . .	82
37. Relationship Between Occupant Impact Velocity and Injury Accident Probability . . . . .	89

## LIST OF TABLES

	<u>Page</u>
1. Concrete Compressive Strength . . . . .	16
2. Native Soil Properties . . . . .	20
3. Test Vehicle Weights . . . . .	23
4. Summary of Crash Test No. 1 . . . . .	31
5. Description of Test No. 1 Sequential Events . . . . .	32
6. Equivalent Test No. 1 Impact Conditions . . . . .	38
7. Summary of Crash Test No. 2 . . . . .	41
8. Description of Test No. 2 Sequential Events . . . . .	42
9. Summary of Crash Test No. 3 . . . . .	49
10. Description of Test No. 3 Sequential Events . . . . .	50
11. Summary of Crash Test No. 4 . . . . .	58
12. Description of Test No. 4 Sequential Events . . . . .	59
13. Summary of Crash Test No. 5 . . . . .	66
14. Description of Test No. 5 Sequential Events . . . . .	67
15. Summary of Crash Test No. 6 . . . . .	75
16. Description of Test No. 6 Sequential Events . . . . .	76
17. Comparative Summary of Crash Test Results . . . . .	85
18. NCHRP 230 Safety Evaluation Guidelines . . . . .	86

## NOMENCLATURE

AASHTO ... American Association of State Highway and Transportation  
Officials

NCHRP ..... National Cooperative Highway Research Program

NDR ..... Nebraska Department of Roads

NSC ..... National Safety Council

## ACKNOWLEDGEMENTS

As the principal investigator, I would like to acknowledge and thank the following people who made a contribution to the successful outcome of this research project.

### Nebraska Department of Roads

Mark Borgmann (Bridge Design Division)  
Kenneth Cheney (Materials and Test Division)  
Leona Kolbet (Materials and Test Division  
and Research Coordinator)  
Robert Miller (Manager of Purchasing and Supply)  
Ron Morton (Materials and Tests Division)  
Dalyce Ronnau (Materials and Test Division  
and Research Engineer)  
Richard Ruby (Roadway Design Division and Project  
Manager)  
Dan Sharp (Bridge Design Division)  
Walter Witt (Roadway Design Division)  
George Woolstrum (Materials and Tests Division)

### Federal Highway Administration

Milo Cress (Lincoln Division Office)  
Charles McDevitt (Wash. D.C. Office of Research)  
William Wendling (Kansas City Regional Office)

### University of Nebraska

Mike Cacak (Manager-Automobile Support Services)  
Jerry Delhay (Manager-Maintenance)  
Jim Dunlap (Manager-Photographic Productions)  
Gerald Fritz (E.E. Technician)  
Tom Grady (E.E. Technician)  
William Kelly (Professor and C.E. Chairman)  
Steve King (C.E. Student)  
Eugene Matson (C.E. Technician)  
Mary Lou Tomka (C.E. Administrative Assistant)  
Vince Ullman (Photographic Technician)  
Bruce Wacker (C.E. Student)  
Mary Lou Wegener (C.E. Secretary)

The New York Public Library, Astor Lenox and Tilden Foundations, is a non-profit corporation organized under the laws of the State of New York. It is a public institution, and its funds are derived from the sale of books, gifts, and bequests. The Library is open to all, and its collections are available to the public. It is a place of learning and research, and it is a source of information and knowledge. The Library is a part of the cultural heritage of the City of New York, and it is a source of pride and honor for the people of the City.

I.

INTRODUCTION

The New York Public Library, Astor Lenox and Tilden Foundations, is a non-profit corporation organized under the laws of the State of New York. It is a public institution, and its funds are derived from the sale of books, gifts, and bequests. The Library is open to all, and its collections are available to the public. It is a place of learning and research, and it is a source of information and knowledge. The Library is a part of the cultural heritage of the City of New York, and it is a source of pride and honor for the people of the City.

## A. PROBLEM STATEMENT

The majority of the bridgerail designs in current use are rigid traffic barriers, whereas, the guardrail designs on the approaches to the bridge structure are semi-rigid traffic barriers. In restraining and redirecting a large size 4,500 lb. automobile at 60 mph and 25 deg., a rigid and semi-rigid traffic barrier will typically undergo deflections of 0 to 6 in. and 30 in., respectively. To provide structural stiffness compatibility between the semi-rigid guardrail and the rigid bridgerail, a guardrail transition section consisting of reduced post spacings and larger size posts is used adjacent to the bridgerail end. A current AASHTO (1)<sup>a</sup> transition section is shown in Figure 1. Referring to Figure 1, it is to be noted that the first 6 wood posts back from the bridgerail end are installed on a reduced spacing of 3 ft-1 1/2 in., and the first 3 wood posts are larger size 10 in. x 10 in. posts.

Many of the bridge structures in the State of Nebraska were constructed with concrete footings that extend back from the end of the bridgerail. The footing has created a field problem in that the first required 10 in. x 10 in. wood post located 3 ft.-1 1/2 in. from the bridgerail end connection as shown in Figure 1 cannot be installed in the ground. In order to compensate for the first post left out or installed further back, the Nebraska Department of Roads

---

<sup>a</sup>

Underlined number is a reference source

Table III-B-3. Operational Roadside Barrier Transition Sections

<div>Metric Conversions</div> <div>1 ft. = 0.305 m</div> <div>1 in. = 25.4 mm</div> <div>1 mph = 1.61 km/hr</div> <div>1 lb. = 0.454 kg</div>		
SYSTEM	T1 G4(1W) Approach Rail to Concrete Parapet	
BARRIER DESCRIPTION	POST SPACING - as shown on sketch; POST TYPE - 8"x8" and 10"x10" Douglas Fir; BEAM TYPE - steel "W" section, 12 GA.; OFFSET BRACKETS - 8"x8" Douglas Fir block; MOUNTINGS - 1" diameter steel bolt; FOOTINGS - none.	
IMPACT PERFORMANCE	IMPACT ANGLE = 15°	IMPACT ANGLE = 25°
<div>IMPACT CONDITIONS</div> <div>Speed (mph)</div> <div>Vehicle Weight (lb.)</div> <div>BARRIER</div> <div>Dynamic Deflection (ft.)</div> <div>VEHICLE ACCELERATIONS (G's)<sup>1</sup></div> <div>Lateral</div> <div>Longitudinal</div> <div>Total</div> <div>VEHICLE TRAJECTORY</div> <div>Exit Angle (deg.)</div> <div>Roll Angle (deg.)</div> <div>Pitch Angle (deg.)</div>	NO TEST	58.8 4297  UNAV  19.0 8.8 UNAV  UNAV UNAV UNAV
BARRIER DAMAGE		UNAV
REFERENCES		18
FIELD PERFORMANCE DATA <sup>2</sup>	NO	
REMARKS	Severe vehicle damage. System that was tested had no flare.	
<div>UNAV - unavailable</div> <div><sup>1</sup>50 millisecond average unless otherwise noted</div> <div><sup>2</sup>If available, see summary in Appendix A</div>		

Figure 1  
AASHTO APPROVED GUARDRAIL-BRIDGERAIL TRANSITION DESIGN



(NDR) has designed four new transition sections consisting of longer 6 ft. posts and stronger guardrail beam members. Because the structural strength performance characteristics of the new transition designs have not been evaluated under full-scale vehicle crash test conditions, the FHWA is concerned that an out-of-control vehicle could possibly (1) penetrate, (2) vault, or (3) pocket and snag on the wood posts or end of the bridgerail.

#### B. OBJECTIVES OF RESEARCH STUDY

The primary objective of this study was to select the most cost-effective of four new guardrail-bridgerail transition designs based on the findings obtained from conducting full-scale vehicle crash tests. In all tests, the first 10 in. x 10 in. wood post located 3 ft.-1 1/2 in. back from the bridgerail end connection was left out. The four new transition designs under consideration were:

1. Single Thrie Beam (Figure 2a)
2. Double Thrie Beam (Figure 2b)
3. Tubular Thrie Beam (Figure 2c)
4. Double W-Beam (Figure 2d)

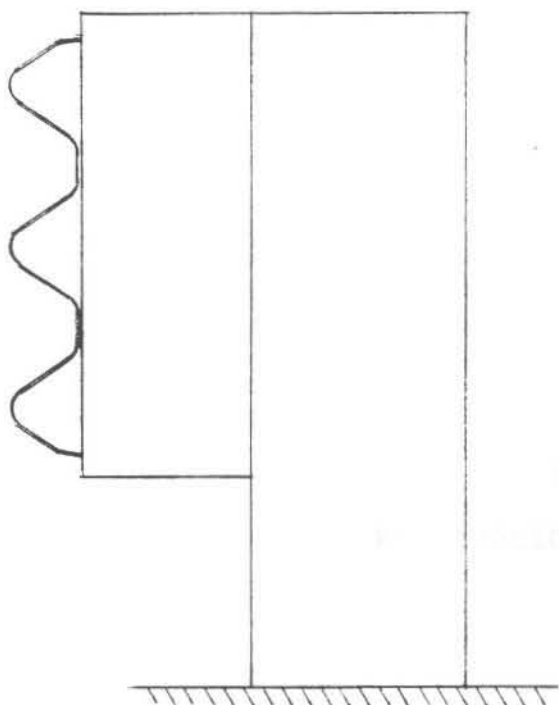


Figure 2a  
SINGLE THRIE BEAM

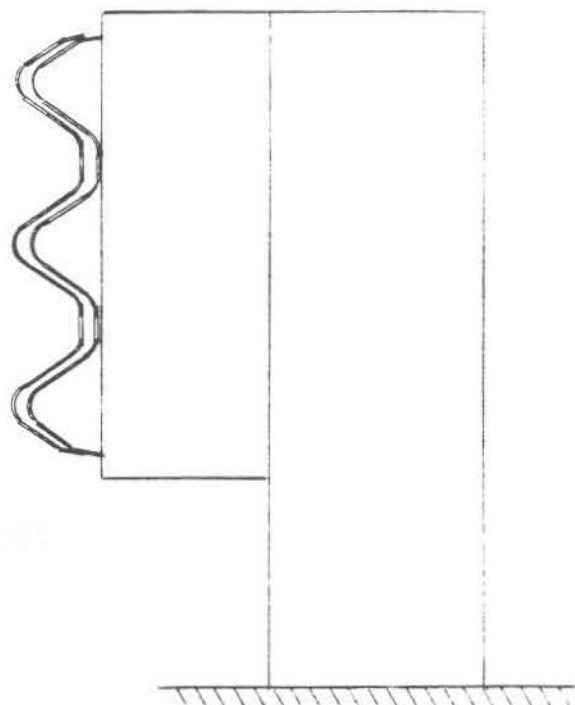


Figure 2b  
DOUBLE THRIE BEAM

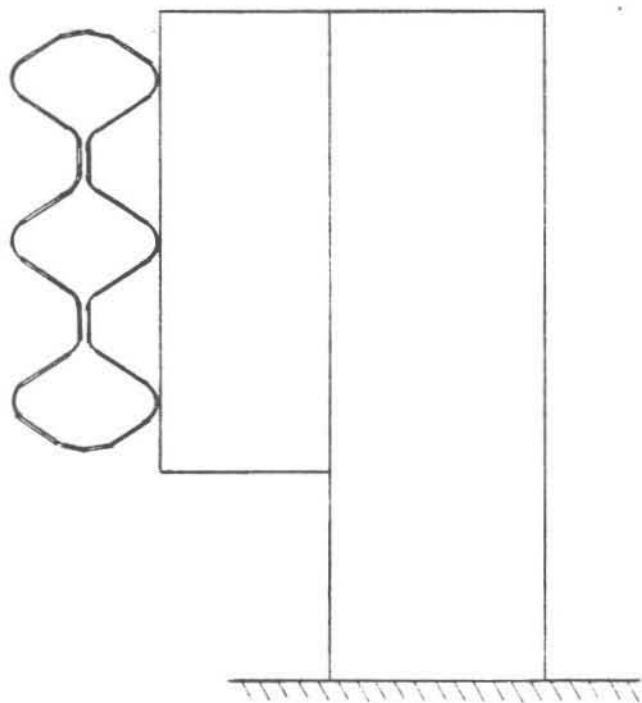


Figure 2c  
TUBULAR THRIE BEAM

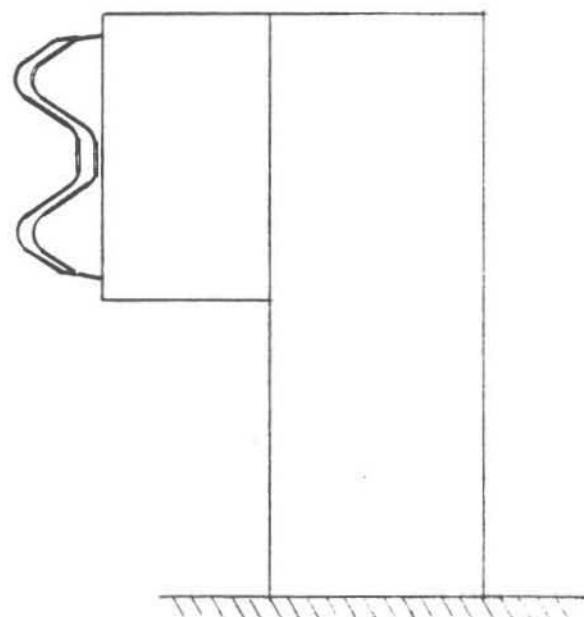


Figure 2d  
DOUBLE W-BEAM

FIGURE 2  
TRANSITION DESIGNS

## II

### TECHNICAL DISCUSSION

## A. TEST CONDITIONS

### A.1. TEST FACILITY

#### Location

The full-scale vehicle crash test site was located at the Lincoln Municipal Airport near Rwy 14. The airport is approximately 7 mi. NW from the University. The test site consisted of a smooth level 30 ft. wide section of an abandoned concrete roadway.

#### Cable Tow System

A cable tow system having a 2:1 mechanical advantage was used to tow the crash test vehicle. Photographs of the system are shown in Figure 3, and a detailed sketch of the system is shown in Figure 4. In this type of system, the test vehicle is travelling at a speed and distance that are exactly two times that of the tow vehicle.

One end of the tow cable was attached to a smooth vertical rod bolted to the front cross-frame member under the engine of the test vehicle, whereas, the other end was clamped to a dead-end anchor. The cable loop attached to the rod on the test vehicle was held-up in place with a piece of soft 18 Ga. wire. The tow cable was pulled down off the rod as the test vehicle passed over the pulley with a chute which was located about 25 ft. in advance of the barrier.

The towing vehicle was a 1981 Chevrolet Pickup truck with a large "454 cubic-inch" engine and a no-spin differential rear-end.



Figure 3  
PHOTOGRAPHS OF CABLE TOW SYSTEM

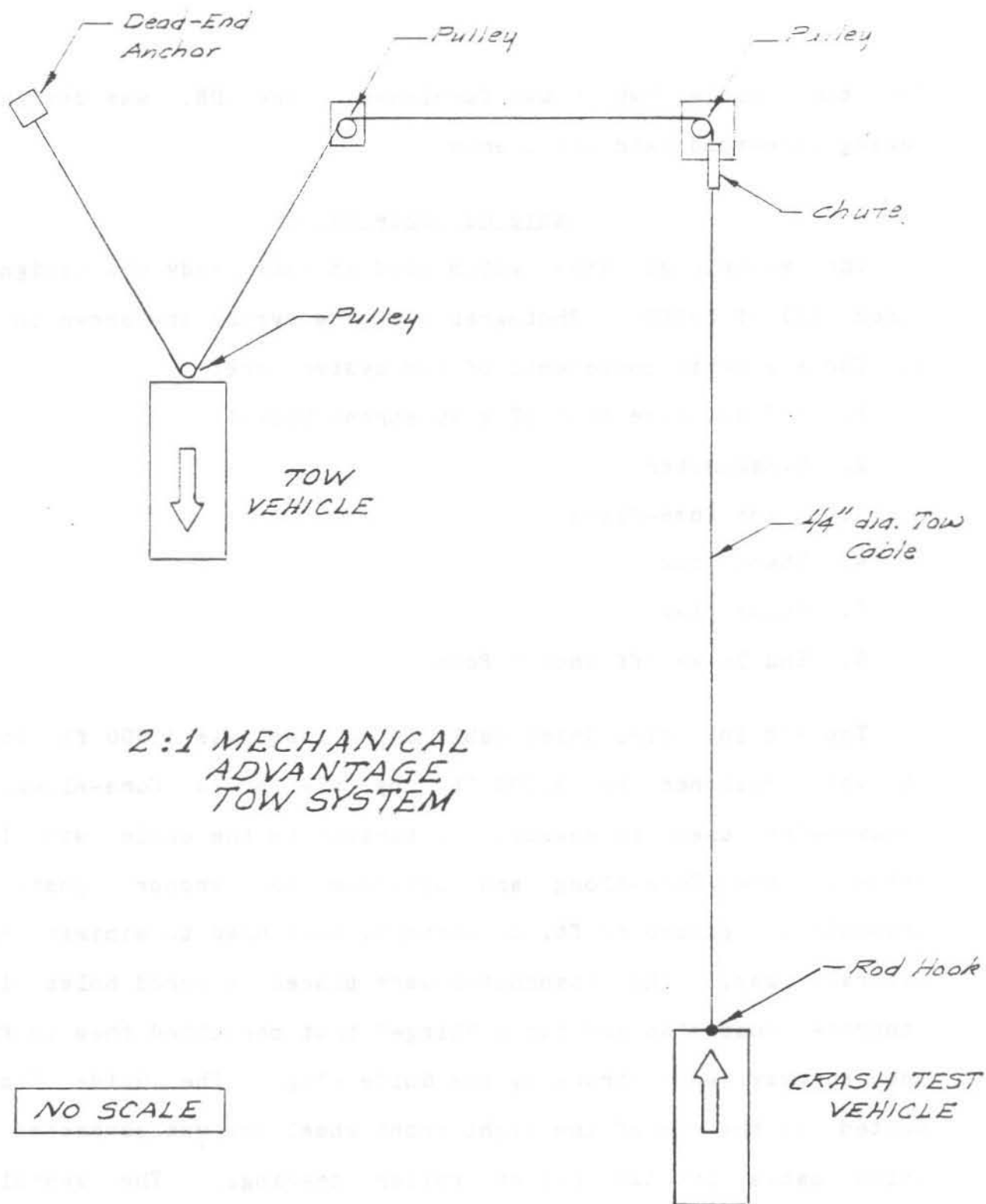


Figure 4  
DETAILED SKETCH OF CABLE TOW SYSTEM

The tow vehicle, which was furnished by the NDR, was designed for making tire-road skid measurements.

#### Cable Guidance System

The vehicle guidance system used in this study was designed by Hinch (2) of ENSCO. Photographs of the system are shown in Figure

5. The six basic components of the system were:

1. 3/8 in. Wire Rope (7 x 19 strand Galv.)
2. Dynamometer
3. 3-Ton Come-Along
4. Stanchions
5. Guide Flag
6. End Break-off Anchor Post

The 3/8 in. dia. Guide Cable (wire rope) was 1,000 ft. long and it was tensioned to 3,000 lb. by use of a Come-Along. The Dynamometer used to measure the tension in the cable was located between the Come-Along and upstream end anchor post. The stanchions, placed 50 ft. on centers, were used to minimize sag and lateral sway. The Stanchions were placed in cored holes in the concrete road slab and had a "hinge" that permitted them to fall to the roadway when struck by the Guide Flag. The Guide Flag was bolted to the rim of the right front wheel and was connected to the guide cable by two sets of roller bearings. The vehicle was released from the guide cable when two small 1/8 in. machine screws were sheared-off as the guide flag impacted the downstream end anchor post. The end anchor post was located so that the vehicle was

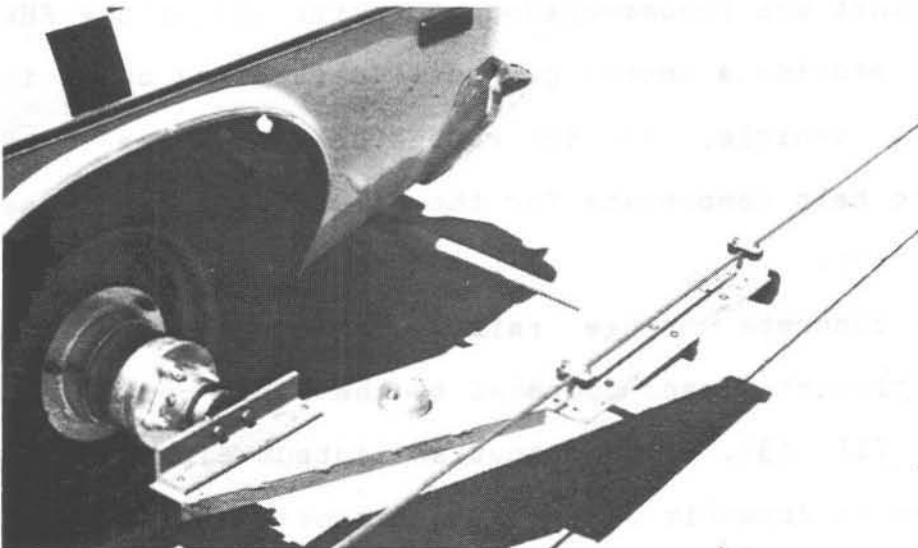


Figure 5  
PHOTOGRAPHS OF CABLE GUIDANCE SYSTEM



"free-wheeling" for a distance of about 25 ft. before impacting the barrier.

## A.2. DESIGN AND CONSTRUCTION OF TEST ARTICLE

### Simulated Bridge Deck and Railing

The simulated concrete bridge railing and deck were designed by the NDR Bridge Division. Design details of the bridge railing and deck are shown in Figure 6 and Appendix B, whereas, photographs of the construction are shown in Figure 7. The railing and deck were constructed by a private contractor who was qualified to bid on NDR bridge contracts. The name of the contractor was M.E. Collins Construction Co. of Wahoo, Nebraska.

The open bridge railing design is a recent design currently in use in Nebraska to help keep the roadway clear of blowing and drifting snow and to facilitate snow removal operations. The cantilevered 4:1 tapered end section was a totally new design feature that was recommended by McDevitt (4) of the FHWA as a method to (1) provide a smooth guardrail deflection curve in redirecting the test vehicle, and (2) reduce the effective unsupported span length to help compensate for the first wood post (Post No. 1) that was left out.

The concrete bridge railing and deck were designed to carry dynamic impact loads computed by the FHWA computer model, named BARRIER VII (5). The input and output data of the model are presented in Appendix C. The simultaneous peak impact loads were 120 kips perpendicular to the barrier and 50 kips parallel to the

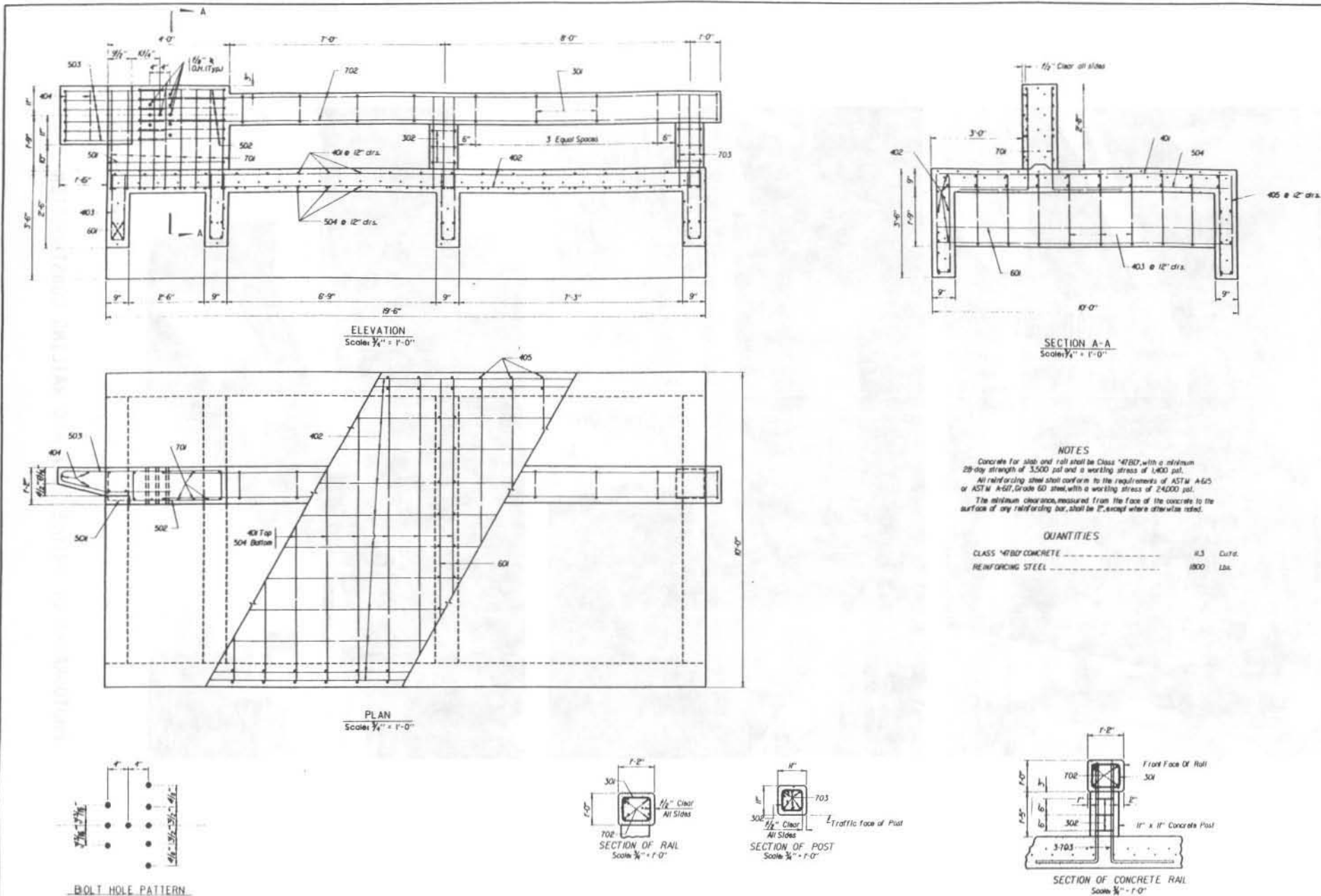


Figure 6  
DESIGN DETAILS OF SIMULATED

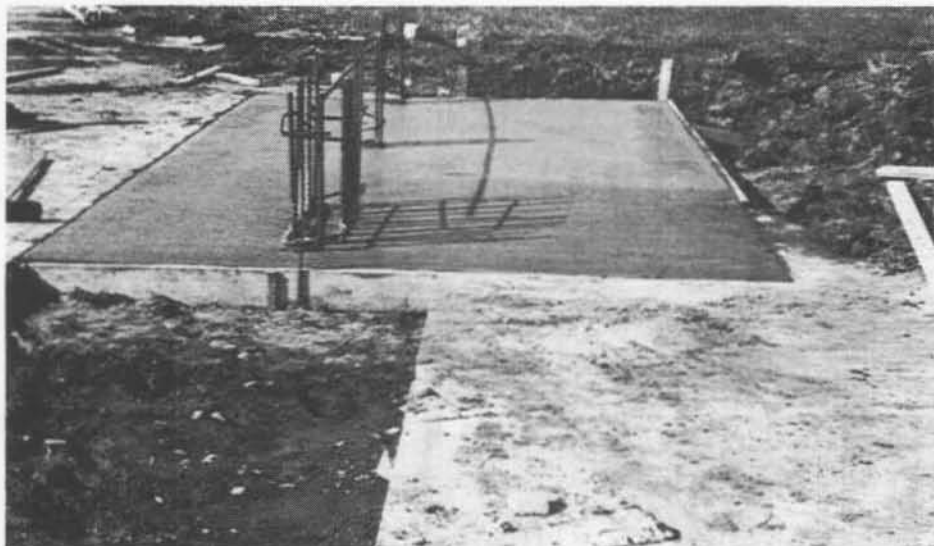
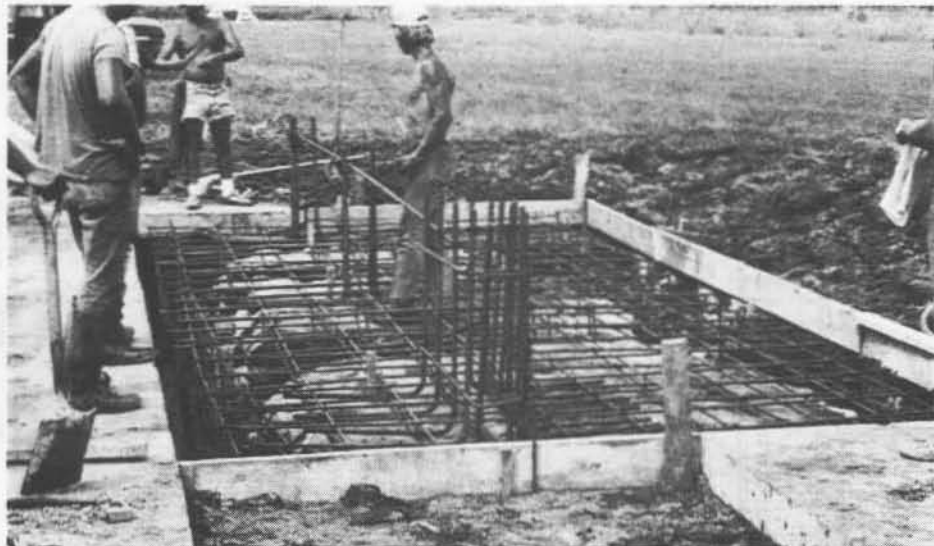


Figure 7  
PHOTOGRAPHS OF BRIDGE DECK AND RAILING CONSTRUCTION

barrier. It is to be noted that the perpendicular impact load is on the order of 12 times higher than the design load of 10 kips specified in the AASHTO Standard Specifications for Highway Bridges (6).

The concrete bridge deck slab was 9-in. deep, 10.0 ft. wide, and 19.5 ft. long. The two longitudinal floor beams were 42 in. deep, whereas, the four transverse floor beams were 21 in. deep. The deck slab and floor beams were reinforced with No. 6 and smaller size rebar (Grade 60) to carry the vehicle impact loads. The deck was constructed in a portion of an area where the concrete roadway slab had been sawcut and removed.

The concrete bridge railing, including the cantilevered 4:1 tapered end section, was 21.5 ft. long. The solid wall portion of the railing was 32 in. high, whereas, the beam portion was 29 in. high. The opening between the deck and railing was 17 in. in the vertical dimension. The two concrete posts, located 7 and 15 ft. from the solid wall portion, were setback 2 in. from the traffic face of the railing to minimize vehicle snagging. The 1 1/8 in. dia. bolt hole pattern in the railing wall was designed to accomodate the end shoes of both the Thrie Beam and the standard W-Beam guardrail sections. The 3 1/4 in. recessed area adjacent to the 4:1 tapered end section was designed to accomodate the added width of the tubular thrie beam guardrail. On the other hand, a 3 1/4 in. wide wood filler block was cut to fill the recessed area and to extend along the length of the tapered end section to accomodate the other non-tubular guardrail designs. The railing was reinforced

with No. 7 and smaller size rebar (Grade 60) to carry the vehicle impact loads.

The compressive strength of concrete bridge deck at 14 days and the railing at 21 days exceeded the NDR specified minimum 28 day strength of 3,500 psi. The concrete cylinder strengths are presented in Table 1.

TABLE 1  
CONCRETE COMPRESSIVE STRENGTH

DAY	S T R E N G T H (psi)	
	Deck	Railing
14	4,952	3,067
	5,164	
21		4,174
		4,025
25	5,801	
	5,518	

#### Approach Guardrail

Design details of the combination W-Beam and Thrie Beam approach guardrail system are shown in Figure 8, and photographs of the installation are shown in Figure 9. The overall length of the guardrail installation was 56 ft.-3 in. A 6 ft. wide strip of the concrete roadway slab was sawcut and removed for the installation of





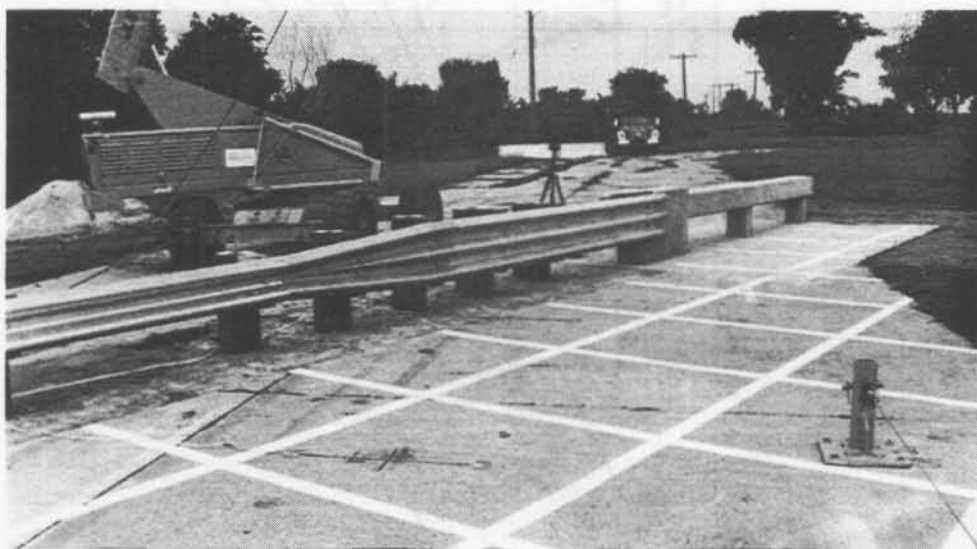
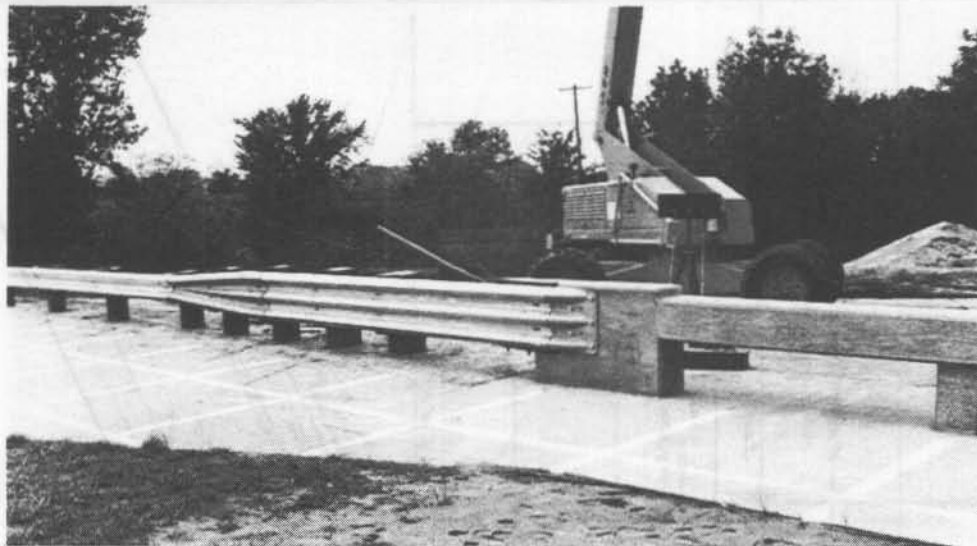


Figure 9  
PHOTOGRAPHS OF APPROACH GUARDRAIL INSTALLATION

the guardrail in native soil. The guardrail was installed at an angle of 25 deg. relative to the centerline of the roadway.

The 12 Ga. Thrie Beam guardrail transition section adjacent to the end of the concrete bridge railing was 12 ft.-6 in. in length. A 12 Ga. 6 ft.-3 in. Adapter section was used to transition from the Thrie Beam section to the upstream standard 12 Ga. W-Beam section. The Thrie Beam was mounted at a height of 31 in., whereas, the standard W-Beam was mounted at a height of 27 in. The upstream end of the W-Beam guardrail was anchored into an 18 in. dia. by 6 ft. deep reinforced concrete shaft.

The first wood guardrail post (Post #2) was installed 7 ft.-7 1/2 in. from the centerline of the bolt hole pattern in the concrete bridge end. The unsupported span length from the 4:1 tapered concrete bridge end to the center of Post No. 2 was 4 ft.-7 in. The post spacings between Post No. 2 and Post No. 6 were 3 ft.-1 1/2 in. on centers, whereas, the post spacings of the remaining posts were 6 ft.-3 in. on centers. The posts were all 6 ft. in length. The size of the first 2 posts were 10 in. x 10 in.; the size of the next 4 posts were 8 in. x 8 in., and the size of the remaining posts were 6 in. x 8 in. The rail blockouts were all 6 in. x 8 in. in size.

#### Soil

The soil, in which the guardrail wood posts were installed, was a "native" silty-clay topsoil. The soil was not in conformance with either the strong soil (S-1) or the weak soil (S-2) defined in NCHRP 230 (3). The decision to deviate from the recommended testing



procedures in NCHRP 230 was made by engineers of the NDR because of the desire to evaluate the guardrail-bridgerail transition designs under typical soil conditions encountered in most of Nebraska. The properties of the soil are shown in Table 2.

TABLE 2  
NATIVE SOIL PROPERTIES

---

Unified Classification (ASTM D-2487)	CL
Liquid Limit (LL)	31
Plastic Limit (PL)	20
Plasticity Index (LL-PL)	11
Optimum Moisture Content	17.6%
Unconfined Shear Strength	1,900 psf

---

The wood posts were placed in 18 to 20 in. dia. holes. The backfill soil around the posts was compacted by hand (as shown in Figure 10) in 6-in. layers to a density of approximately 92%. The soil tests conducted by the NDR and a private soil testing agency (Geotechnical Services, Inc.) are presented in Appendix A. The field density of the soil was measured by a Troxler Nuclear Density Meter.



Figure 10  
PHOTOGRAPHS OF WOOD POST INSTALLATION

### A.3. TEST VEHICLES

The six test vehicles used in the full-scale crash tests were 1977 Plymouth Fury 4-door sedans. Ballast was added to bring the weight of the vehicles in conformance with the  $4,500 \pm 200$  lb. requirement in NCHRP 230 (3). The ballast was equally distributed fore and aft of the vehicle center-of-gravity. The ballasted weights of the vehicles are presented in Table 3.

Referring to Figure 5 (p11), the two reference targets used in the analysis of the high-speed film and mounted on the centerline of the roof of the vehicle were spaced 5 ft. on centers. The forward target was mounted directly above the center-of-gravity of the vehicle.

The braking system installed in the test vehicle was bolted to the floor of the rear compartment area. The system consisted of a ram that was operated by high-pressure bottled nitrogen gas. A 1/8 in. dia. cable was attached to the ram and the vehicle brake pedal. In turn, the cable ran under the front seat and around a pulley that was bolted to the floor directly under the brake pedal. The cable pulled the brake pedal downward in the same manner that a driver would apply the brakes. The brakes were applied when the test vehicle was about 50 ft. clear of the test barrier.

TABLE 3  
TEST VEHICLE WEIGHTS

Test No.	Curb Weight <sup>(1)</sup> (lb)	Equipment <sup>(2)</sup> Weight (lb)	Ballast Weight (lb)	Test <sup>(3)</sup> Weight (lb)
1	4,060	64	260	4,384
2	3,940	64	336	4,340
3	4,000	64	336	4,400
4	3,960	64	336	4,360
5	3,920	64	336	4,320
6	4,160	64	336	4,560

Notes:

- (1) Rear seat removed
- (2) Weight includes brake system, roof reference targets, and accelerometer hardware.
- (3) Weight of 160 lb. Anthropometric Dummy not included.

#### A.4. DATA ACQUISITION SYSTEMS

##### High-Speed Photography System

Four high-speed cameras were used to film the crash tests at a film rate of approximately 500 frames/sec. One camera (Photex IV) was located at a distance of 300 ft. perpendicular to the barrier. A second camera (Photex IV) was located 200 ft. downstream and offset 6 ft. from an extended centerline of the traffic barrier. The downstream camera (see Figure 32) was protected by a row of Concrete Median Barriers to prevent the test vehicle from hitting the camera. In the first three crash tests, a third camera (Redlake Lo-Cam) was located at a distance of 50 ft. perpendicular to the barrier, and a fourth camera (Photex IV) was located 50 ft. overhead in the basket of the Cherry-Picker, whereas, in the remaining three crash tests, both of these cameras were located overhead.

Each camera was equipped with an electronic internal timing device for determining the exact operating speed of the camera. The timing device placed a red mark on the edge of the film every 10 msec.

A Vanguard Motion Analyzer was used to analyze the high-speed film frame by frame.

##### Electronic Speed Trap System

Three electronic pressure tape switches were used to determine the impact speed of the vehicle. The tape switches were mounted exactly 3.00, 15.00, and 30.00 ft. from the point of barrier impact. As the left front tire of the vehicle rode over the pressure switch,

the switch would close the circuit and a 6-volt battery would fire a blue 5-B flashbulb which was mounted in the field of view of all four high-speed cameras. The vehicle speed between two switches was determined by the following equation:

$$\text{Veh. Speed (fps)} = \frac{\text{Distance Between Switches (ft)} \times \text{Calibrated Camera Speed (fr/sec)}}{\text{Number of Film Frames Between Flashes (fr.)}}$$

#### Metraplex Accelerometer System

Photographs of the 160 lb. Anthropometric Dummy in the test vehicle, the tri-axial accelerometer unit on the C.G. of the test vehicle, and the data acquisition system placed in a van vehicle are shown in Figure 11. A schematic diagram of the electronic data acquisition system is presented in Figure 12. In addition to the accelerometers on the vehicle, a tri-axial accelerometer unit was placed inside the head of the dummy. The data from the six accelerometers on-board the test vehicle was transmitted to the Metraplex System and Honeywell Magnetic Recorder through a 1,200 ft. length of a an 18 pair, 36 conductor cable.

The analytical method described in NCHRP 230 for analyzing the accelerometer data was used in this study to determine the occupant risk factors of impact velocity and ridedown accelerations.



Figure 11  
PHOTOGRAPHS OF DUMMY AND ELECTRONIC EQUIPMENT

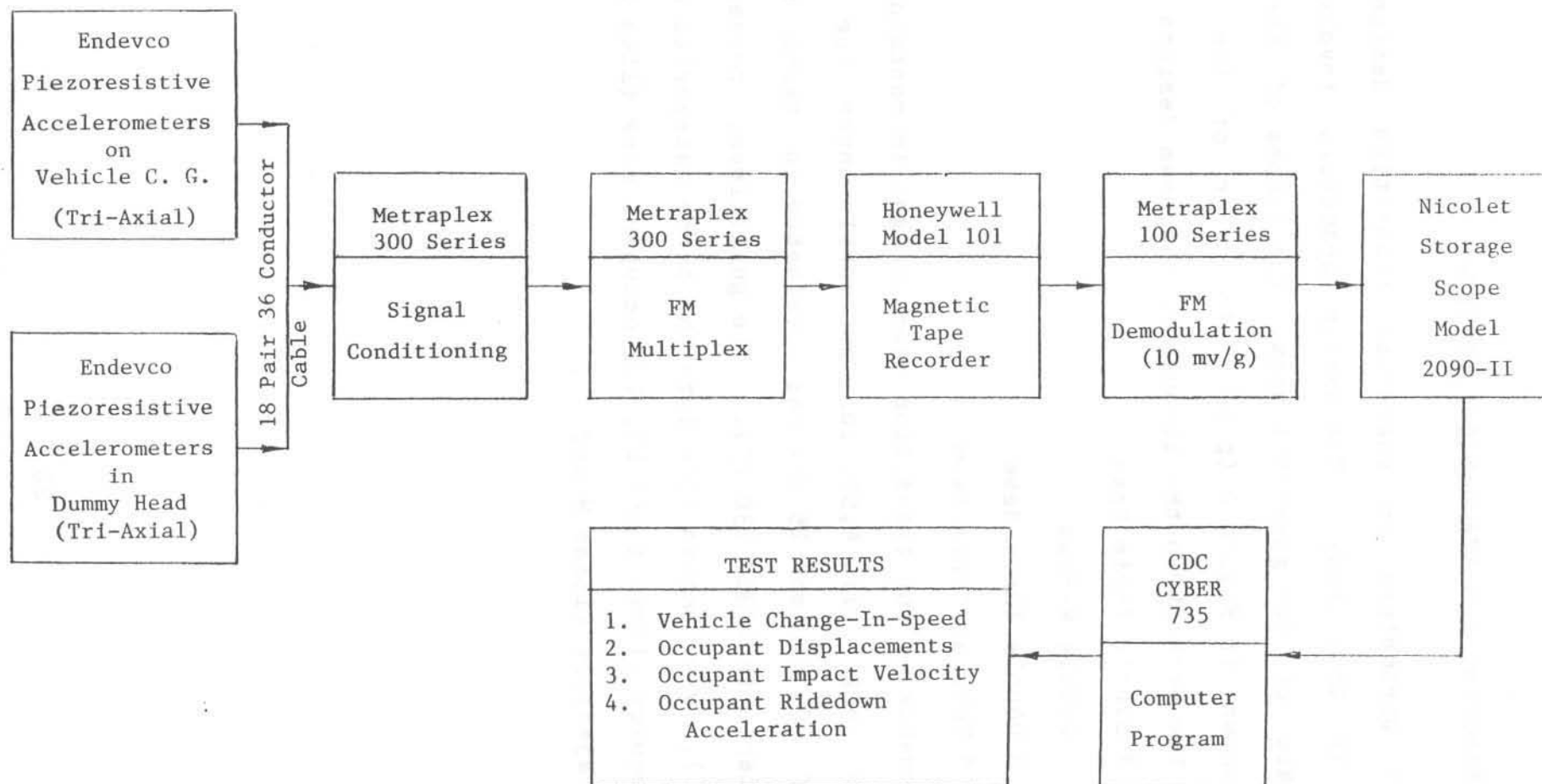


Figure 12 ELECTRONIC DATA ACQUISITION SYSTEM



#### A.5. TEST PARAMETERS AND EVALUATION CRITERIA

Four test parameters on guardrail transition designs were investigated in this study. The design parameters involved the geometric shape of the guardrail beam. The shapes of the beams tested are shown in Figure 2 (p 5). In order of the bending strength from the weakest to the strongest, the beam designs were:

- \* Single Thrie Beam
- \* Double W-Beam
- \* Double Thrie Beam
- \* Tubular Thrie Beam

The performance of the transition beam designs in containing and redirecting a large size 4,500 lb. automobile under the impact conditions of 60 mph and 25 deg was evaluated in terms of the guideline criteria in NCHRP 230 (3). The guidelines, presented in Table 18 (p 86), were broken down into the three categories of: (1) structural adequacy (Items A and D), (2) occupant risk (Item E), and (3) vehicle trajectory (Items H and I).

## B. TEST RESULTS

### \*\*\* Special Note \*\*\*

Due to electronic technical problems, no valid accelerometer data was obtained to evaluate the occupant risk factors in NCHRP 230 (Item F). However, the occupant risk factors of impact velocity and ridedown accelerations were obtained from the backup high-speed film analysis data acquisition system in conjunction with an analytical method in NCHRP 86 (see Appendix D). It is to be noted that the occupant risk factor in NCHRP 230 is not a required item for testing a guardrail transition.

#### B.1. TEST NO. 1: TUBULAR THRIE BEAM TRANSITION

A summary of the full-scale vehicle crash test on the Tubular Thrie Beam Transition is presented in Table 4. Due to technical problems with the tow vehicle, the impact speed was 13 mph below the recommended target speed of 60 mph in NCHRP 230. The point of impact was between Post Nos. 2 and 3.

Sequential photographs of Test No. 1 are shown in Figure 13, and a description of the sequential events is presented in Table 5. At a time of 76 msec after impact, the vehicle reached its greatest depth of crushing into the guardrail. At a time of 194 msec, the "lateral" velocity component of the vehicle was zero as the vehicle became parallel to an extended centerline of the traffic barrier. Somewhere in between 76 and 194 msec, an occupant would have moved laterally 12 in. and struck the side of the vehicle.

Photographs of the guardrail damage are shown in Figure 14, and measurements of the guardrail permanent set deflections are shown in Figure 15. The tubular thrie beam was fabricated by a local steel manufacturer by shop welding two thrie beams back-to-back (see Figure 2c). The end shoe was welded on the outside of the tubular thrie beam. As evident, the damage to the guardrail was very minor with a maximum guardrail permanent set of only 2 1/2 in. Due to a technical problem with the overhead camera, no measurement was made of the maximum guardrail dynamic deflection. Assuming a typical impact factor of 1.5, an estimate of the maximum dynamic deflection would be 4 in.

TABLE 4  
SUMMARY OF CRASH TEST NO. 1

TEST VEHICLE

Make . . . . . 1977 Plymouth Fury  
Weight (excluding dummy) . . . . . 4,384 lb.

TRAFFIC BARRIER INSTALLATION

Concrete Bridgerail  
Type . . . . . Open Rail/Post; Tapered End  
Length . . . . . 21 ft.-6 in.  
Guardrail Beam Members (12 Ga)  
Transition  
Type . . . . . Tubular Thrie Beam  
Length . . . . . 12 ft.-6 in.  
Adapter  
Length . . . . . 6 ft.-3 in.  
Approach  
Type . . . . . Standard W-Beam  
Length . . . . . 37 ft.-6 in.  
Guardrail Wood Posts  
Post No. 1 . . . . . Left Out  
Post Nos. 2 and 3 . . . . . 10 x 10 x 72 in.  
Post Nos. 4 thru 7 . . . . . 8 x 8 x 72 in.  
Post Nos. 8 thru 12 . . . . . 6 x 8 x 72 in.  
Native Soil  
Type . . . . . Silty-Clay (CL)  
Optimum Moisture . . . . . 18%  
Relative Compaction . . . . . 92%  
Test Conditions . . . . . Dry

TEST RESULTS

Vehicle Speed  
Impact . . . . . 47 mph  
Exit . . . . . 38 mph  
Vehicle Angle  
Impact . . . . . 25 deg.  
Exit . . . . . 15 deg.  
Vehicle Rebound Distance . . . . . 72 ft.  
Vehicle Damage . . . . . TAD LFQ-3  
Traffic Barrier  
Impact Location . . . . . Between Post Nos. 2 and 3  
Max. Dynamic Deflection . . . . . 4 in. (est.)  
Max. Permanent Set . . . . . 2 1/2 in.  
Snagging . . . . . None  
Occupant Risk (NCHRP 230)  
Lateral Impact Velocity . . . . . Not Measured  
Ridedown Accelerations . . . . . Not Measured  
Occupant Risk (NCHRP 86)  
Injury Accident Probability . . . . . 18%

TABLE 5

## DESCRIPTION OF TEST NO. 1 SEQUENTIAL EVENTS

Time (msec)	E V E N T
0	Vehicle Impact
76	Max. Vehicle Crushing of 22 in.
194	Vehicle Becomes Parallel to Center Line of Traffic Barrier
294	Vehicle Exit



Impact



76 msec



194 msec



294 msec

Figure 13  
SEQUENTIAL PHOTOGRAPHS OF TEST NO. 1

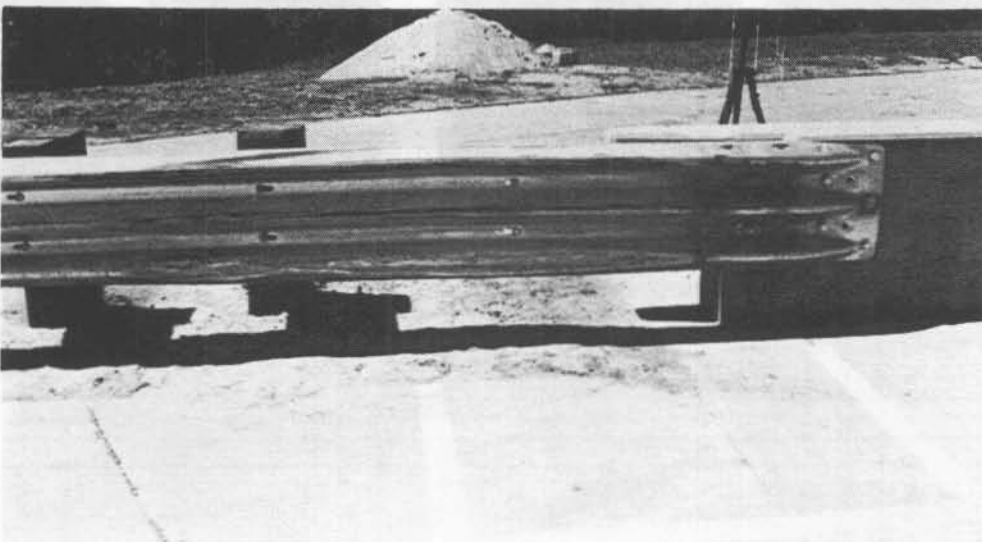
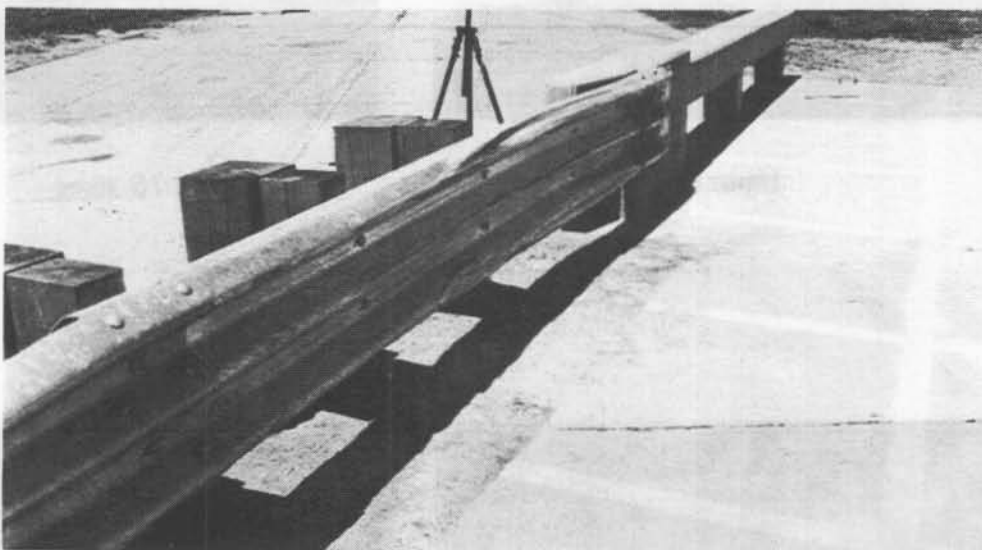
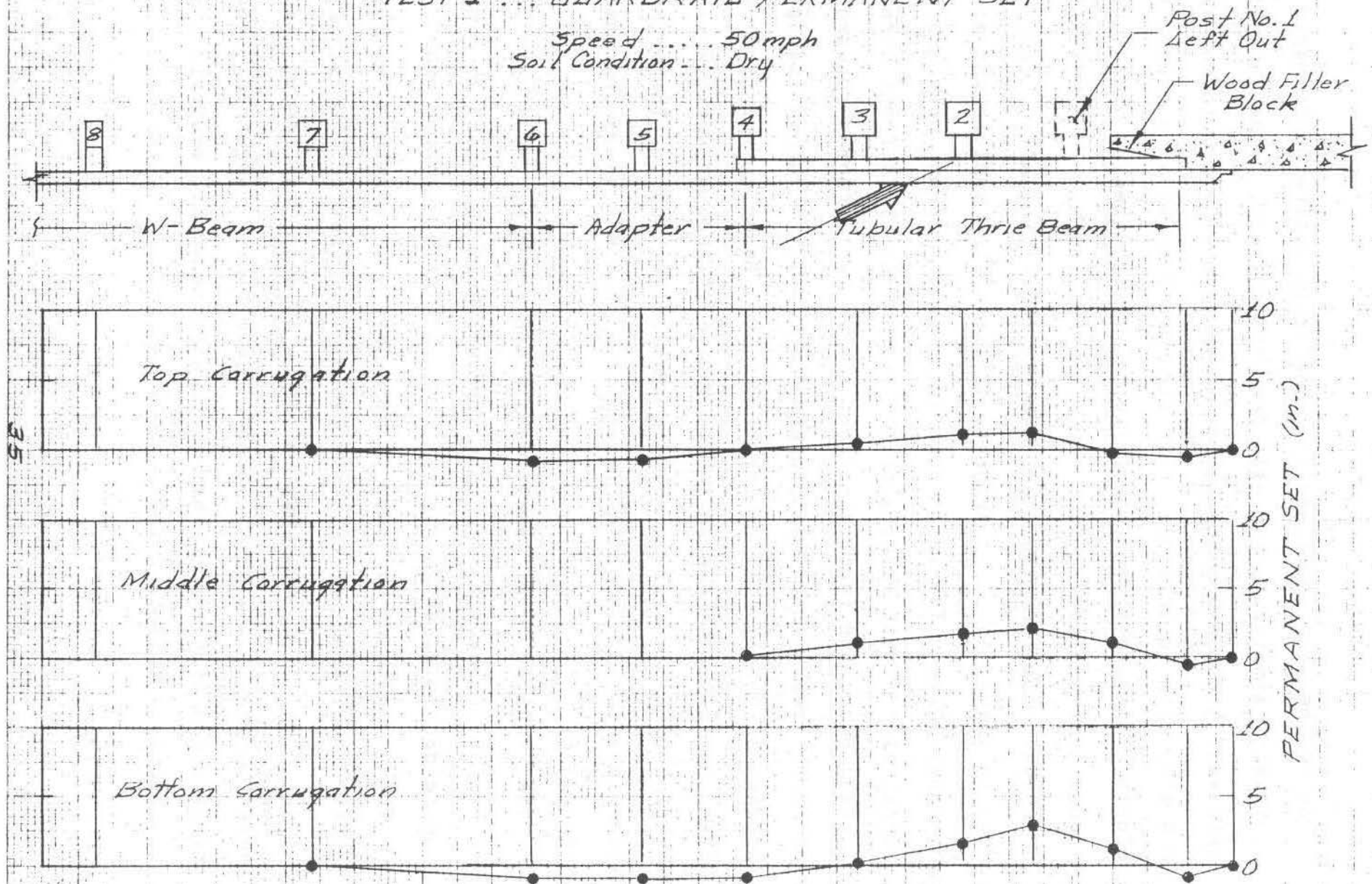


Figure 14  
PHOTOGRAPHS OF TEST NO. 1 GUARDRAIL DAMAGE



Figure 15  
TEST 1 ... GUARDRAIL PERMANENT SET

Speed ... 50 mph  
Soil Condition ... Dry





As can be seen in Figure 14, the vehicle tire scuff marks were relatively straight after exit from the barrier. The vehicle exit angle was 15 deg, and the vehicle travelled 270 ft. before it came to a stop with no braking. The tire scuff marks were caused by the deformed inward alignment of the two front wheels. The vehicle rebound distance was 72 ft.

Photographs of the test vehicle before and after impact are shown in Figure 16. As evident, damage to the vehicle was moderate and repairable. The left front door was not sprung open under the lateral side impact loading of the dummy. The left front corner was crushed 15 in. and the right front corner was deformed outward 3 in. The left rear corner was crushed 4 in. The vehicle damage was assigned a NSC (7) TAD rating of LFQ-3. Based on the findings in NCHRP 86 (8), the damage rating indicates that injuries will occur in 18% of the vehicles damaged to this extent that. The method to determine injury accident probability in NCHRP 86 is presented in Appendix E.

The vehicle impact speed was 47 mph and the exit speed was 38 mph. The change-in-speed of 9 mph was well below the 15 mph limit recommended in NCHRP 230 (3).

The results of Test No. 1 were used to determine "equivalent" impact conditions presented in Table 6 by equating lateral kinetic energy. At an impact angle of about 20 deg, the same guardrail damage shown in Figures 14 and 15 would have occurred under an impact speed of 60 mph. The equation to determine equivalent speeds is presented in Table 6.



Figure 16  
PHOTOGRAPHS OF TEST VEHICLE BEFORE AND AFTER TEST NO. 1

TABLE 6  
EQUIVALENT TEST NO. 1 IMPACT CONDITIONS

Actual Test Speed . . . 47 mph

Actual Test Angle . . . 25 deg

Impact Angle (deg)	Equivalent Impact Speed (mph)
15	77
16	72
17	68
18	64
19	61
20	58

$$\frac{1}{2} \frac{W}{g} (V \sin \theta)^2 = \left[ \frac{1}{2} \frac{W}{g} (V \sin \theta)^2 \right]_{\text{test}}$$

$$V^2 = \frac{(V \sin \theta)_{\text{test}}^2}{\sin^2 \theta}$$

$$V^2 = \frac{394.5}{\sin^2 \theta}$$

In a similar manner, the results of Test No. 1 were used to estimate that a dynamic deflection of 6 to 7 in. would have occurred in a 60 mph impact. This estimate is based on the assumption that the guardrail deflection is directly proportional to the vehicle lateral kinetic energy as follows:

$$\frac{D}{\frac{1}{2} \frac{W}{g} (V \sin \theta)^2} = \frac{D}{\frac{1}{2} \frac{W}{g} (V \sin \theta)^2}_{\text{test}}$$

$$D = \frac{V^2}{V_{\text{test}}^2} D_{\text{test}}$$

$$D = 1.63 D_{\text{test}}$$

Based on the estimate that the guardrail dynamic deflections would have only been on the order of 6 to 7 in. under a 60 mph impact, the decision was made by NDR to not rerun the test because the test would most likely be successful. It is interesting to note that the BARRIER VII Computer Model (see Appendix C) predicted a dynamic deflection of 9 in. No attempt was made to "fine tune" the computer model in this study.

## B.2. TEST NO. 2: SINGLE THRIE BEAM TRANSITION

A summary of the full-scale vehicle crash test on the Single Thrie Beam Transition is presented in Table 7. The vehicle impact point was between Post Nos. 2 and 3. Due to technical problems with the tow vehicle, the vehicle impact speed of 46 mph was 14 mph below the speed of 60 mph recommended in NCHRP 230.

Sequential photographs of Test No. 2 are shown in Figure 17, and a description of the sequential events is presented in Table 8. The maximum vehicle crushing of 16 in. occurred at a time of 70 msec after impact. At a time of 193 msec, the "lateral" velocity component of the vehicle was zero as the vehicle became parallel to the centerline of the traffic barrier. The vehicle exit from the barrier occurred at a time of about 331 msec.

Photographs of the guardrail damage are shown in Figure 18, and measurements of the guardrail permanent set deflections are shown in Figure 19. As evident, the damage was relatively minor and there was evidence of vehicle snagging. The maximum permanent set was approximately 6 in. Due to technical problems with the overhead camera, no measurements were made of the guardrail dynamic deflections. Assuming an impact factor of 1.5, it was estimated that the maximum dynamic deflection was 9 in.

Photographs of the vehicle before and after the test are shown in Figure 20. To reemphasize, the line of concrete median barriers (CMB) were set in place to protect the downstream camera from the possibility of being struck by the vehicle. It was estimated that

TABLE 7

## SUMMARY OF CRASH TEST NO. 2

TEST VEHICLE

Make . . . . . 1977 Plymouth Fury  
 Weight (excluding dummy) . . . . . 4,340 lb.

TRAFFIC BARRIER INSTALLATION

Concrete Bridgerail  
   Type . . . . . Open Rail/Post; Tapered End  
   Length . . . . . 21 ft.-6 in.  
 Guardrail Beam Members (12 Ga)  
   Transition  
     Type . . . . . Single Thrie Beam  
     Length . . . . . 12 ft.-6 in.  
   Adapter  
     Length . . . . . 6 ft.-3 in.  
   Approach  
     Type . . . . . Standard W-Beam  
     Length . . . . . 37 ft.-6 in.  
 Guardrail Wood Posts  
   Post No. 1 . . . . . Left Out  
   Post Nos. 2 and 3 . . . . . 10 x 10 x 72 in.  
   Post Nos. 4 thru 7 . . . . . 8 x 8 x 72 in.  
   Post Nos. 8 thru 12 . . . . . 6 x 8 x 72 in.  
 Native Soil  
   Type . . . . . Silty-Clay (CL)  
   Optimum Moisture . . . . . 18%  
   Relative Compaction . . . . . 92%  
   Test Conditions . . . . . Dry

TEST RESULTS

Vehicle Speed  
   Impact . . . . . 46 mph  
   Exit . . . . . 35 mph  
 Vehicle Angle  
   Impact . . . . . 25 deg.  
   Exit . . . . . 15 deg.  
 Vehicle Rebound Distance . . . . . 20 ft.  
 Vehicle Damage . . . . . TAD LFQ-3 (moderate)  
 Traffic Barrier  
   Impact Location . . . . . Between Post Nos. 2 and 3  
   Max. Dynamic Deflection . . . . . 9 in. (est.)  
   Max. Permanent Set . . . . . 6 in.  
   Snagging . . . . . None  
 Occupant Risk (NCHRP 230)  
   Lateral Impact Velocity . . . . . Not Measured  
   Ridedown Accelerations . . . . . Not Measured  
 Occupant Risk (NCHRP 86)  
   Injury Accident Probability . . . . . 18%

TABLE 8  
DESCRIPTION OF TEST NO. 2 SEQUENTIAL EVENTS

Time (msec)	E V E N T
0	Vehicle Impact
70	Max. Vehicle Crushing of 16 in.
193	Vehicle Becomes Parallel to Center Line of Traffic Barrier
331	Vehicle Exit



Impact



70 msec



193 msec



331 msec

Figure 17  
SEQUENTIAL PHOTOGRAPHS OF TEST NO. 2



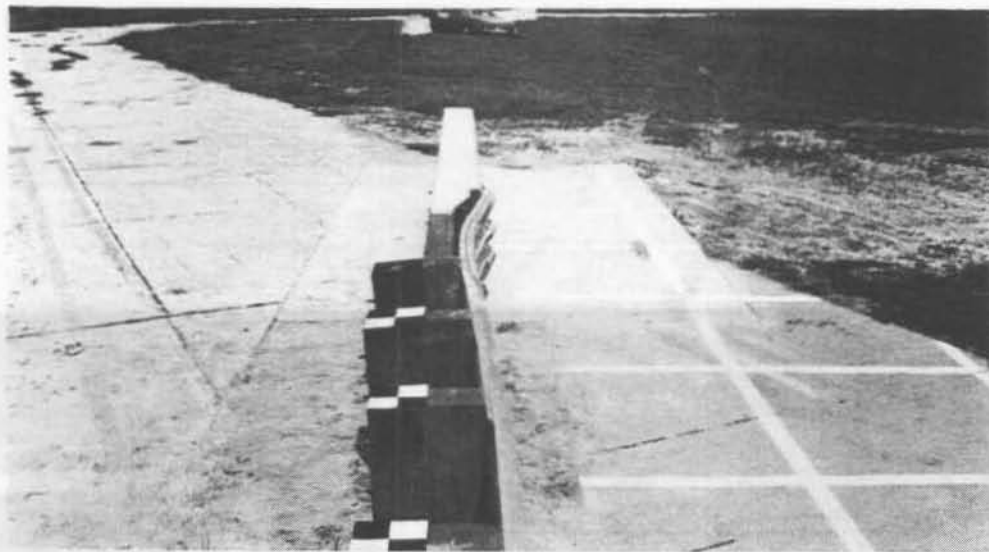


Figure 18  
PHOTOGRAPHS OF TEST NO. 2 GUARDRAIL DAMAGE

Speed... 50 mph  
Soil Condition... Dry

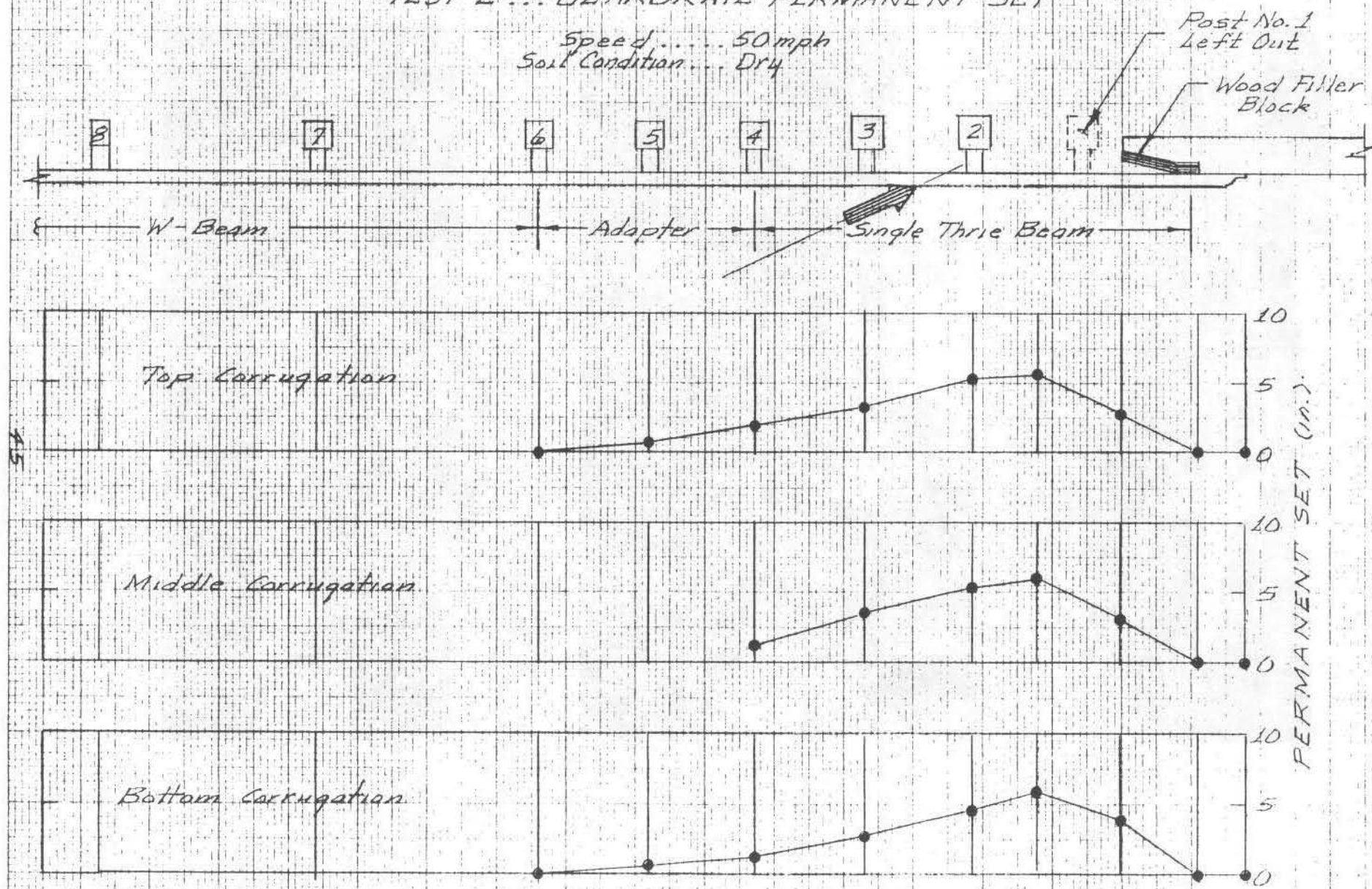




Figure 20  
PHOTOGRAPHS OF TEST VEHICLE BEFORE AND AFTER TEST NO. 2

the vehicle was travelling at a speed of 10 mph or less when it was stopped by the CMB. Because the 20 ft. CMB sections were not connected and were free to slide and rotate as an individual section, it was assumed that most of the damage to the vehicle had occurred during impact with the traffic barrier. As evident, the damage to the vehicle was moderate and repairable. The damage was assigned a NSC (7) TAD rating of LFQ-3. Based on the findings in NCHRP 86 (8), it was predicted that in vehicles damaged to this extent that injuries would occur in 18% of the accidents.

Based upon the methodology discussed earlier in Test No. 1, it was estimated that under a 60 mph and 25 deg impact that the dynamic deflections of the guardrail would have been on the order of 6 to 7 in. greater than at the impact speed of 46 mph. Due to the uncertainty of the larger deflections on the performance of the guardrail at a higher impact speed of 60 mph, and due to the simple fact that the test speed was not in conformance with NCHRP 230, the decision was made by NDR to rerun the test.

### B.3. TEST NO. 3: SINGLE THRIE BEAM TRANSITION

A summary of the full-scale vehicle crash test on the Single Thrie Beam Transition is presented in Table 9. The point of impact was between Post Nos. 2 and 3. The vehicle impact speed was 60 mph and the exit speed was 39 mph.

Sequential photographs of Test No. 3 are shown in Figure 21, and a description of the sequential events is presented in Table 10. During the primary (vehicle front-end) impact stage at a time of 89 msec, the maximum guardrail deflection was 13 in. At a time of 108 msec, the lateral occupant displacement of 12 in. occurred nearly simultaneously to the time in which the front door sprung open under a dummy side impact loading force of 10 g's. The methodology used to determine occupant lateral displacement, impact velocity, and ridedown accelerations by high-film analyses is presented in Appendix D. It was interesting to observe that the largest guardrail deflection of 14 in. occurred during the secondary (vehicle rear-end) impact stage at a time of 231 msec. Vehicle exit from the barrier occurred at a time of about 280 msec.

Photographs of the guardrail damage are shown in Figure 22 (2 pages), and measurements of the guardrail permanent set deflections are shown in Figure 23. The area where the upstream end anchor was bolted to the W-Beam guardrail buckled inward under the tensile loading of about 48 kips. as computed by the BARRIER VII model (see Appendix C). As clearly visible in the photographs, a "moderate" amount of vehicle snagging occurred in the lower half of the thrie beam in the area of the tapered end of the concrete bridgerail. The



TABLE 9

## SUMMARY OF CRASH TEST NO. 3

TEST VEHICLE

Make . . . . . 1977 Plymouth Fury  
 Weight (excluding dummy) . . . . . 4,400 lb.

TRAFFIC BARRIER INSTALLATION

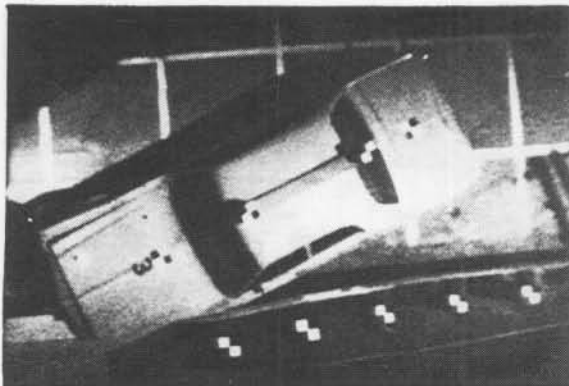
Concrete Bridgerail  
   Type . . . . . Open Rail/Post; Tapered End  
   Length . . . . . 21 ft.-6 in.  
 Guardrail Beam Members (12 Ga)  
   Transition  
     Type . . . . . Single Thrie Beam  
     Length . . . . . 12 ft.-6 in.  
   Adapter  
     Length . . . . . 6 ft.-3 in.  
   Approach  
     Type . . . . . Standard W-Beam  
     Length . . . . . 37 ft.-6 in.  
 Guardrail Wood Posts  
   Post No. 1 . . . . . Left Out  
   Post Nos. 1 and 2 . . . . . 10 x 10 x 72 in.  
   Post Nos. 3 thru 6 . . . . . 8 x 8 x 72 in.  
   Post Nos. 7 thru 12 . . . . . 6 x 8 x 72 in.  
 Native Soil  
   Type . . . . . Silty-Clay (CL)  
   Optimum Moisture . . . . . 18%  
   Relative Compaction . . . . . 92%  
   Test Conditions . . . . . Dry

TEST RESULTS

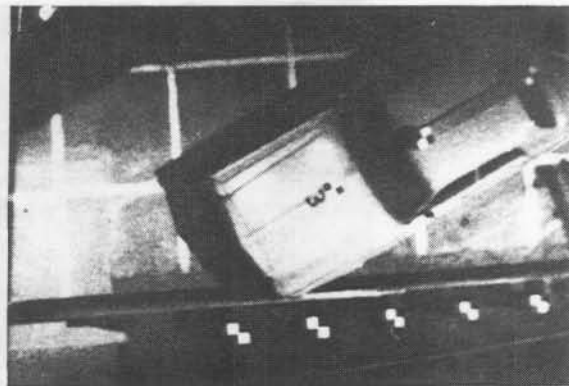
Vehicle Speed  
   Impact . . . . . 60 mph  
   Exit . . . . . 39 mph  
 Vehicle Angle  
   Impact . . . . . 25 deg.  
   Exit . . . . . 11 deg.  
 Vehicle Rebound Distance . . . . . 20 ft.  
 Vehicle Damage . . . . . TAD FLQ-6 1/2 (major)  
 Traffic Barrier  
   Impact Location . . . . . Between Post Nos. 2 and 3  
   Max. Dynamic Deflection . . . . . 14 in.  
   Max. Permanent Set . . . . . 10 in.  
   Snagging . . . . . Moderate  
 Occupant Risk (NCHRP 230)  
   Lateral Impact Velocity . . . . . 21 fps  
   Ridedown Accelerations . . . . . 10 g  
 Occupant Risk (NCHRP 86)  
   Injury Accident Probability . . . . . 86%

TABLE 10  
DESCRIPTION OF TEST NO. 3 SEQUENTIAL EVENTS

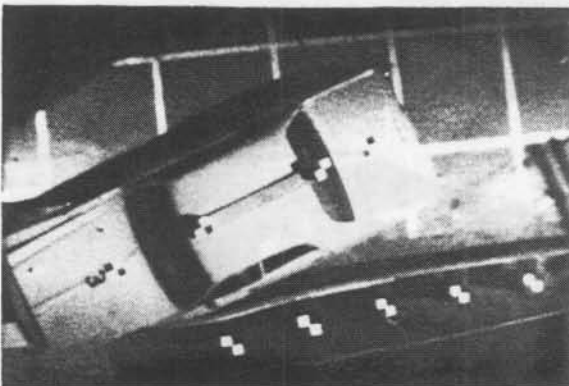
Time (msec)	E V E N T
0	Vehicle Impact
89	Max. Guardrail Deflection of 13 in. During Primary Impact Stage
108	Lateral Occupant Displacement of 12 in.
109	Front Door Springs Open Under Dummy Side Loading
185	Vehicle Becomes Parallel to Center Line of Traffic Barrier
231	Max. Guardrail Deflection of 14 in. During Secondary Impact Stage
280	Vehicle Exit



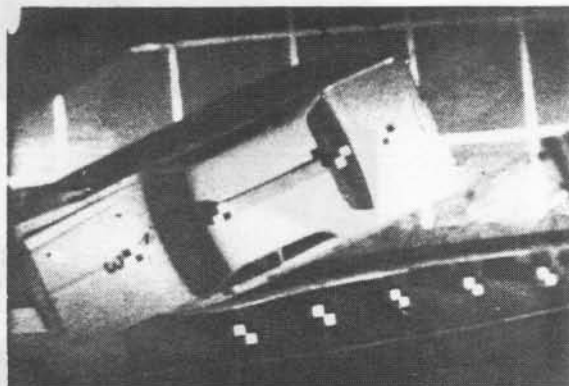
89 msec



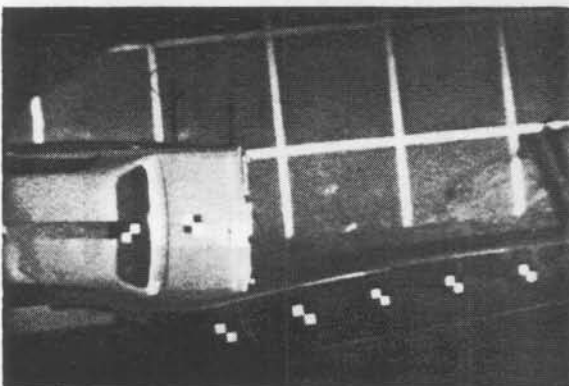
Impact



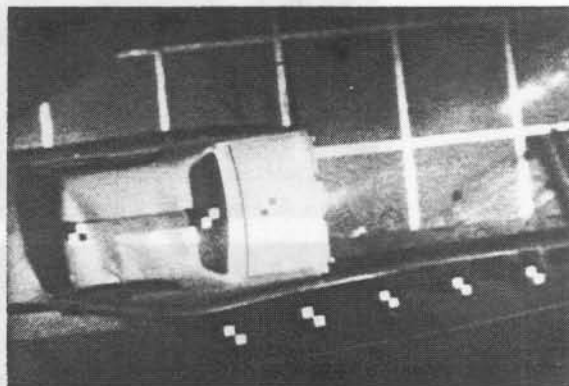
109 msec



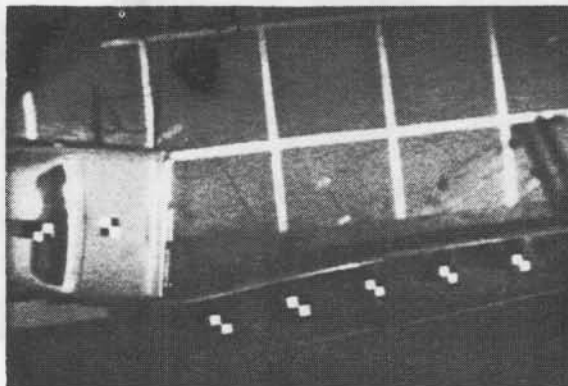
108 msec



231 msec



185 msec



280 msec

Figure 21

SEQUENTIAL PHOTOGRAPHS OF TEST NO. 3



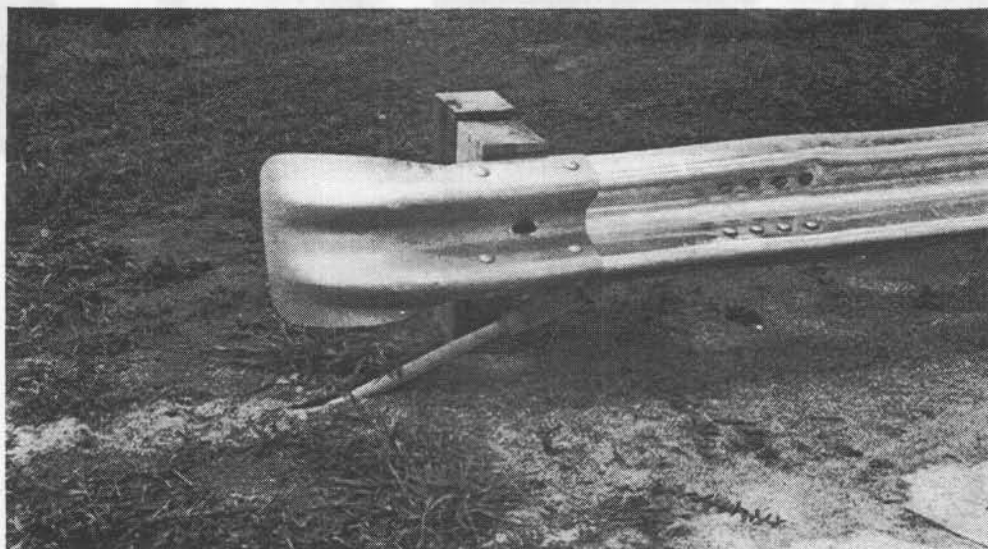
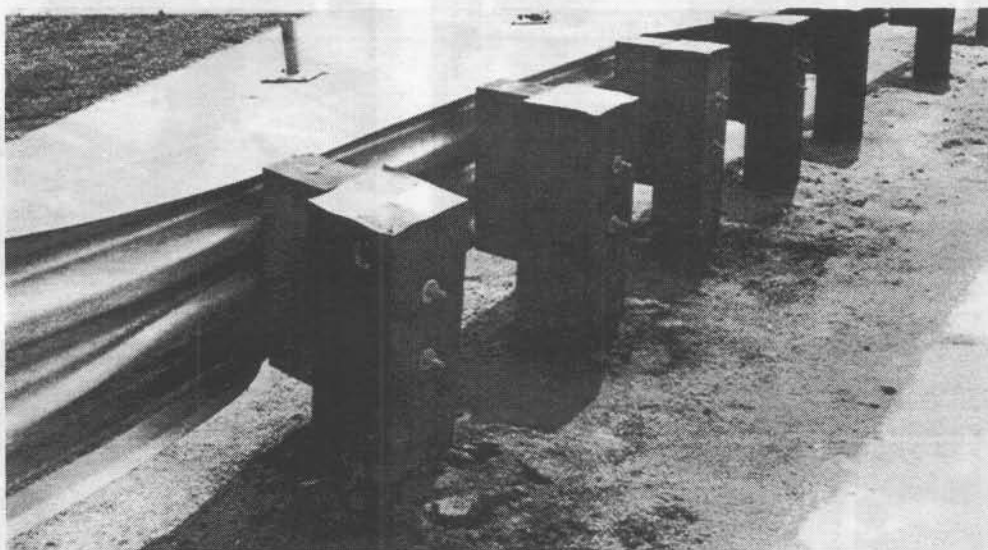


Figure 22  
PHOTOGRAPHS OF TEST NO. 3 GUARDRAIL DAMAGE

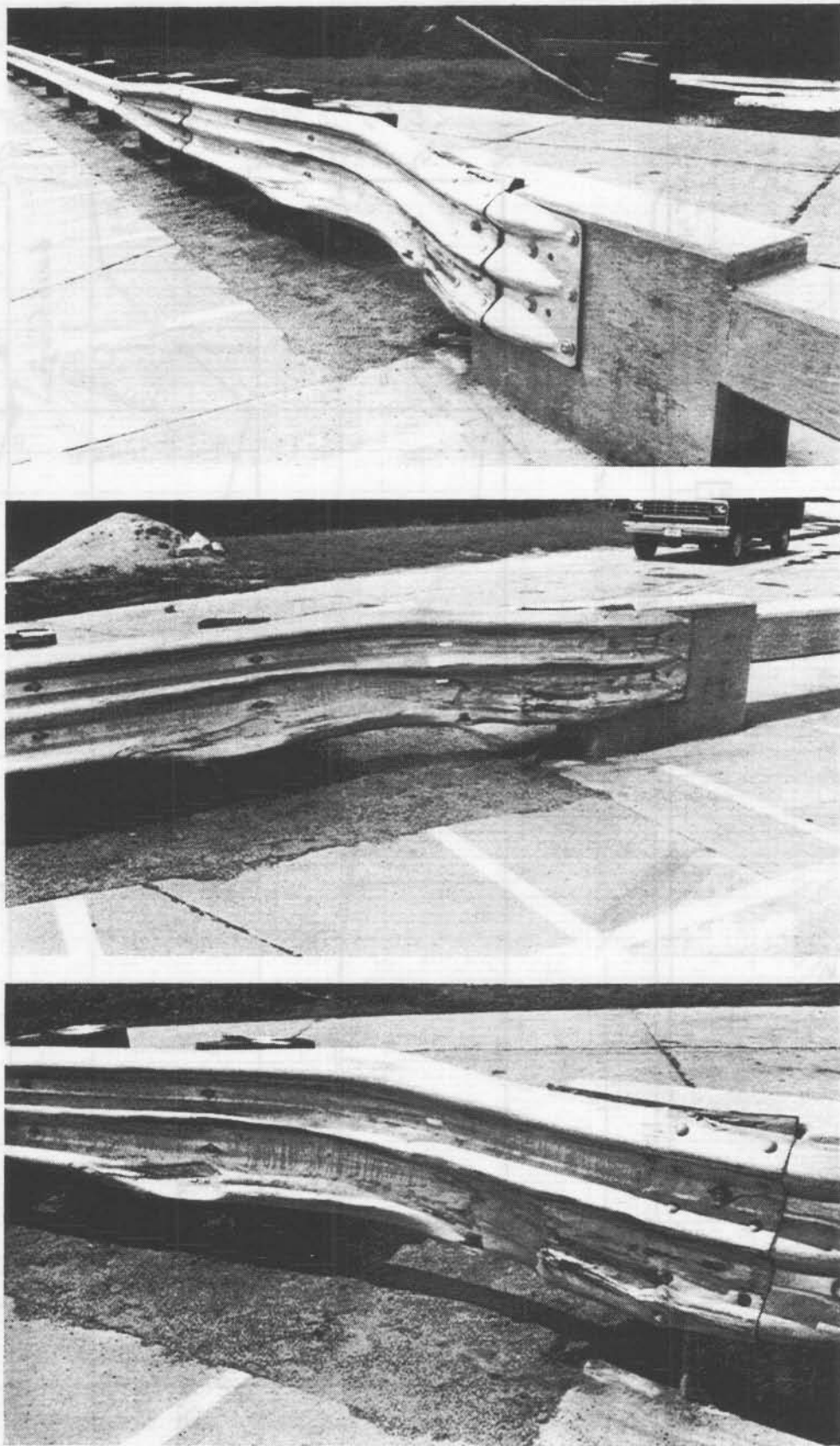
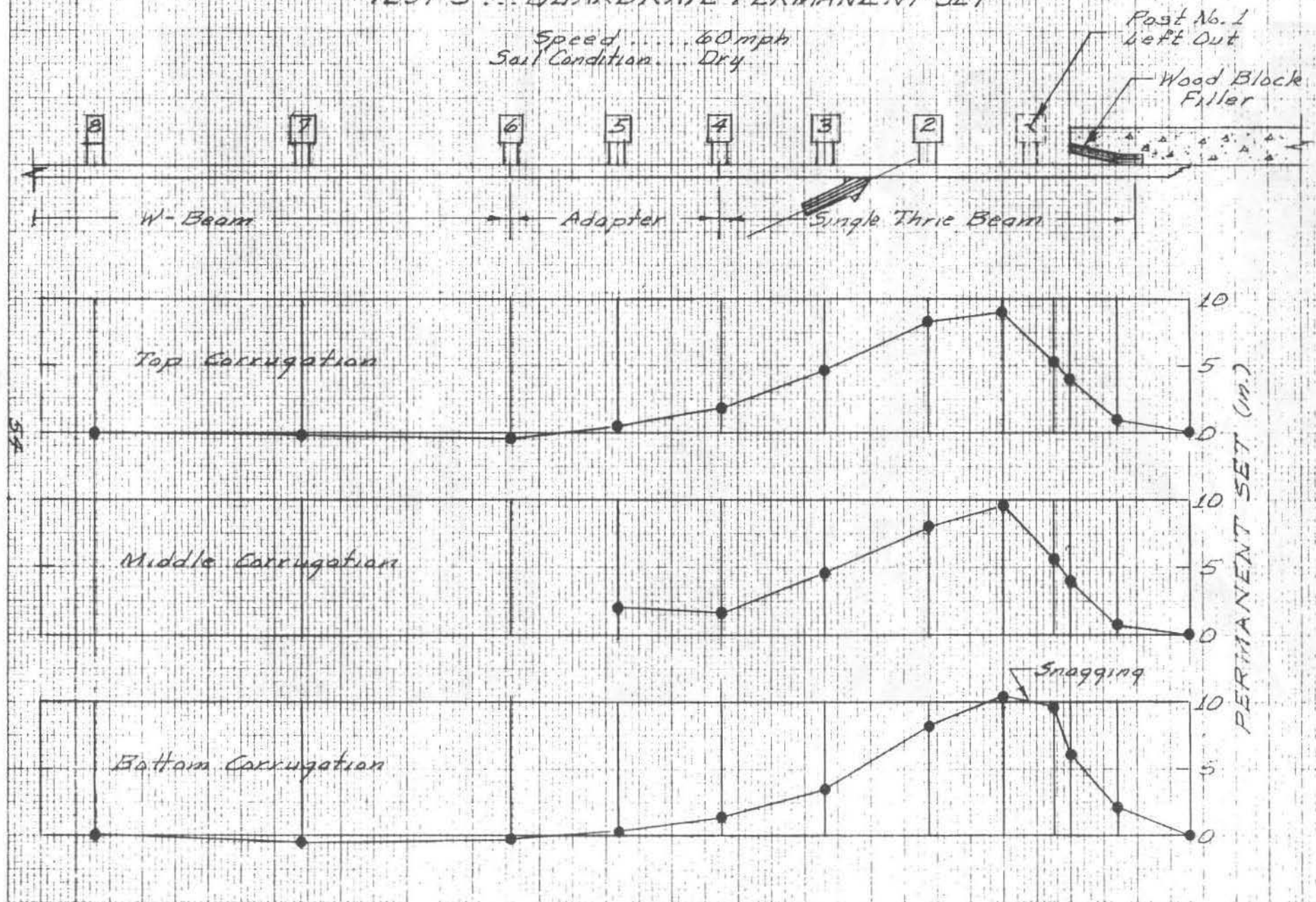


Figure 22  
PHOTOGRAPHS OF TEST NO. 3 GUARDRAIL DAMAGE

Figure 23  
TEST 3 ... GUARDRAIL PERMANENT SET

Speed ... 60 mph  
Soil Condition ... Dry





The vehicle change-in-speed of 21 mph was also a clear indication of a moderate amount of snagging as the change-in-speed was greatly in excess of the 15 mph limit specified in NCHRP 230.

The vehicle exit angle, as visible in one of the photographs in Figure 22, was 11 deg. Due to the high drag forces from the badly damaged left front wheel, the vehicle turned back-in toward an extended centerline of the traffic barrier after it had travelled a distance of 78 ft. The maximum rebound distance of the vehicle C.G. path was 20 ft.

Photographs of the vehicle before and after the test are shown in Figure 24. It was assumed that the vehicle was travelling at a speed of 10 to 15 mph when it was stopped by the CMB protecting the downstream high-speed camera visible in the background. Due to the snagging, the damage to the vehicle was major and not repairable. Most of the damage was incurred during impact with the traffic barrier. The vehicle damage was assigned a NSC TAD rating of LFQ-6 1/2. Based on the findings in NCHRP 86 (8), the damage rating indicates that injuries will occur in 86% of the vehicles damaged to this extent.

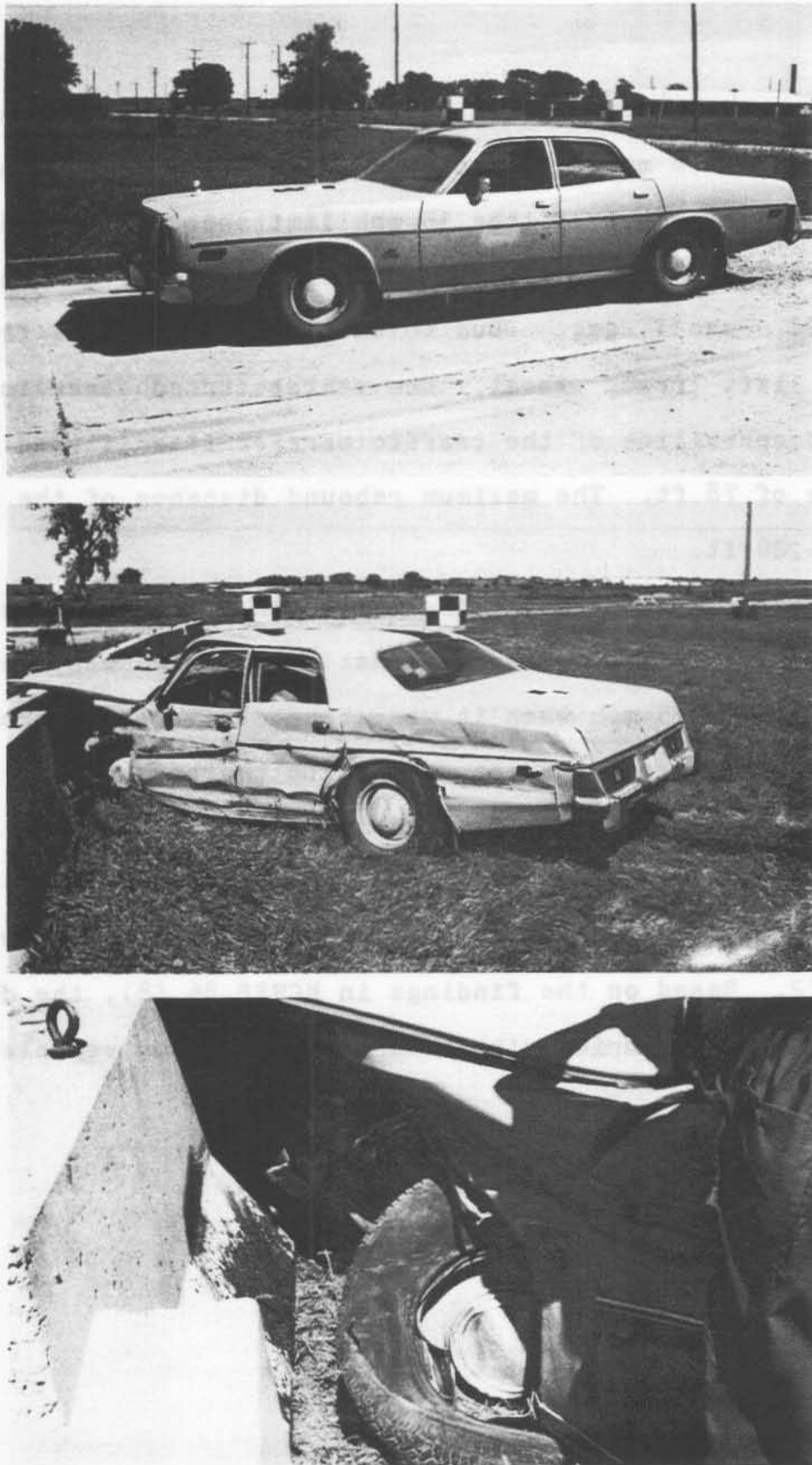


Figure 24  
PHOTOGRAPHS OF TEST VEHICLE BEFORE AND AFTER TEST NO. 3

#### B.4. TEST NO. 4: DOUBLE THRIE BEAM TRANSITION

A summary of the full-scale vehicle crash test on the Double Thrie Beam Transition is presented in Table 11. The point of impact was between Post Nos. 2 and 3. The vehicle impact speed was 61 mph and the exit speed was 47 mph.

Sequential photographs of Test No. 4 are shown in Figure 25, and a description of the sequential events is presented in Table 12. During the primary (vehicle front-end) impact stage at a time of 86 msec, the maximum guardrail deflection was 9 in. At a time of 114 msec, the lateral occupant displacement of 12 in. occurred nearly simultaneously to the time in which the front door sprung open under a dummy side impact loading force of 10 g's. The methodology used to determine occupant lateral displacement, impact velocity, and ridedown accelerations by high-speed analyses is presented in Appendix D. It was interesting to observe that the largest guardrail deflection of 10 in. occurred during the secondary (vehicle rear-end) impact stage at a time of 194 msec. Vehicle exit from the barrier occurred at a time of about 250 msec.

Photographs of the guardrail damage are shown in Figure 26, and measurements of the guardrail permanent set deflections are shown in Figure 27. The damaged guardrail shows no indication of vehicle snagging. The vehicle change-in-speed of 14 mph was also supportive of the fact that no snagging occurred as the change-in-speed was below the 15 mph limit specified in NCHRP 230. Overall, the guardrail "smoothly" redirected the vehicle. The maximum permanent set in the guardrail was 7 1/2 in.

TABLE 11

## SUMMARY OF CRASH TEST NO. 4

TEST VEHICLE

Make . . . . . 1977 Plymouth Fury  
 Weight (excluding dummy) . . . . . 4,360 lb.

TRAFFIC BARRIER INSTALLATION

Concrete Bridgerail  
   Type . . . . . Open Rail/Post; Tapered End  
   Length . . . . . 21 ft.-6 in.  
 Guardrail Beam Members (12 Ga)  
   Transition  
     Type . . . . . Double Thrie Beam  
     Length . . . . . 12 ft.-6 in.  
   Adapter  
     Length . . . . . 6 ft.-3 in.  
   Approach  
     Type . . . . . Standard W-Beam  
     Length . . . . . 37 ft.-6 in.  
 Guardrail Wood Posts  
   Post No. 1 . . . . . Left Out  
   Post Nos. 2 and 3 . . . . . 10 x 10 x 72 in.  
   Post Nos. 4 thru 7 . . . . . 8 x 8 x 72 in.  
   Post Nos. 8 thru 12 . . . . . 6 x 8 x 72 in.  
 Native Soil  
   Type . . . . . Silty-Clay (CL)  
   Optimum Moisture . . . . . 18%  
   Relative Compaction . . . . . 92%  
   Test Conditions . . . . . Dry

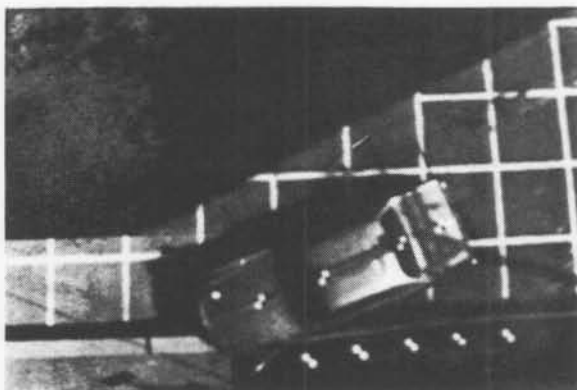
TEST RESULTS

Vehicle Speed  
   Impact . . . . . 61 mph  
   Exit . . . . . 47 mph  
 Vehicle Angle  
   Impact . . . . . 25 deg.  
   Exit . . . . . 11 deg.  
 Vehicle Rebound Distance . . . . . 20 ft.  
 Vehicle Damage . . . . . TAD FLQ-4 1/2  
 Traffic Barrier  
   Impact Location . . . . . Between Post Nos. 2 and 3  
   Max. Dynamic Deflection . . . . . 10 in.  
   Max. Permanent Set . . . . . 7 1/2 in.  
   Snagging . . . . . None  
 Occupant Risk (NCHRP 230)  
   Lateral Impact Velocity . . . . . 19 fps  
   Ridedown Accelerations . . . . . 10 g  
 Occupant Risk (NCHRP 86)  
   Injury Accident Probability . . . . . 41%

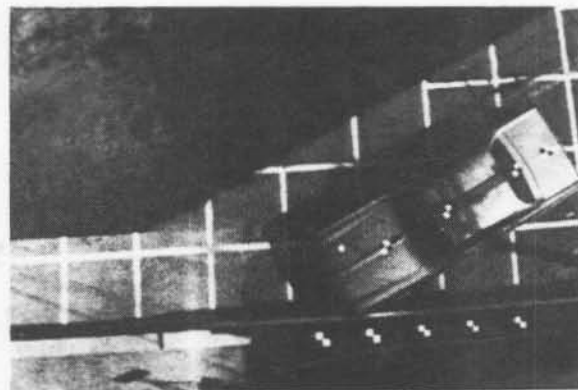
TABLE 12  
DESCRIPTION OF TEST NO. 4 SEQUENTIAL EVENTS

Time (msec)	E V E N T
0	Vehicle Impact
86	Max. Guardrail Deflection of 9 in. During Primary Impact Stage
114	Lateral Occupant Displacement of 12 in.
116	Front Door Springs Open Under Dummy Side Loading
166	Vehicle Becomes Parallel to Center Line of Traffic Barrier
194	Max. Guardrail Deflection of 10 in. During Secondary Impact Stage
250	Vehicle Exit

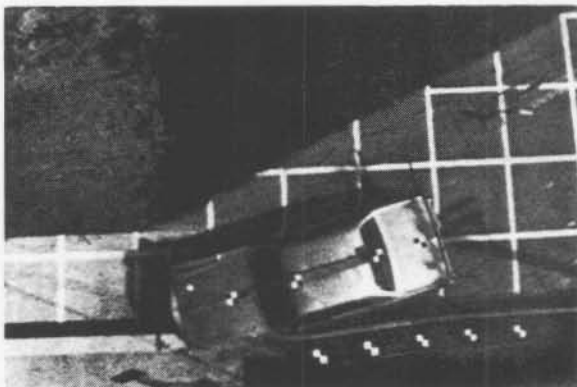




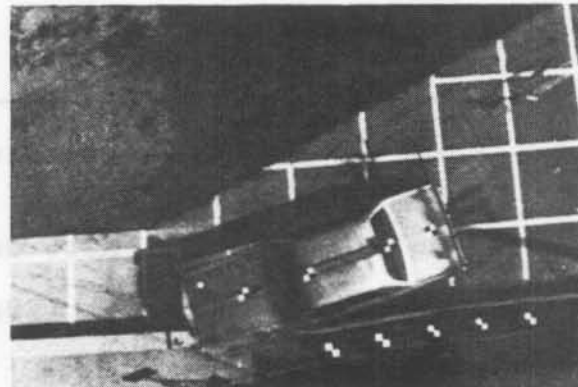
86 msec



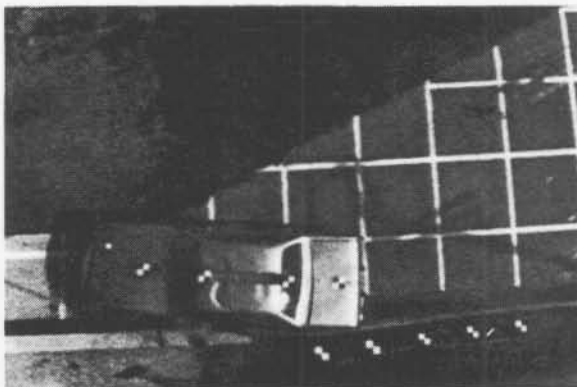
Impact



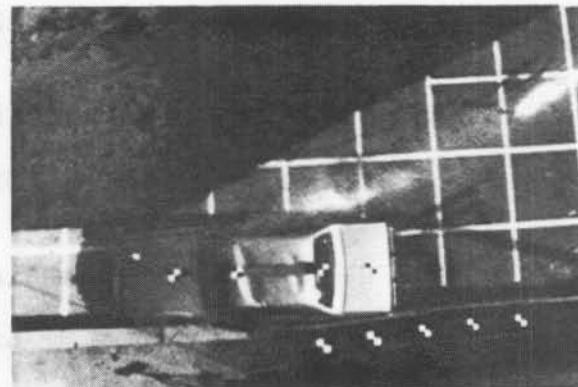
116 msec



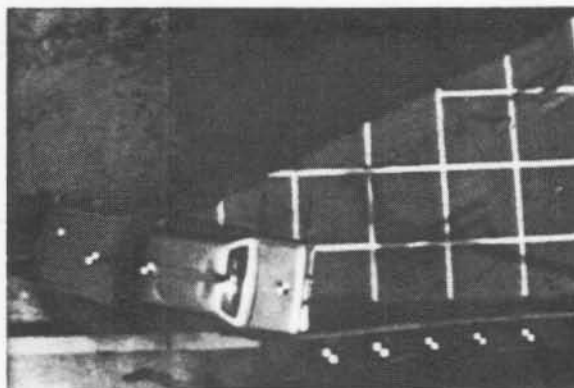
114 msec



194 msec



166 msec



250 msec

Figure 25  
SEQUENTIAL PHOTOGRAPHS OF TEST NO. 4

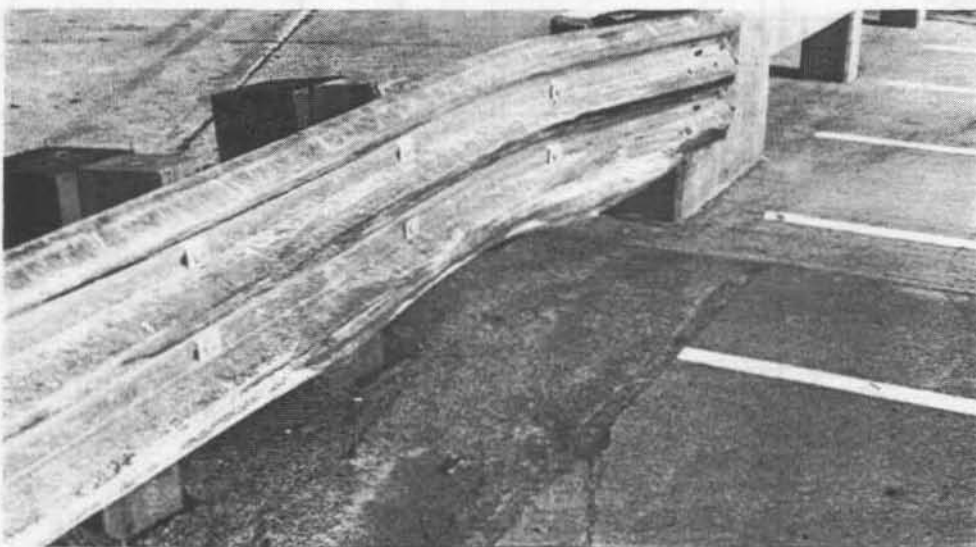
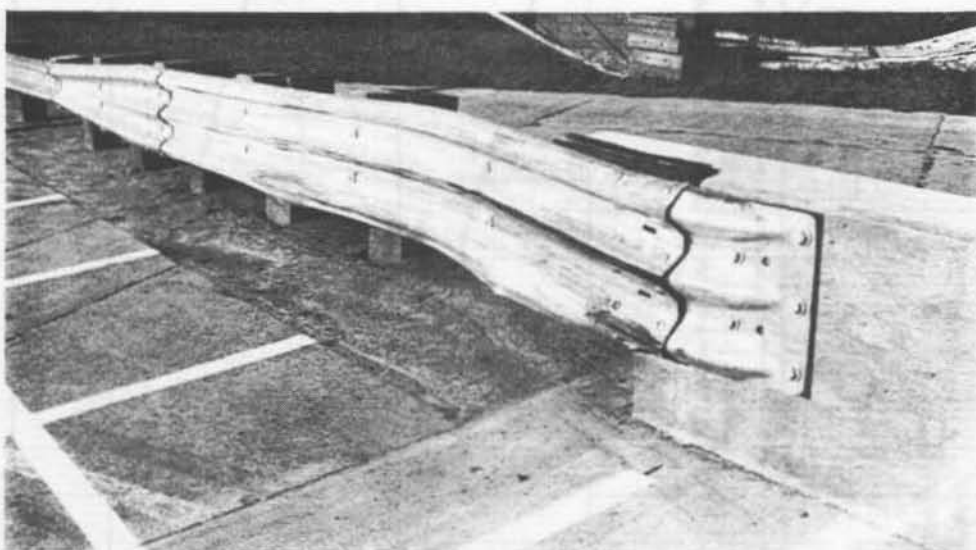
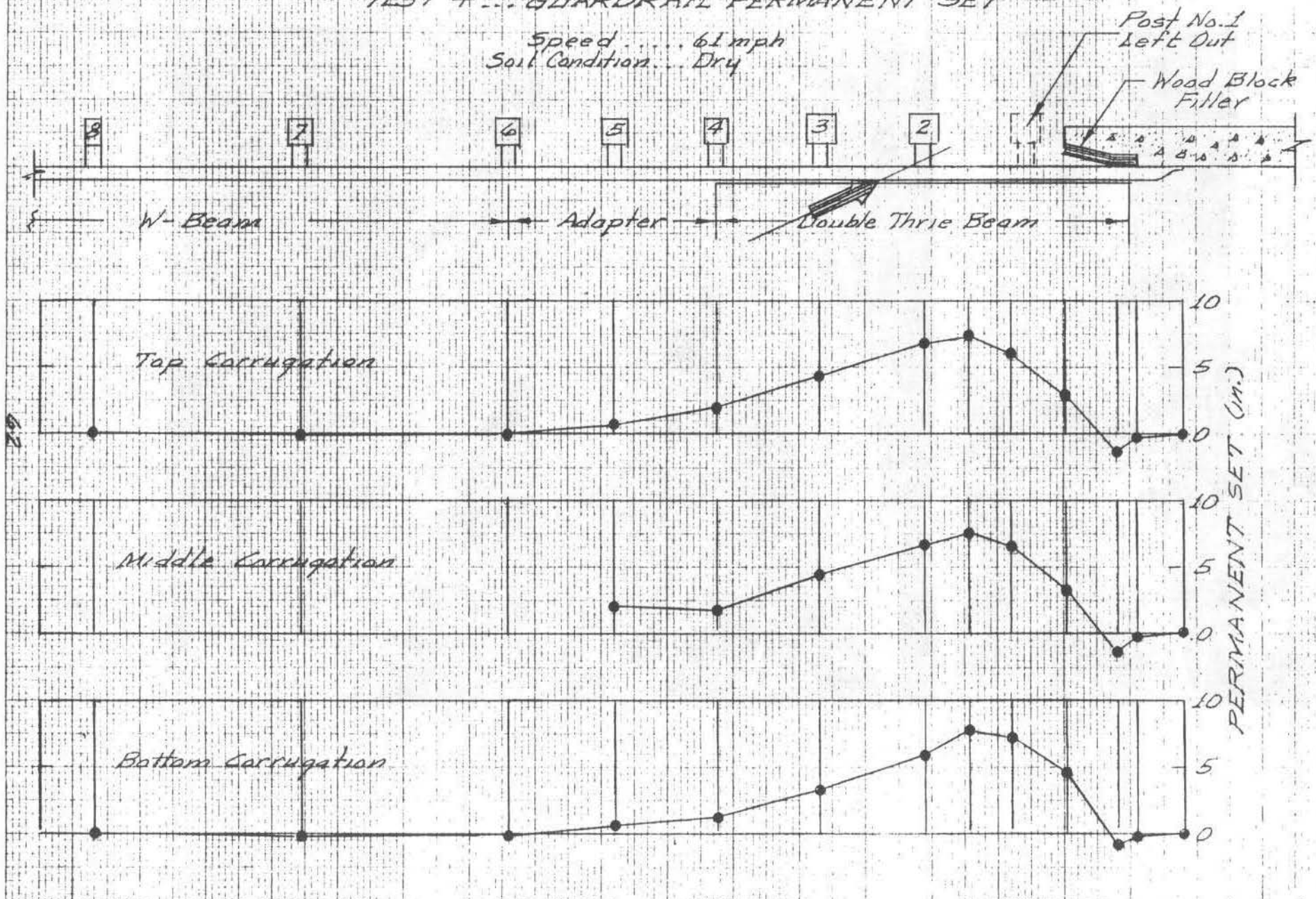


Figure 26  
PHOTOGRAPHS OF TEST NO. 4 GUARDRAIL DAMAGE

Figure 27  
TEST 4... GUARDRAIL PERMANENT SET

Speed..... 61 mph  
Soil Condition... Dry



The vehicle exit angle, as measured from the high-speed film analyses of the overhead camera and the tire scuff marks, was 11 deg. which is well below the limit of 15 deg. recommended in NCHRP 230. Due to slight damage of the left front wheel, the vehicle turned slowly back-in toward an extended centerline of the traffic barrier. The maximum rebound distance of the vehicle C.G. path was approximately 20 ft.

Photographs of the vehicle before and after the test are shown in Figure 28. It was estimated that the vehicle was travelling at a speed of 10 to 15 mph when it was stopped by the CMB protecting the downstream high-speed camera. Most of the damage was incurred during impact with the Double Thrie Beam Transition. The vehicle damage was assigned a NSC TAD rating of LFQ-4 1/2. Based on the findings in NCHRP 86 (8), it was predicted that injuries would occur in vehicles damaged to this extent in 41% of the accidents.





Figure 28  
PHOTOGRAPHS OF TEST VEHICLE BEFORE AND AFTER TEST NO. 4

#### B.5. TEST NO. 5: DOUBLE THRIE BEAM TRANSITION

A summary of the full-scale vehicle crash test on the Double Thrie Beam Transition is presented in Table 13. The point of impact was at Post No. 4; whereas, in the preceding test (Test No. 4) on the identical guardrail design, the impact point was between Post Nos. 2 and 3. The decision to run the second test was based on the need to determine the most critical impact location in terms of guardrail performance. The vehicle impact speed was 61 mph and the exit speed was 48 mph.

Sequential photographs of Test No. 5 are shown in Figure 29, and a description of the sequential events is presented in Table 14. During the primary (vehicle front-end) impact stage at a time of 90 msec, the maximum guardrail deflection was 16 in. At a time of 99 msec, the lateral occupant displacement of 12 in. occurred nearly simultaneously to the time in which the front door sprung open under a dummy side impact loading force of 8 g's. The methodology used to determine occupant lateral displacement, impact velocity, and ridedown accelerations by high-speed film analyses is presented in Appendix D. It was interesting to observe that the largest guardrail deflection of 17 in. occurred during the secondary (vehicle rear-end) impact stage at a time of 201 msec. Vehicle exit from the barrier occurred at a time of about 283 msec.

Photographs of the guardrail damage are shown in Figure 30 (2 pages), and measurements of the guardrail permanent set deflections are shown in Figure 31. The soil was saturated from a heavy 2 day storm preceding the day of the test. The decision to test under a

TABLE 13

## SUMMARY OF CRASH TEST NO. 5

TEST VEHICLE

Make . . . . . 1977 Plymouth Fury  
 Weight (excluding Dummy) . . . . . 4,320 lb.

TRAFFIC BARRIER INSTALLATION

Concrete Bridgerail  
 Type . . . . . Open Rail/Post; Tapered End  
 Length . . . . . 21 ft.-6 in.  
 Guardrail Beam Members (12 Ga)  
 Transition  
 Type . . . . . Double Thrie Beam  
 Length . . . . . 12 ft.-6 in.  
 Adapter  
 Length . . . . . 6 ft.-3 in.  
 Approach  
 Type . . . . . Standard W-Beam  
 Length . . . . . 37 ft.-6 in.  
 Guardrail Wood Posts  
 Post No. 1 . . . . . Left Out  
 Post Nos. 2 and 3 . . . . . 10 x 10 x 72 in.  
 Post Nos. 4 thru 7 . . . . . 8 x 8 x 72 in.  
 Post Nos. 8 thru 12 . . . . . 6 x 8 x 72 in.  
 Native Soil  
 Type . . . . . Silty-Clay (CL)  
 Optimum Moisture . . . . . 18%  
 Relative Compaction . . . . . 92%  
 Test Conditions . . . . . Wet

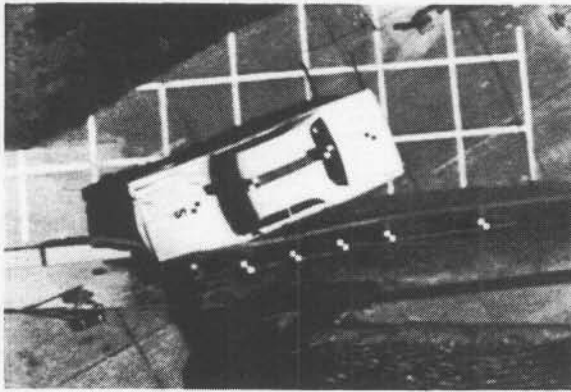
TEST RESULTS

Vehicle Speed  
 Impact . . . . . 61 mph  
 Exit . . . . . 48 mph  
 Vehicle Angle  
 Impact . . . . . 25 deg.  
 Exit . . . . . 15 deg.  
 Vehicle Rebound Distance . . . . . 20 ft.  
 Vehicle Damage . . . . . TAD LFQ-4  
 Traffic Barrier  
 Impact Location . . . . . Post No. 4  
 Max. Dynamic Deflection . . . . . 17 in.  
 Max. Permanent Set . . . . . 11 in.  
 Snagging . . . . . None  
 Occupant Risk (NCHRP 230)  
 Lateral Impact Velocity . . . . . 17 fps  
 Ridedown Accelerations . . . . . 8 g  
 Occupant Risk (NCHRP 86)  
 Injury Accident Probability . . . . . 33%

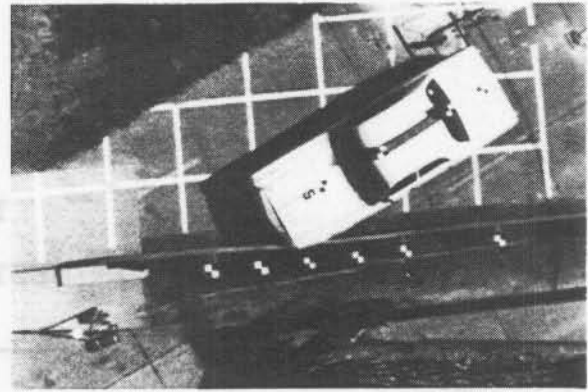
TABLE 14  
DESCRIPTION OF TEST NO. 5 SEQUENTIAL EVENTS

Time (msec)	E V E N T
0	Vehicle Impact
90	Max. Guardrail Deflection of 16 in. During Primary Impact Stage
99	Lateral Occupant Displacement of 12 in.
101	Front Door Springs Open Under Dummy Side Loading
155	Vehicle Becomes Parallel to Center Line of Traffic Barrier
201	Max. Guardrail Deflection of 17 in. During Secondary Impact Stage
283	Vehicle Exit

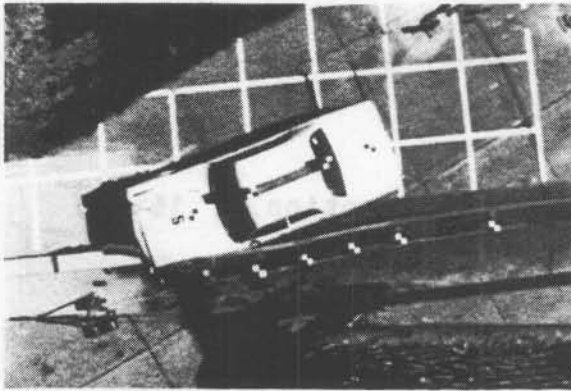




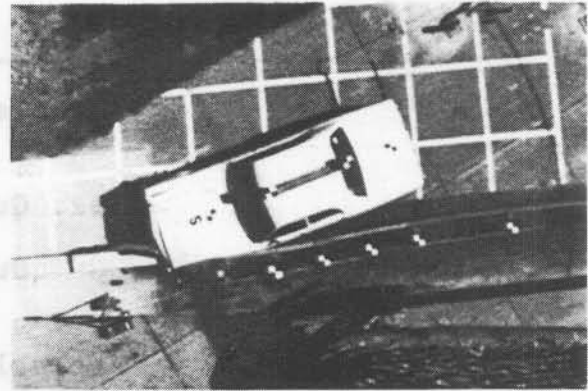
90 msec



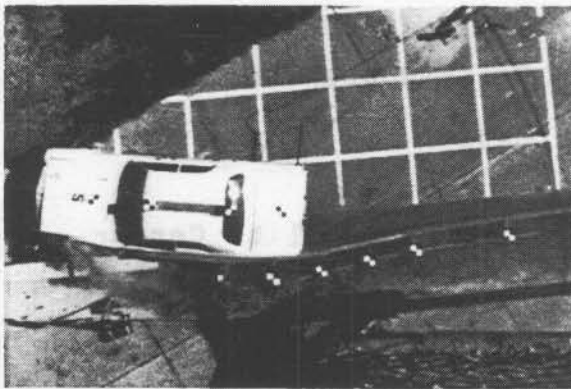
Impact



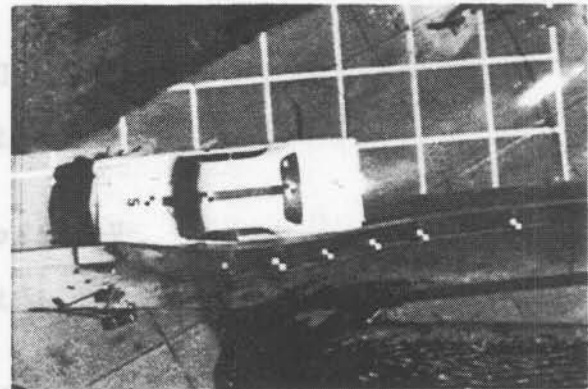
101 msec



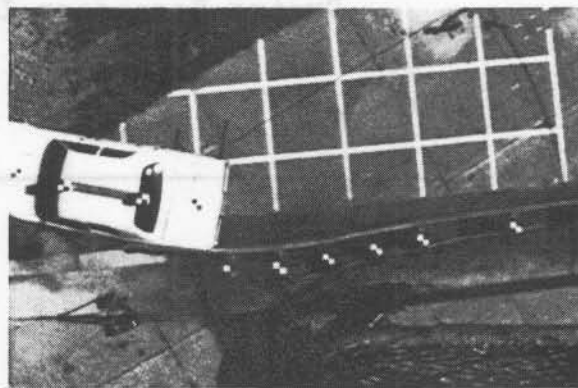
99 msec



201 msec



155 msec



283 msec

Figure 29

SEQUENTIAL PHOTOGRAPHS OF TEST NO. 5

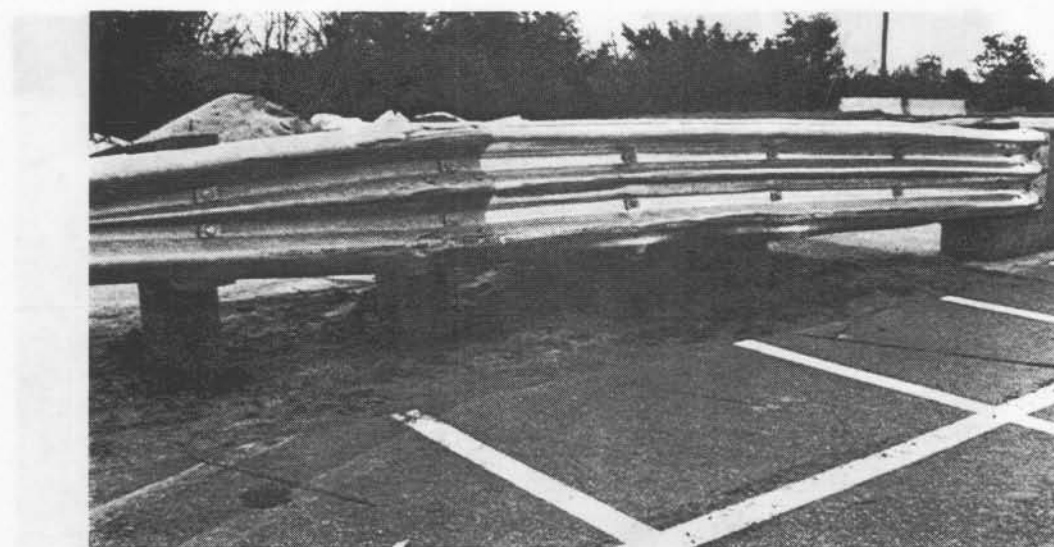


Figure 30  
PHOTOGRAPHS OF TEST NO. 5 GUARDRAIL DAMAGE

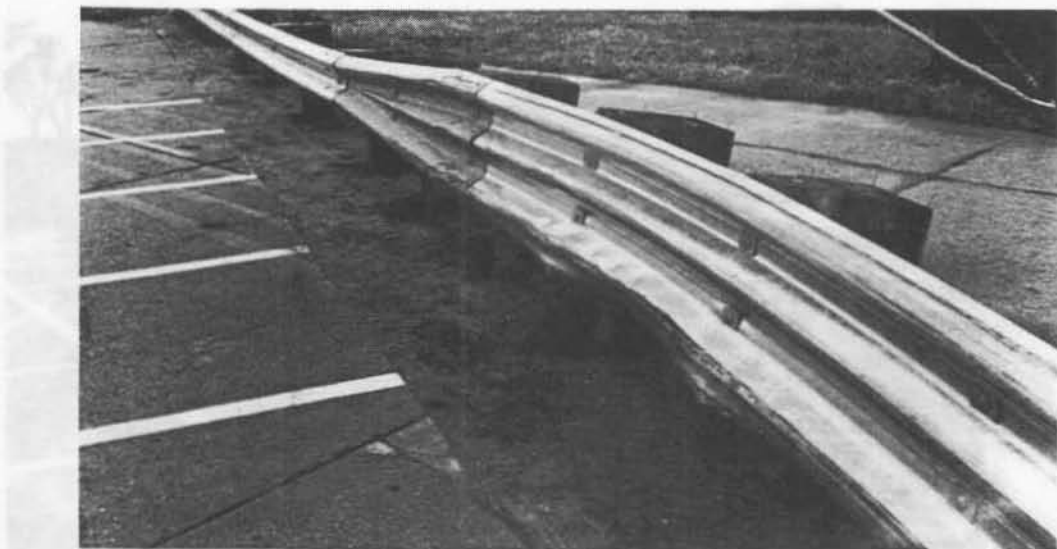
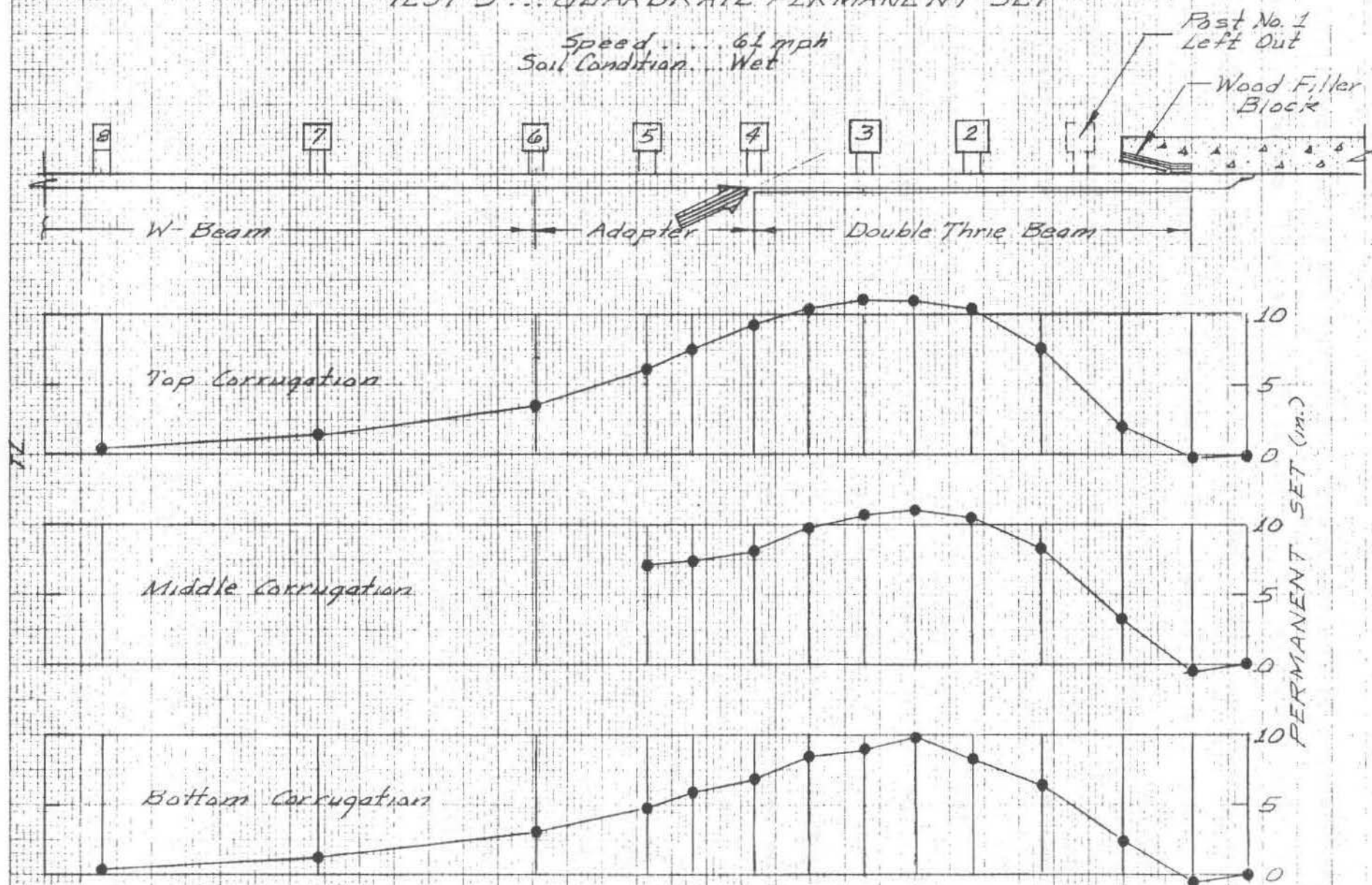


Figure 30  
PHOTOGRAPHS OF TEST NO. 5 GUARDRAIL DAMAGE



Figure 31  
TEST 5... GUARDRAIL PERMANENT SET

Speed..... 61 mph  
Soil Condition... Wet



saturated soil condition was made by the NDR as this condition would be representative of the lowest possible soil shearing strength. The damaged guardrail shows no indication of vehicle snagging. The vehicle change-in-speed of 13 mph was also supportive of the fact that no snagging occurred as the change-in-speed was below the 15 mph limit specified in NCHRP 230. Overall, the guardrail "smoothly" redirected the vehicle. The maximum permanent set in the guardrail was 11 in.

The vehicle exit angle, as measured from the high-speed analysis of the overhead camera, was 15 deg. Due to slight damage of the left front wheel, the vehicle turned slowly back-in toward an extended centerline of the traffic barrier. The maximum rebound of the vehicle C.G. path was approximately 20 ft.

Photographs of the vehicle before and after the test are shown in Figure 32. It was assumed that the vehicle was travelling at a speed of 10 to 15 mph when it was stopped by the CMB protecting the downstream high-speed camera. Most of the damage was incurred during impact with the Double Thrie Beam Transition. The vehicle damage was assigned a NSC TAD rating of LFQ-4. Based on the findings in NCHRP 86 (8), it was predicted that injuries would occur in vehicles damaged to this extent in 33% of the accidents.



Figure 32  
PHOTOGRAPHS OF TEST VEHICLE BEFORE AND AFTER TEST NO. 5

#### B.6. TEST NO. 6: DOUBLE W-BEAM TRANSITION

The Double W-Beam Transition was similar to an "old" design that was in wide use several years ago in Nebraska. The old design was different in that it had smaller size 6 x 8 in. posts spaced on longer 6 ft.-3 in. centers.

A summary of the full-scale vehicle crash test on the Double W-Beam Transition is presented in Table 15. The point of impact was between Post Nos. 2 and 3. The vehicle impact speed was 62 mph and the exit speed was 39 mph.

Sequential photographs of Test No. 6 are shown in Figure 33, and a description of the sequential events is presented in Table 16. During the primary (vehicle front-end) impact stage at a time of 75 msec, the maximum guardrail deflection was 9 in. At a time of 113 msec, the lateral displacement of an occupant would have been 12 in., however, there was no sign of the front door being sprung open under the side impact loading of the dummy as had occurred in the three previous tests. The largest guardrail deflection of 10 in. occurred during the secondary (vehicle rear-end) impact stage at a time of 212 msec. Vehicle exit from the barrier occurred at a time of 262 msec.

Photographs of the guardrail damage are shown in Figure 34 (2 pages), and measurements of the guardrail permanent set deflections are shown in Figure 35. The soil was frozen to a depth of 8 to 10 in. The effect of the frozen soil was readily apparent by comparing the permanent set deflections in Test No. 4 (Figure 27) with this

TABLE 15

## SUMMARY OF CRASH TEST NO. 6

TEST VEHICLE

Make . . . . . 1977 Plymouth Fury  
 Weight (excluding Dummy) . . . . . 4,560 lb.

TRAFFIC BARRIER INSTALLATION

Concrete Bridgerail  
 Type . . . . . Open Rail/Post; Tapered End  
 Length . . . . . 21 ft.-6 in.  
 Guardrail Beam Members (12 Ga)  
 Transition  
 Type . . . . . Double W-Beam  
 Length . . . . . 12 ft.-6 in.  
 Adapter  
 Length . . . . . 6 ft.-3 in.  
 Approach  
 Type . . . . . Standard W-Beam  
 Length . . . . . 37 ft.-6 in.  
 Guardrail Wood Posts  
 Post No. 1 . . . . . Left Out  
 Post Nos. 2 and 3 . . . . . 10 x 10 x 72 in.  
 Post Nos. 4 thru 7 . . . . . 8 x 8 x 72 in.  
 Post Nos. 8 thru 12 . . . . . 6 x 8 x 72 in.  
 Native Soil  
 Type . . . . . Silty-Clay (CL)  
 Optimum Moisture . . . . . 18%  
 Relative Compaction . . . . . 92%  
 Test Conditions . . . . . Ground Frozen 8 to 10 in.

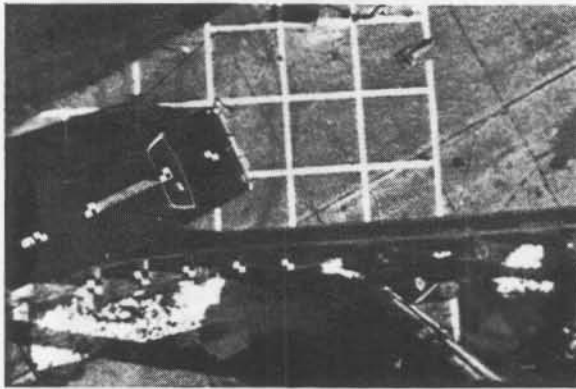
TEST RESULTS

Vehicle Speed  
 Impact . . . . . 62 mph  
 Exit . . . . . 39 mph  
 Vehicle Angle  
 Impact . . . . . 25 deg.  
 Exit . . . . . 9 deg.  
 Vehicle Rebound Distance . . . . . 20 ft.  
 Vehicle Damage . . . . . TAD FLQ-7 (extensive)  
 Traffic Barrier  
 Impact Location . . . . . Between Post Nos. 2 and 3  
 Max. Dynamic Deflection . . . . . 10in.  
 Max. Permanent Set . . . . . 6 in.  
 Snagging . . . . . severe  
 Occupant Risk (NCHRP 230)  
 Lateral Impact Velocity . . . . . 24 fps  
 Ridedown Accelerations . . . . . 6 g  
 Occupant Risk (NCHRP 86)  
 Injury Accident Probability . . . . . 100%

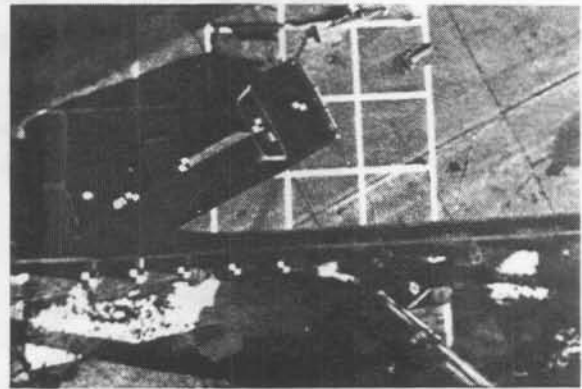


TABLE 16  
DESCRIPTION OF TEST NO. 6 SEQUENTIAL EVENTS

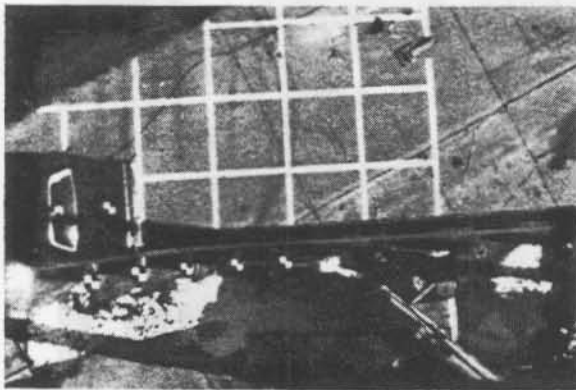
Time (msec)	E V E N T
0	Vehicle Impact
75	Max. Guardrail Deflection of 9 in. During Primary Impact
113	Lateral Occupant Displacement of 12 in.
182	Vehicle Becomes Parallel to Center Line of Traffic Barrier
212	Max. Guardrail Deflection of 10 in. During Secondary Impact
262	Vehicle Exit



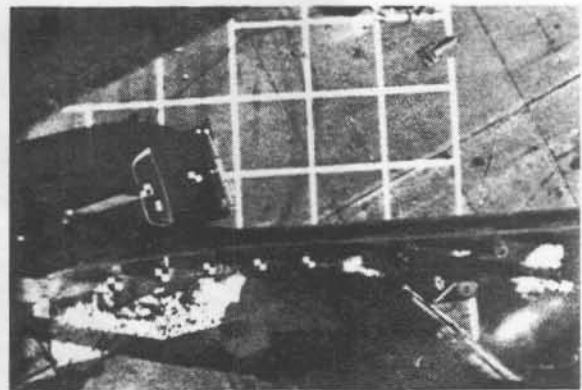
75 msec



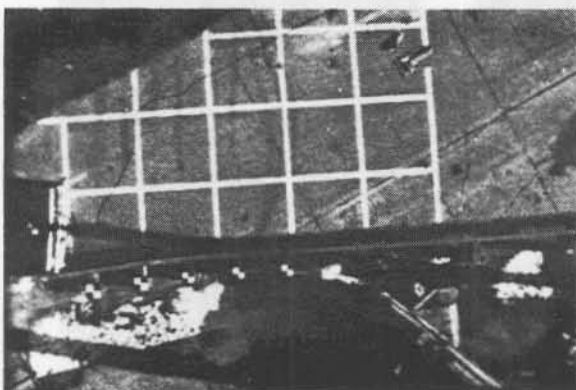
Impact



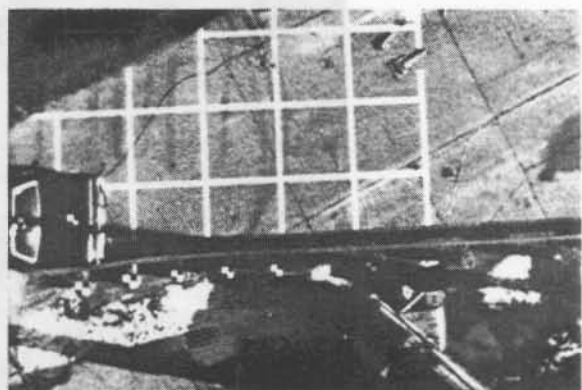
182 msec



113 msec



262 msec



212 msec

Figure 33

SEQUENTIAL PHOTOGRAPHS OF TEST NO. 6



Figure 34  
PHOTOGRAPHS OF TEST NO. 6 GUARDRAIL DAMAGE

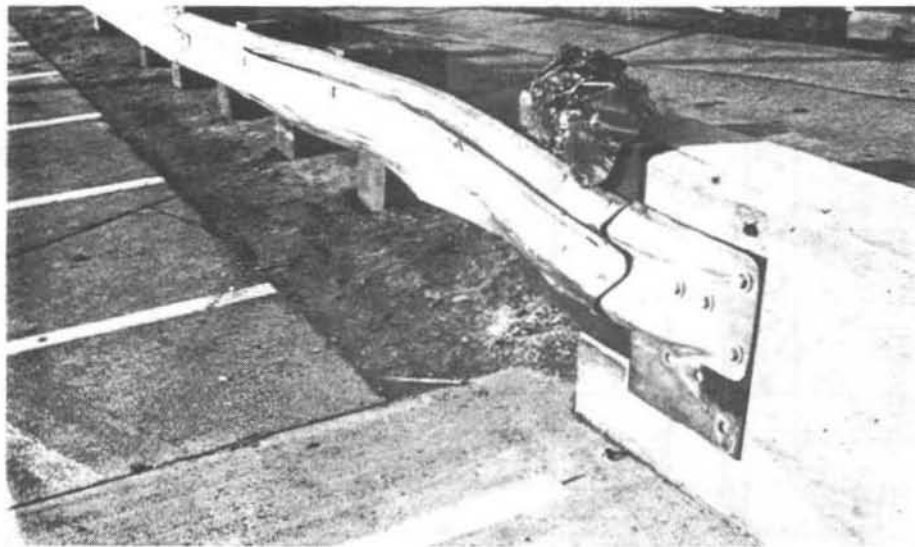
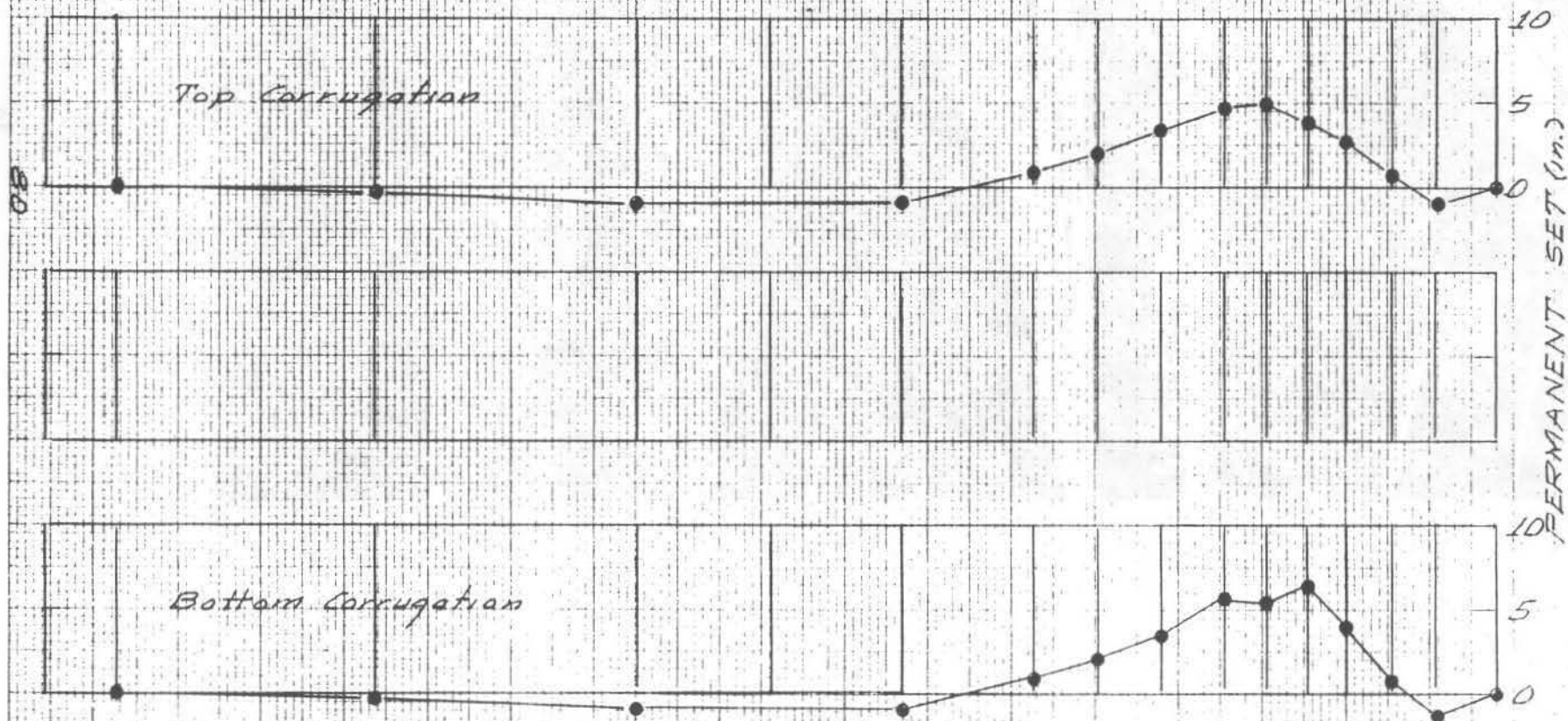
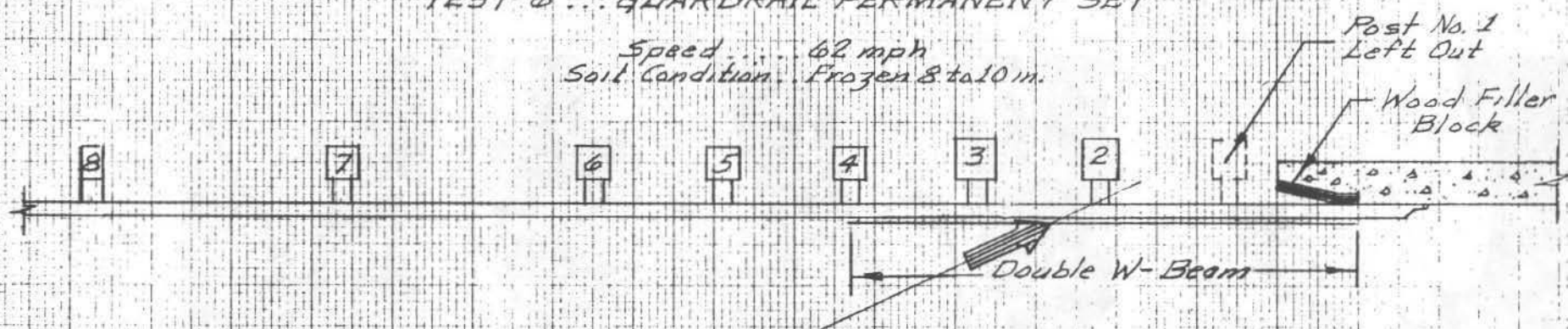


Figure 34  
PHOTOGRAPHS OF TEST NO. 6 GUARDRAIL DAMAGE

Figure 35  
TEST 6 ... GUARDRAIL PERMANENT SET

Speed ... 62 mph  
Soil Condition ... Frozen 8 to 10 in.





test. Aside from the fact that the strength of the Double Thrie Beam in Test No. 4 was much stronger than the strength of the Double W-Beam, the permanent set deflections of the Double W-Beam were much less. The damaged guardrail in Figure 34 shows severe vehicle snagging. The vehicle change-in-speed of 23 mph was also supportive of the fact that severe snagging occurred as the change-in-speed greatly exceeded the 15 mph limit specified in NCHRP 230. The snagging was the result of the vehicle frame and wheel assembly getting under the guardrail and impacting the tapered-end of the concrete bridgerail. As can be seen in Figure 34, sheet metal was torn from the vehicle and wedged in between the guardrail and the wood filler block in the recessed area of the bridgerail tapered-end.

The vehicle exit angle, as measured from an analysis of the high-speed film of the overhead camera, was 9 deg. Due to the badly damaged left front wheel, the vehicle turned rapidly back-in toward an extended centerline of the traffic barrier.

Photographs of the vehicle before and after the test are shown in Figure 36. It was estimated that the vehicle was travelling at a speed of 10 to 15 mph when it was stopped by the CMB protecting the downstream high-speed camera. Most of the damage was incurred during impact with the Double W-Beam Transition. As evident, the vehicle was extensively damaged as a result of the severe snagging. The vehicle damage was assigned a NSC TAD rating of LFQ-7. Based on the findings in NCHRP 86 (8), it was predicted that injuries would occur in vehicles damaged to this extent in 100% of the accidents.



Figure 36  
PHOTOGRAPHS OF TEST VEHICLE BEFORE AND AFTER TEST NO. 6



### III

### SUMMARY AND CONCLUSIONS

A comparative summary of the crash test results is presented in Table 17, and the performance of the traffic barrier measured in terms of the NCHRP 230 (3) safety evaluation guidelines is presented in Table 18.

Due to technical problems with the tow vehicle, the impact speeds in Test No. 1 and Test No. 2 were approximately 14 mph below the recommended target speed of 60 mph in NCHRP 230. Test No. 1 on the Tubular Thrie Beam transition was not rerun because it was estimated that the dynamic deflection would have only been on the order of 3 in. greater at the higher 60 mph impact speed, and hence, the 60 mph test would have most likely been satisfactory. On the other hand, Test No. 2 on the Single Thrie Beam transition was rerun (1) because of the uncertainty that existed due to an estimated dynamic deflection on the order of 7 in. greater at the higher 60 mph impact speed, (2) due to the simple fact that the test speed was not in conformance with NCHRP 230. The estimated deflections were determined on the assumption that the deflection of the guardrail was directly proportional to the lateral kinetic energy of the vehicle.

After impact with the guardrail transition, the vehicle trajectory (C.G. path) in each of the six tests was unsatisfactory in accordance with NCHRP 230 (Item H) as each vehicle would have been redirected back into the adjacent lanes of traffic. In order to compensate for this type of situation, it is specified in NCHRP 230 (Item I) that (1) the change-in-speed of the vehicle should be less than 15 mph, and (2) the exit angle should be less than 15 deg.

TABLE 17

## COMPARATIVE SUMMARY OF CRASH TEST RESULTS

TEST NO.	1	2	3	4	5	6
TRANSITION BEAM DESIGN	Tubular Thrie	Single Thrie	Single Thrie	Double Thrie	Double Thrie	Double W-Beam
SOIL (Silty-Clay)	Dry	Dry	Dry	Dry	Wet	Frozen <sup>(a)</sup>
VEHICLE WEIGHT (lb)	4,384	4,340	4,400	4,360	4,320	4,560
VEHICLE SPEED						
Impact (mph)	47	46	60	61	61	62
Exit (mph)	38	35	39	47	48	39
Change (mph)	9	11	21	14	13	23
VEHICLE ANGLE						
Impact (deg)	25	25	25	25	25	25
Exit (deg)	15	15	11	11	15	9
VEHICLE REBOUND DISTANCE (ft)	72	20	20	20	20	20
VEHICLE DAMAGE (TAD LFQ)	3 (moderate)	3 (moderate)	6 1/2 (major)	4 1/2 (moderate)	4 (moderate)	7 (extensive)
TRAFFIC BARRIER						
Impact Post Location	Bet. 2&3	Bet. 2&3	Bet. 2&3	Bet. 2&3	4	Bet. 2&3
Max. Dynamic Deflection (in)	4	9	14	10	17	10
Max. Permanent Set (in)	2½	6	10	7½	11	6
Snagging	None	None	Moderate	None	None	Severe
OCCUPANT RISK (NCHRP 230)						
Lateral Impact Velocity (fps)	12 <sup>b</sup>	12 <sup>b</sup>	21	19	17	24
Ridedown Accelerations (g)	-	-	10	10	8	6
OCCUPANT RISK (NCHRP 86)						
Injury Accident Probability	18	18	86	41	33	100

Notes: (a) Soil Frozen to Depth of 8 to 10 in.

(b) Estimated . . . See Figure 37

TABLE 18

NCHRP 230 SAFETY EVALUATION GUIDELINES  
 Appurtenance . . . . Longitudinal Barrier  
 Test Designation . . . . No. 30 (Transition)

Evaluation Factor	Evaluation Criteria	TRANSITION DESIGN <sup>(1)</sup>					
		Tubular Thrie Beam (Test 1)	Single Thrie Beam (Test 2)	Single Thrie Beam (Test 3)	Double Thrie Beam (Test 4)	Double Thrie Beam (Test 5)	Double Safety Beam (Test 6)
Impact Conditions	58 to 60 mph/25 deg	U	U	S	S	S	S
Structural	A. Test article shall <u>smoothly</u> redirect the vehicle.	S	S	U	S	S	U
	The vehicle shall not penetrate or go over the installation although controlled lateral deflection of the test article is acceptable.	S	S	S	S	S	S
	D. Detached elements, fragments or other debris from the test article shall not penetrate or show potential for penetrating the passenger compartment or present undue hazard to other traffic.	S	S	S	S	S	S
Occupant Risk	E. The vehicle shall remain upright during and after collision although moderate roll, pitching and yawing are acceptable.	S	S	S	S	S	S
	Integrity of the passenger compartment must be maintained with essentially no deformation or intrusion.	S	S	M	S	S	M
Vehicle Trajectory	H. After collision, the vehicle trajectory and final stopping position shall intrude a minimum distance, if at all, into adjacent traffic lanes.	U	U	U	U	U	U
	I. In test where the vehicle is judged to be re-directed into or stopped while in adjacent traffic lanes, vehicle speed change during test article collision should be less than 15 mph and the exit angle from the test article should be less than 60 percent of test impact angle, both measured at time of vehicle loss of contact with test device.	S	S	U	S	S	U

In Test No. 3 on the Single Thrie Beam transition, a moderate amount of vehicle snagging occurred in the lower half of the thrie beam adjacent to the tapered end of the concrete bridgerail. As a result, the test was considered to be unsatisfactory because the vehicle change-in-speed of 21 mph was significantly higher than the limit of 15 mph specified in NCHRP 230. Due to vehicle snagging on the Single Thrie Beam transition, a decision was made by the NDR to run the next test on a Double Thrie Beam transition in favor of the much stronger and costly Tubular Thrie Beam transition that was used earlier in the study.

In Test No. 6 on the Double W-Beam transition, an extensive amount of vehicle snagging occurred under the guardrail on the tapered end of the concrete bridgerail. As a result, the test was considered to be unsatisfactory because the vehicle change-in-speed of 23 mph greatly exceeded the limit of 15 mph specified in NCHRP 230. In addition, the integrity of the passenger compartment area in terms of occupant risk (Item E) was considered to be marginal as the engine firewall was pushed backward on the side of the driver. The last item of concern was the soil that was frozen to a depth of 5 to 6 in. It is predicted that if the soil had not been frozen that the vehicle would have penetrated deeper under the flexible guardrail, and as a result, the vehicle would most-likely have been abruptly stopped and spunout on the tapered end of the concrete bridgerail.

From an overall consideration, the Double Thrie Beam transition in Test Nos. 4 and 5 was satisfactory in terms of the NCHRP 230

performance categories of structural adequacy (Items A and D), occupant risk (Item E), and vehicle trajectory (Item I). Two tests were conducted at different points of impact to be certain that the transition design was tested under the most critical condition of impact. Also, in Test No. 5 the soil was saturated from a heavy 2 day storm preceding the day of the test. The decision to test under a saturated soil condition was made by the NDR as this condition would be representative of the lowest possible soil shearing strength.

In NCHRP 230, it is to be noted that no evaluation guidelines are specified for conducting tests on a guardrail transition in regard to the "Impact Velocity of a Hypothetical Front Seat Passenger Against the Vehicle Interior". However, data on occupant impact velocity was presented in this study because it was felt that the data provided further insight into the evaluation of the transition designs tested. To supplement the NCHRP 230 data on occupant impact velocity, data on "Injury Accident Probability" contained in NCHRP 86 (8) was also presented in this study. The two sets of data on the tests are presented in Table 17, and a graphical relationship between the two sets of data is presented in Figure 37. An occupant impact velocity of 20 fps is recommended in NCHRP 230 as an "acceptable" design value, whereas, a value of 30 fps is a recommended design "limit". The effects of vehicle snagging are very evident in Figure 37.

In Test No. 6, severe snagging on the Double W-Beam transition would result in an injury accident probability of 100%; whereas, in

Test No. 3, moderate snagging on the Single Thrie Beam transition would result in an injury accident probability of 86%. In Test Nos. 4 and 5, an impact with the Double Thrie Beam transition in which no snagging occurred would result in an injury accident probability of 35 to 40%. Lastly, in Test Nos. 1 and 2 at a lower impact speed of 47 mph, an impact into either the Single Thrie Beam transition or the Tubular Thrie Beam transition in which no snagging occurred would result in an injury accident probability of about 20%.

In summary, the following conclusions were reached in regard to the overall performance of the four new guardrail-bridgerail transition designs in restraining and smoothly redirecting a large size 4,500 lb. automobile under the impact conditions of 60 mph and 25 deg.

1. Tubular Thrie Beam Transition . . . . . Satisfactory
2. Single Thrie Beam Transition . . . . . Unsatisfactory
3. Double Thrie Beam Transition . . . . . Satisfactory
4. Double W-Beam Transition . . . . . Unsatisfactory

It is to be emphasized that the above conclusions are based on the condition that a new design in the field will be constructed to the same exact design details under which the full-scale vehicle crash tests were conducted. In particular careful attention must be given to insure that: (1) the soil has the properties of a type "CL" soil, (2) the wood posts are of the proper size, spacing and clear of knots, (3) the 4:1 tapered-end is installed to the dimensions



tested, and (4) the size and quantity of rebar in the concrete bridge end are adequate to carry a lateral impact load of 120 kips and a longitudinal load of 50 kips.

IV  
REFERENCES

1. AASHTO, "Guide for Selecting, Locating, and Designing Traffic Barriers", American Association of State Highway and Transportation Officials, 1977.
2. Hinch, J., Yang, T-L, and Owings, R., "Guidance Systems for Vehicle Testing", ENSCO Inc., Springfield, VA, 1986.
3. NCHRP Report 230, "Recommended Procedures for the Safety Performance Evaluation of Highway Appurtenances", National Cooperative Highway Research Program Report, Transportation Research Board, March 1981.
4. McDevitt, C.F., Structural Research Engineer, Federal Highway Administration, Office of Research, Fairbank Highway Research Station, Washington, D.C. 20590.
5. Powell, G.H. "BARRIER VII: A Computer Program for Evaluation of Automobile Barrier Systems", Report No. FHWA-RD-73-51, Final Report, April 1973.
6. AASHTO, "Standard Specifications for Highway Bridges", American Association of State Highway and Transportation Officials, Sect. 1.1.8-Railings, 12th. Edition, 1977.
7. National Safety Council, "Vehicle Damage Scale for Traffic Accident Investigators", TAD Project Technical Bulletin No. 1, 1971.
8. Olson, R.M., Post, E.R., and McFarland, W.F., "Tentative Service Requirements for Bridge Rail Systems", National Cooperative Highway Research Board, NCHRP 86, 1970.

## APPENDICIES

APPENDIX A  
SOIL TESTS

DATE August 19, 1986  
TO Richard Ruby  
FROM Kenneth Cheney  
THRU  
SUBJECT Guard Rail Post Backfill

A bag of material used for backfill around guard rail posts was submitted to Materials and Tests. Tests performed were moisture-density and unconfined compression to determine shear strength.

The results are listed below.

Moisture - Density Tests  
Maximum dry density 1.71 gm/cc  
Optimum Moisture 17.9%

Unconfined Compression Test

Moisture %	Dry Density gm/cc	Shear Strength P.S.F.
16.6	1.76	3575
18.8	1.70	1900
20.6	1.66	1230

A shear strength of 1900 P.S.F. would best represent maximum density-optimum moisture condition.

The moisture content around the guard rail post was 21.0% on August 13, 1986 which may have been affected by recent rains.

  
Kenneth Cheney  
Soils and Aggregates Engineer

KC/pr

xc: W. Ramsey





# GEOTECHNICAL SERVICES, INC.

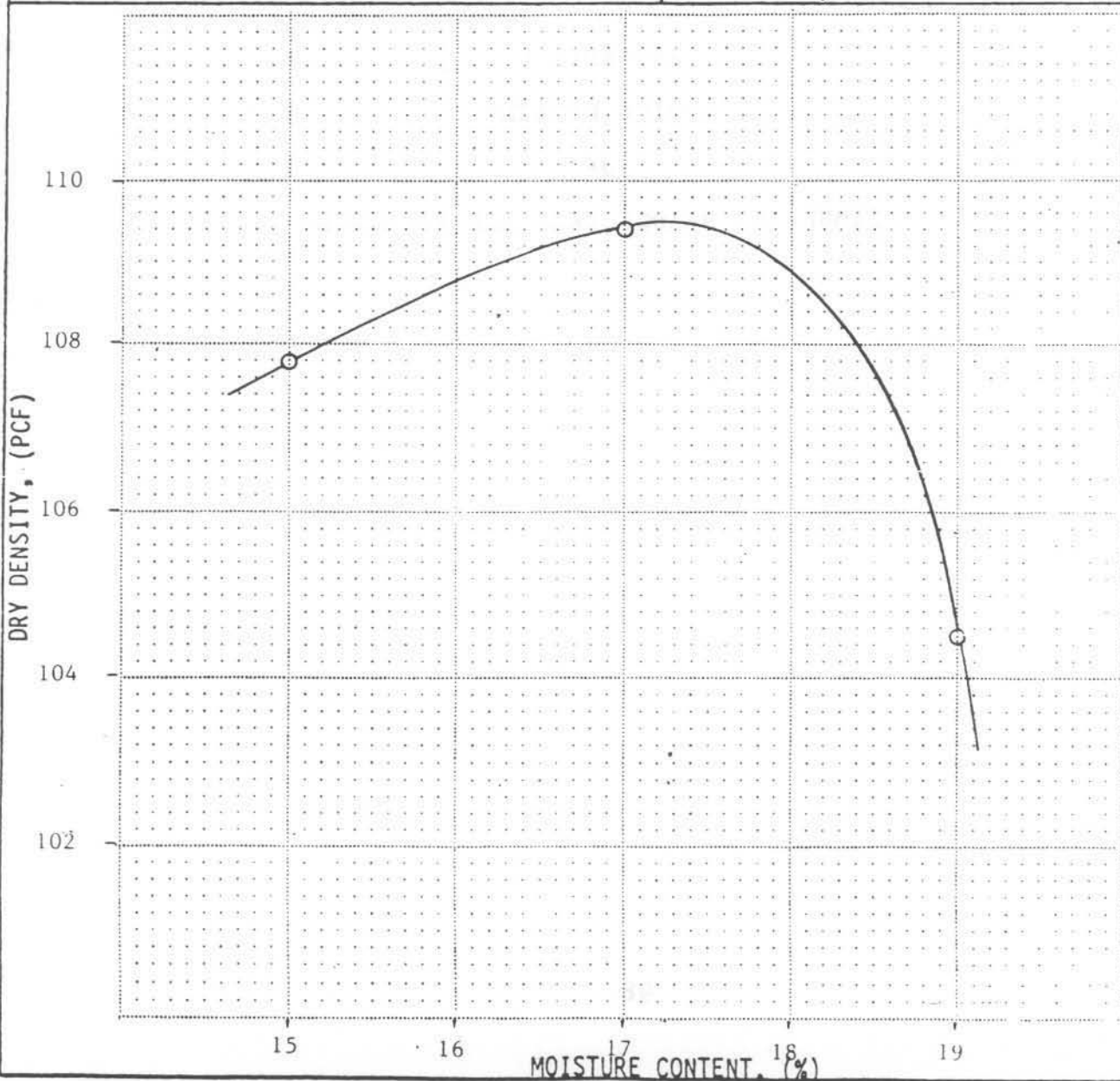


Soil and Foundation Consultants

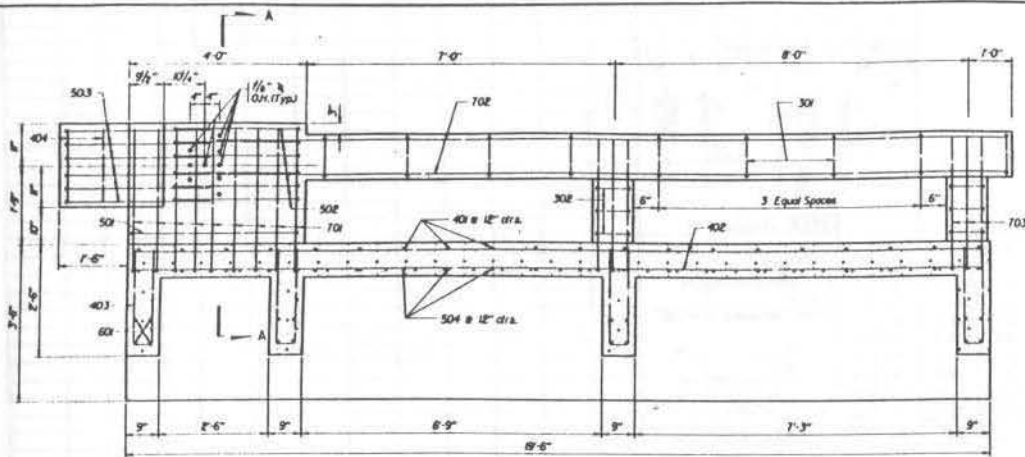
OMAHA, LINCOLN &  
GRAND ISLAND, NEBRASKA  
SALINA, KANSAS

## MOISTURE - DENSITY RELATIONSHIP REPORT

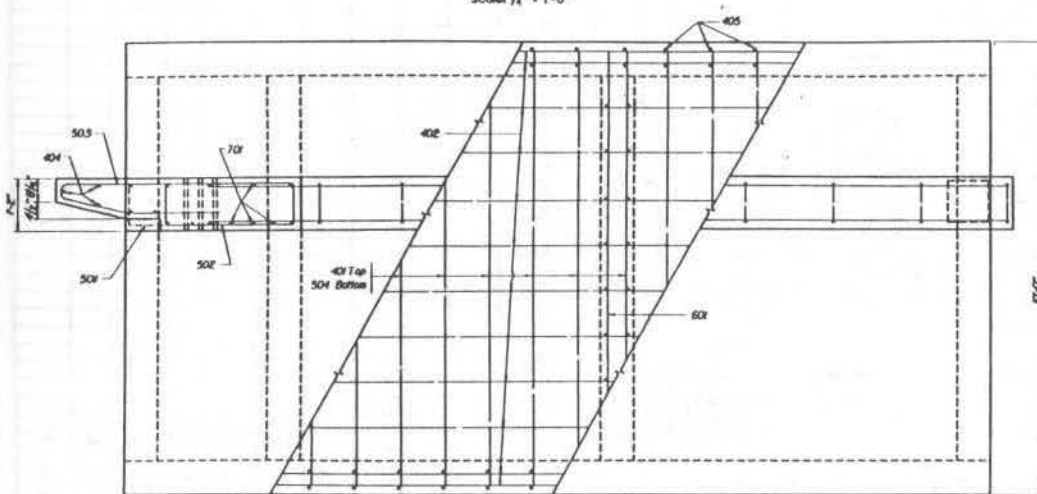
TYPE OF TEST ASTM D 698 Method "A"		OPTIMUM DRY DENSITY (pcf) 109.5		OPTIMUM WATER CONTENT (%) 17.3	
JOB NO. 335AL14	LAB NO. A-333	DATE TESTED 11/6/86	SUBMITTED BY: Wm. C. Arneson, P.E. <i>Wm. C. Arneson</i>		
LOCATION SAMPLED Base of Guard Rail Post			SAMPLE NO. MB02-126	SAMPLE DEPTH 0-3'	
SOIL DESCRIPTION Brown Black Silty Clay			ATTERBERG LIMITS LL 31 PL 20 PI 11	SOIL CLASSIFICATION CL	
PROJECT Barrier Crash Site			ARCHITECT/ENGINEER/CONTRACTOR Dr. Post-College of Engineering Science and Technologies		
LOCATION OF PROJECT Air Park, Lincoln, Nebraska			OWNER University of Nebraska-Lincoln		



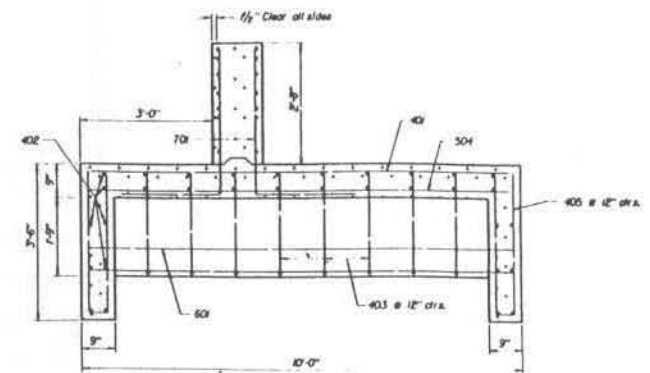
APPENDIX B  
DESIGN DETAILS  
OF  
SIMULATED BRIDGE DECK AND RAILINGS



ELEVATION  
Scale  $\frac{1}{4}'' = 1'-0''$



PLAN  
Scale  $\frac{1}{4}'' = 1'-0''$



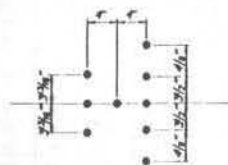
SECTION A-A  
Scale  $\frac{1}{4}'' = 1'-0''$

#### NOTES

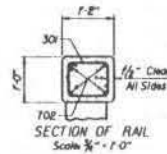
Concrete for slab and rail shall be Class "4780" with a minimum 28-day strength of 3,500 psi and a working stress of 1,400 psi.  
All reinforcing steel shall conform to the requirements of ASTM A-615 or ASTM A-617, Grade 60 steel, with a working stress of 24,000 psi.  
The minimum clearance, measured from the face of the concrete to the surface of any reinforcing bar, shall be 2", except where otherwise noted.

#### QUANTITIES

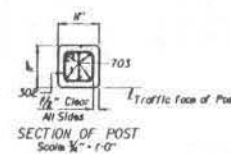
CLASS "4780" CONCRETE	8.3	Cu/Yd.
REINFORCING STEEL	1800	Lbs.



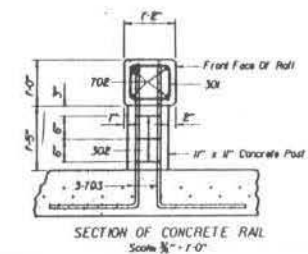
BOLT HOLE PATTERN



SECTION OF RAIL  
Scale  $\frac{1}{4}'' = 1'-0''$



SECTION OF POST  
Scale  $\frac{1}{4}'' = 1'-0''$



SECTION OF CONCRETE RAIL  
Scale  $\frac{1}{4}'' = 1'-0''$

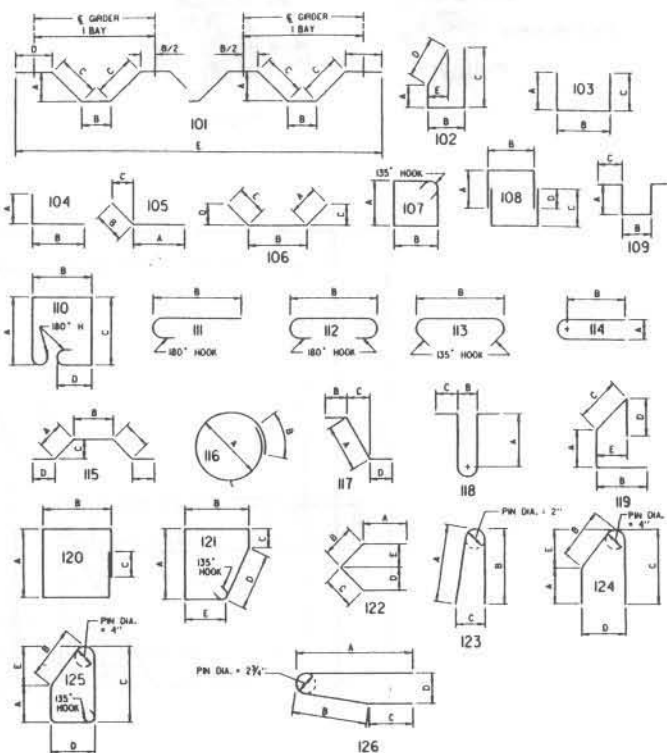
## B I L L O F B A R S

[illegible]

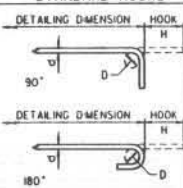
## BENDING DIAGRAMS

ALL DIMENSIONS ARE OUT TO OUT

NOT TO SCALE



## STANDARD HOOKS



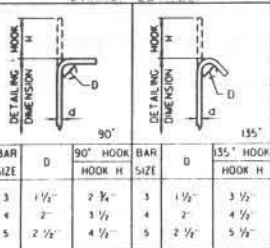
(PRIMARY STRESS BARS)

BAR SIZE	D	90° HOOK	180° HOOK
		HOOK H	HOOK H
4	3"	6 3/4"	6"
5	5 3/8"	8 1/2"	7"
6	4 1/2"	10 1/4"	8 1/2"
7	5 1/4"	12 0"	9 3/4"
8	6"	14 1/4"	11"
9	9"	17 0"	13 3/4"
10	10 1/2"	19 6"	15 4 3/4"
11	11 1/4"	21 8"	17 6 1/2"

## BAR SETS

[illegible]

## STIRRUP DETAILS



The barrier VII computer model simulations were used to determine the effect of barrier VII on the rate of reaction between the reactants and the products. The results of the simulations are shown in Figure 1. The rate of reaction was found to be significantly lower in the presence of barrier VII than in its absence. This is due to the fact that barrier VII acts as a physical barrier to the reaction, preventing the reactants from coming into contact with each other. The rate of reaction was also found to be lower in the presence of barrier VII than in the presence of barrier VI. This is due to the fact that barrier VII is a higher energy barrier than barrier VI, and therefore it is more difficult for the reactants to overcome it.

## APPENDIX C

### BARRIER VII COMPUTER MODEL SIMULATIONS

The barrier VII computer model simulations were used to determine the effect of barrier VII on the rate of reaction between the reactants and the products. The results of the simulations are shown in Figure 1. The rate of reaction was found to be significantly lower in the presence of barrier VII than in its absence. This is due to the fact that barrier VII acts as a physical barrier to the reaction, preventing the reactants from coming into contact with each other. The rate of reaction was also found to be lower in the presence of barrier VII than in the presence of barrier VI. This is due to the fact that barrier VII is a higher energy barrier than barrier VI, and therefore it is more difficult for the reactants to overcome it.

The BARRIER VII computer simulation model developed by Powell (5) was used in this study to determine (1) design impact loading on the end of the concrete bridgerail, and (2) the most critical point-of-impact on the guardrail transition. The "input" data on the vehicle crushing properties and the cohesive soil were obtained from results published by other research agencies. It is to be noted that no attempt was made to "fine tune" or calibrate the model after the full-scale testing was underway because the results on the dynamic deflections in Test No. 1 were in good agreement with the model.

The traffic barrier was idealized as a plane framework composed of inelastic one-dimensional elements of a variety of types. The automobile was idealized as a plane rigid body surrounded by a cushion of springs. A large-displacement dynamic structural analysis problem was solved by numerical methods.

The analysis is two-dimensional in the horizontal plane. Out-of-plane effects, which include vertical displacements of both the automobile and the barrier, are not considered. The automobile slides along the barrier, and the effects of normal force, friction forces, and wheel drag forces are considered in determining its motion. The necessary input data consist of the barrier configuration, the properties of the barrier members and the automobile, and the velocity and trajectory of the automobile before impact. Output consists of barrier member forces, barrier deflections, time histories of automobile positions, and velocities and accelerations of the automobile.

A final comment should be made about the BARRIER VII program. It is a two-dimensional program and it therefore has limitations. BARRIER VII cannot predict the roll motion of the vehicle, wheel snagging, or vehicle vaulting, nor will it predict situations in which the vehicle could break through the guardrail.



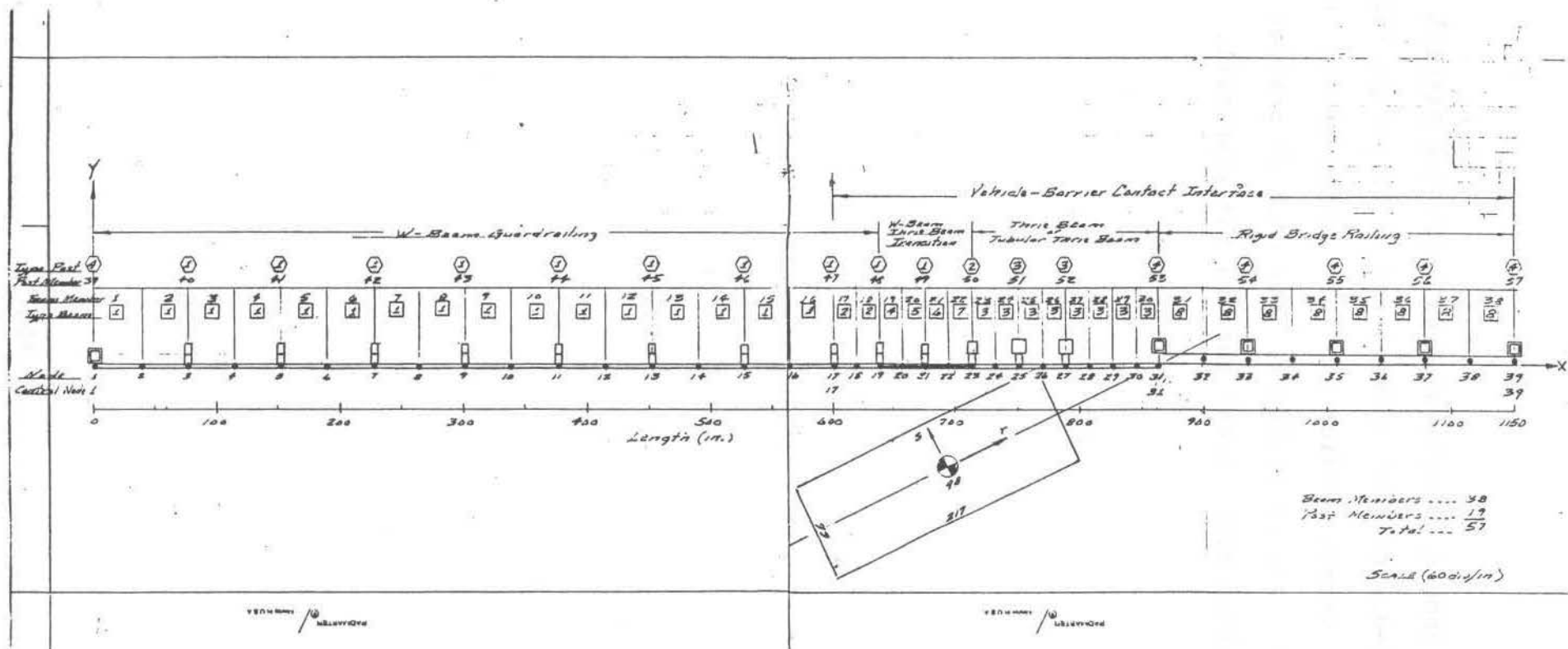


Figure C1  
TRAFFIC BARRIER SETUP

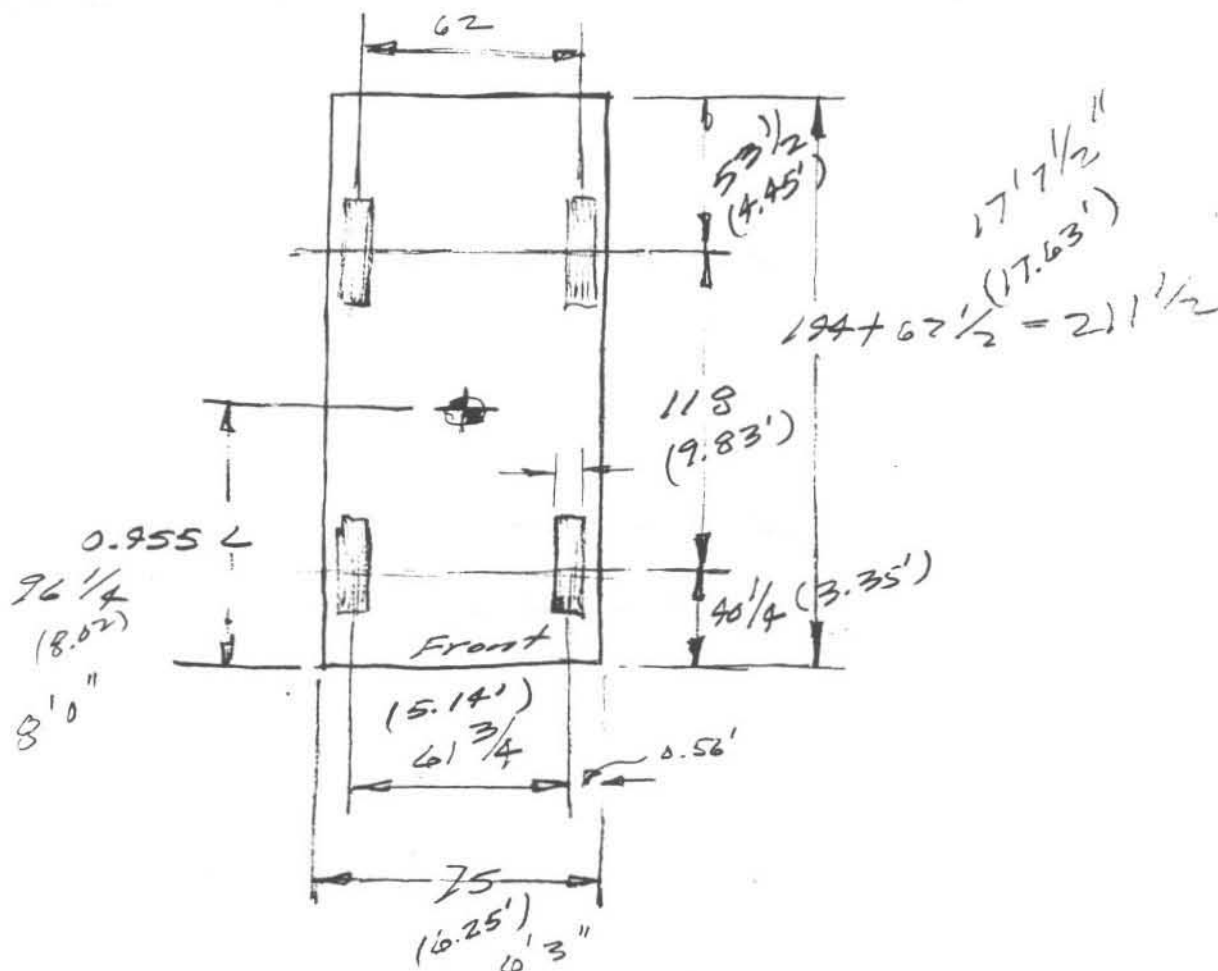
ER PET

2/3)

HP & R 86-52

CRASH  
VEHICLES

1. Vehicle Dimensions



$$W_t = 4,100 \text{ lb}$$

2. Vehicle Yaw Moment-of-Inertia

$$\begin{aligned} I_{zz}^{cgt} &= (1.26 W_t - 1750) 12 \\ &= [1.26 (4100) - 1750] 12 \\ &= 40,992 \text{ in-lb-sec}^2 \end{aligned}$$

3. Weight Distribution

$$2W_F (118") = W_t (62")$$

$$W_F = \frac{4100 \text{ lb} (62")}{2 (118")} = 1,077.1 \text{ lb}$$

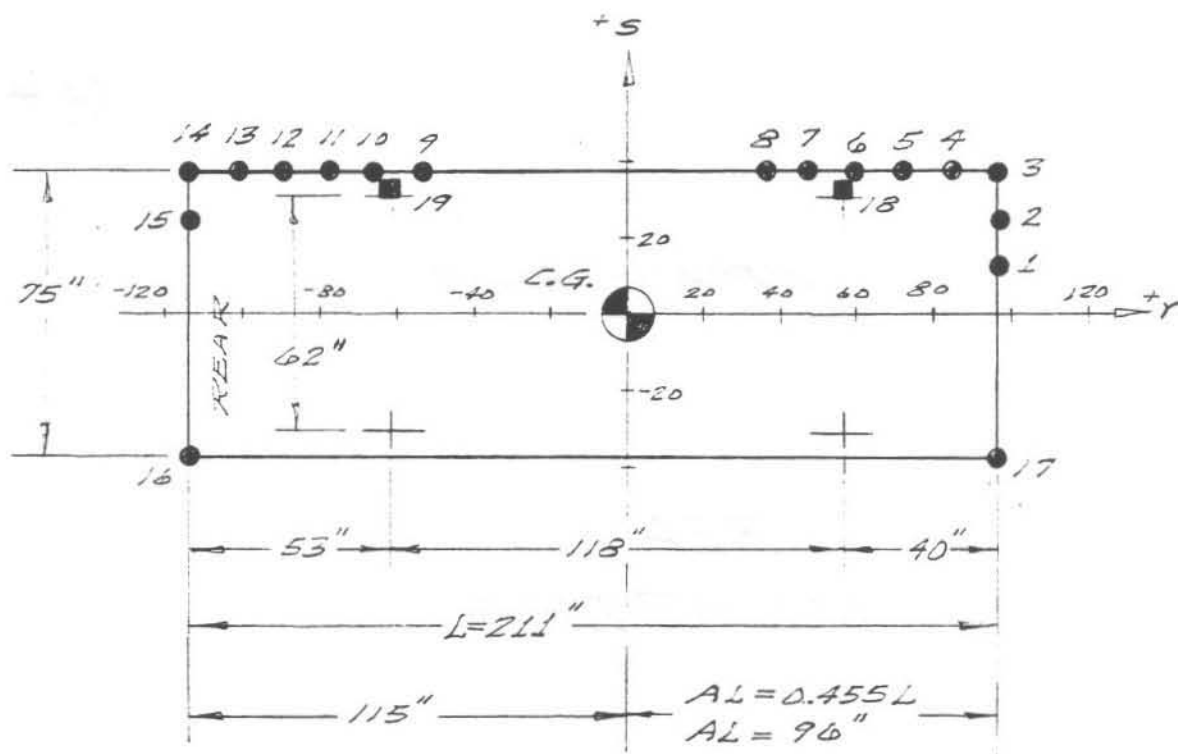
$$2W_R = 4100 - 2(1077.1)$$

$$W_R = 972.9 \text{ lb}$$

AUTOMOBILE  
1937 Plymouth Fury

(33)

## 3. Contact Points



SCALE 50 div./in

Contact Point No.	Coordinates		Stiffnesses			Deflection Before Bottoming (in.)	Length (in.)
	r (in.)	s (in.)	Before Bottoming (K/in/in)	After Bottoming (K/in/in)	Unloading (K/in/in)		
1	96.0	13.5	0.04	0.24	0.33	15.0	12.0
2	96.0	25.5					12.0
3	96.0	37.5					12.0
4	84.0	37.5					12.0
5	72.0	37.5					12.0
6	60.0	37.5					12.0
7	48.0	37.5					12.0
8	36.0	37.5					12.0
9	-55.0	37.5					12.0
10	-67.0	37.5					12.0
11	-79.0	37.5					12.0
12	-91.0	37.5					12.0
13	-103.0	37.5					12.0
14	-115.0	37.5					12.0
15	-115.0	25.5					12.0
16	-115.0	-37.5					1.0
17	96.0	-37.5					1.0
Wire Wheel Hubs (Unit #2)							
18	56.0	33.0	1.00	2.00	1.50	10.0	1.0
19	-62.0	33.0	1.00	2.00	1.50		1.0

E. R. Post

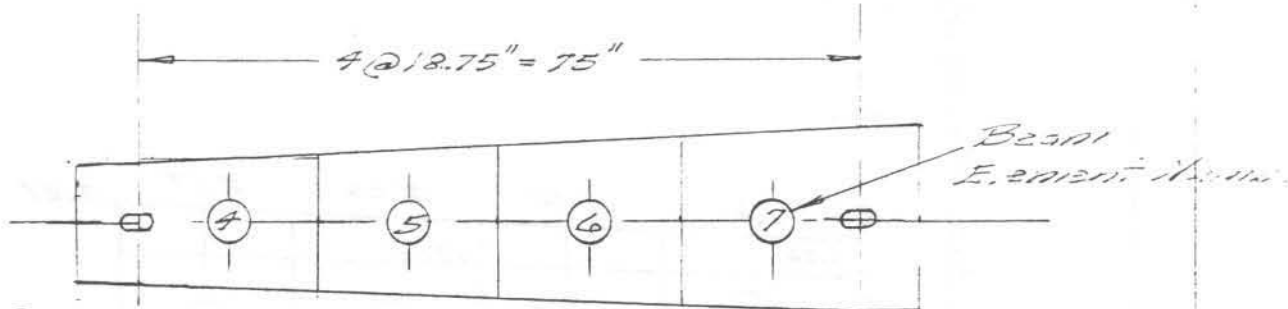
27 Apr 85

(14)

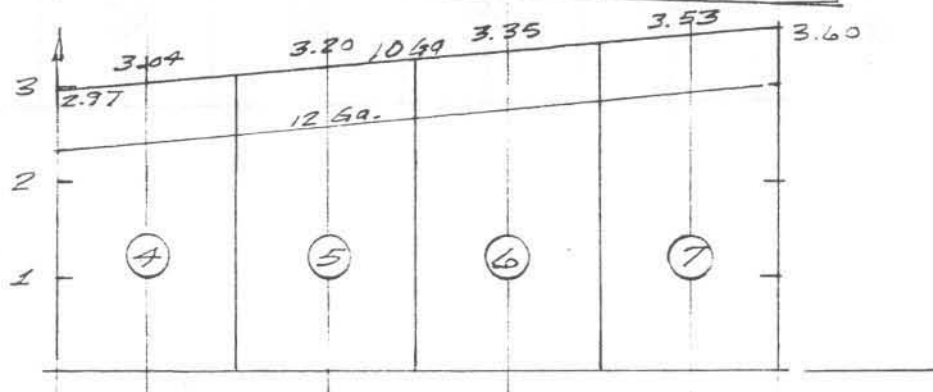
HP&R 86-2

BEAM  
MEMBERS

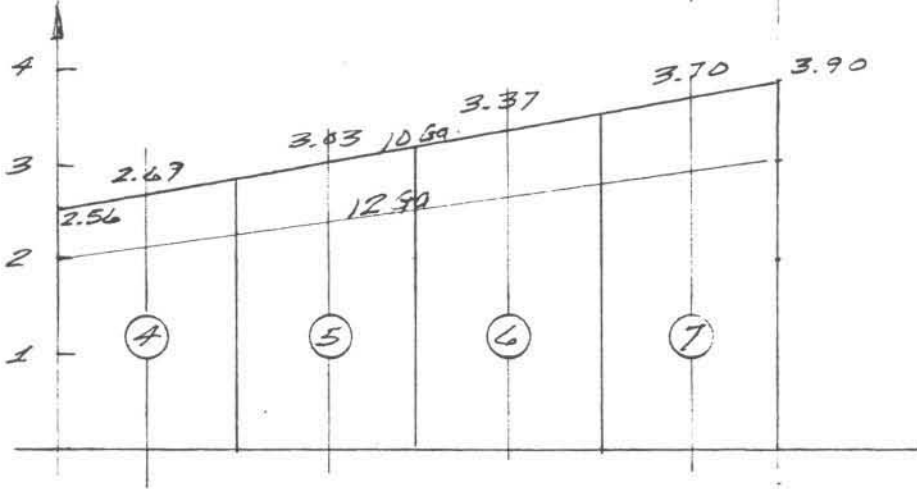
1. TAPIE BEAM TRANSITION (10 GA.)



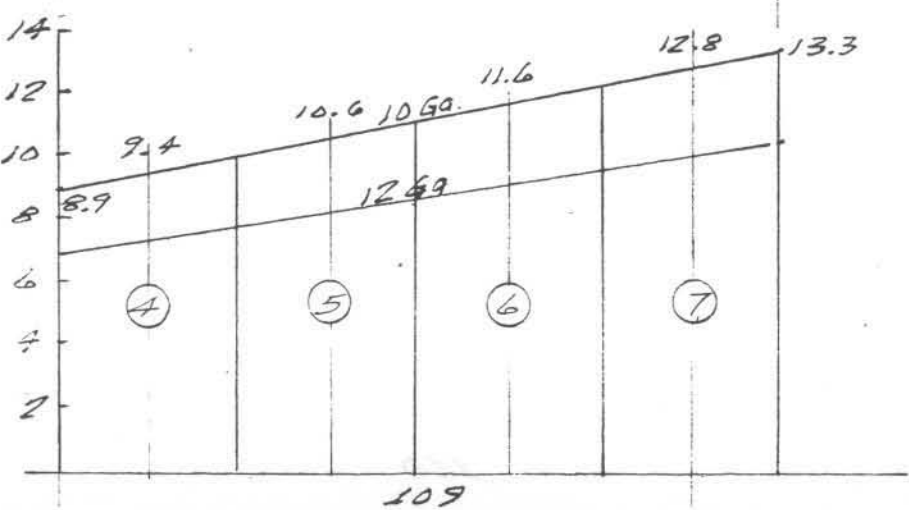
$I$   
Moment of Inertia ( $in^4$ )



$A$   
Area ( $in^2$ )

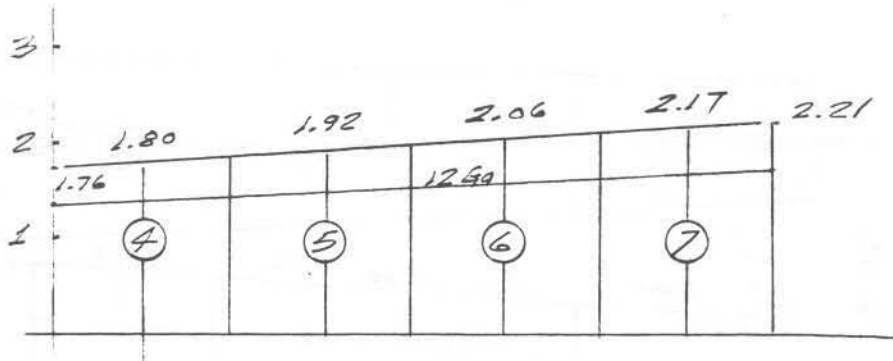


$W$   
Weight (lb)



1. Time Brn. Transition (10 Gs)

Section Mass. 25 (10 Gs)





(7/7)

$$I_{\text{rotular}} = 2 \left\{ I_{yy} + A d^2 \right\}$$

$$23.35 = 2 \left\{ 3.60 + 3.9 d^2 \right\}$$

$$2(3.9)d^2 = 16.15$$

$$d = 1.44 \text{ in.}$$

$$I_{1240} = 2 \left\{ 2.87 + 3.0 (1.44)^2 \right\}$$

$$= 18.22$$

$$S_{1240} = \frac{18.22}{3.25} =$$

E. K. Post

29 Apr 33

(4/3)

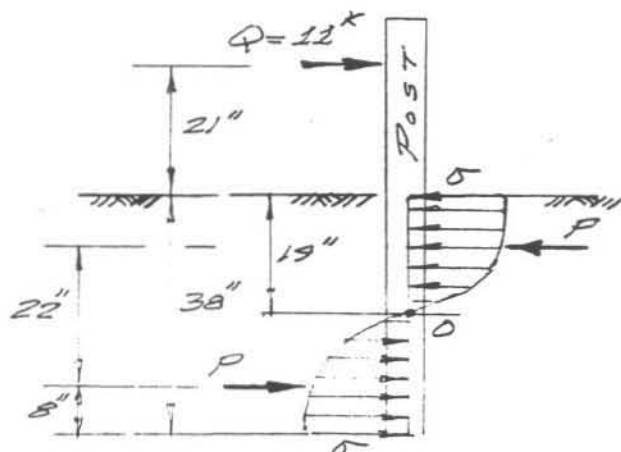
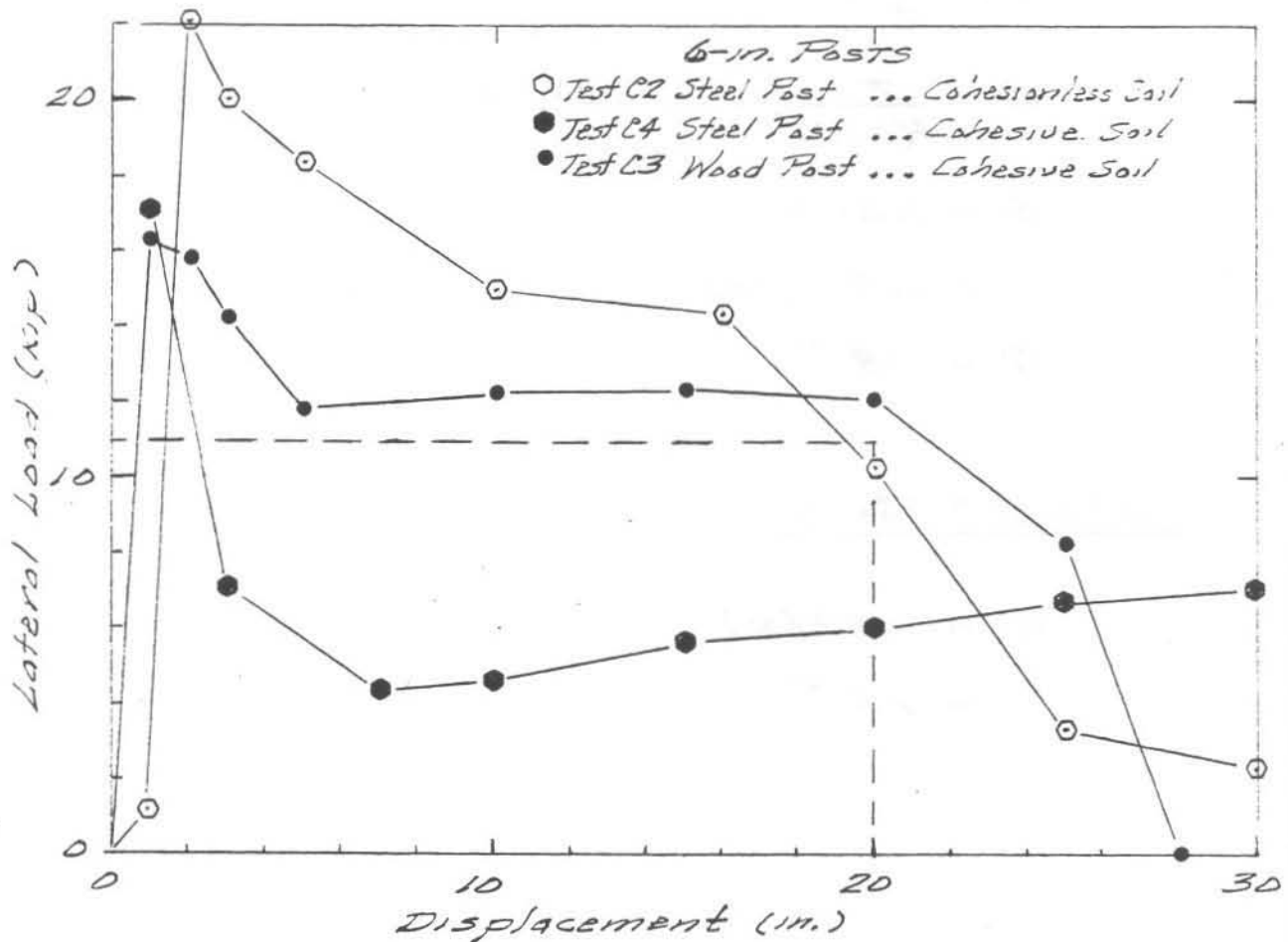
HP&R 86-2

POST  
MEMBERS

DYNAMIC TESTS  
ON  
GUARDRAIL POSTS

(2, 4)

(TTI...TRR 970)



$$\Sigma M = 0 \quad P = \left( \frac{40}{22} \right) Q = 1.82 Q$$

also,

$$P = \frac{\pi}{4} (19)(\sigma)(6)$$

$$= \frac{\pi}{4} (19)(6) \sigma$$

$$P = 89.5 \sigma$$

thus,

$$\sigma = \frac{1.82 Q}{89.5} = \frac{1.82 (12)}{89.5}$$

$$\sigma = 0.224 \text{ ksi}$$

Ellipsoidal Pressure  
Distribution  
(2014)

(2'4)

10" x 10" Posts

$$1.82 Q = \frac{\pi}{4} (19)(6)(5)$$

$$Q = \frac{\pi}{4(1.82)} (19)(0.224) 6$$

$$Q = 1.84 6$$

$$= 1.84 (10)$$

$$Q = 18^*$$

8" x 8" Posts

$$Q = 1.84(8)$$

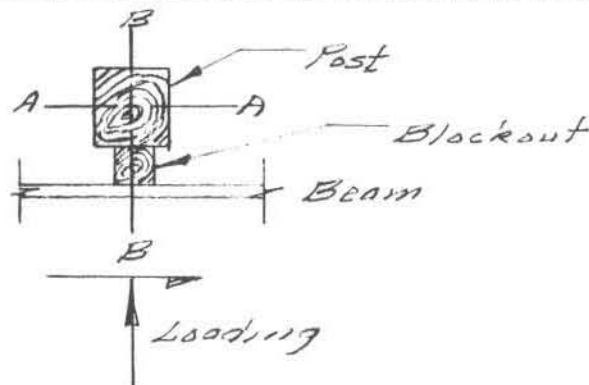
$$= 15^*$$

E.R. Post

29 Apr '86  
 (3/4)

# POST MEMBERS

Post Position	Type No.	Beam Height		Stiffness		Effective Weight (lb)	Base Moment		Yield Accuracy	Shear Force <sup>1</sup>		Deflection	
		Node 1 (in)	Node 2 (in)	A-axis (K/in)	B-axis (K/in)		B-axis (K-in)	A-axis (K-in)		A-axis (K)	B-axis (K)	A-axis (in)	B-axis (in)
Approach GR End (stiff) <sup>2</sup>	1	21.0	0.0	2955.0	2955.0	200.0	2670.0	2670.0	0.10	127.0	127.0	1.0	1.0
	2			15.0	11.0	50.0	315.0	231.0		18.8	13.8	20.0	20.0
	3			15.0	15.0	77.0	315.0	315.0		18.8	18.8	20.0	20.0
	4			18.0	18.0	121.0	378.0	378.0		22.5	22.5	20.0	20.0
Bridge (stiff) <sup>2</sup>	1			2955.0	2955.0	200.0	2670.0	2670.0		127.0	127.0	1.0	1.0



## Notes

1. Shear values increased 25% above yield in order to suppress post failure in shear at base

2. Effective Weights

$$W_2 = (0.022 \text{ pci} \times 6") \times (3") \times (47") = 50.0 \text{ lbs}$$

$$W_3 = (0.022 \times 8") \times (8") \times (47+8") = 77.0 \text{ lbs}$$

$$W_4 = (0.022 \times 10) \times (10) \times (47+8) = 121.0 \text{ lbs}$$

3. Stiff Posts (End GR & Bridge)

$$TS \ 10 \times 10 \times 0.6250$$

$$M_p = \sigma_y (1.22 S_x) = 36 (1.22 \times 60.7) = 2,670 \text{ K-in.}$$

$$P_u = \frac{M_p}{L} = \frac{2,670}{21} = 127 \text{ K}$$

$$K = \frac{P}{\Delta} = \frac{3EI}{L^3} = \frac{3(30 \times 10^6) \times (30.7)}{(21)^3} = 2,954,325 \text{ lb/in}$$

$$W_4 = 74 \text{ lb} (2.7 \text{ ft}) = 200.0 \text{ lb}$$

INPUT  
DATA

1BARRIER VII - ANALYSIS OF AUTOMOBILE BARRIERS - U.C. BERKELEY, 1972

\*\*\*\*\*

UNL RUN NO. 2E 12 GA. TUBULAR THRIE BEAM GUARDRAIL TRANSITION

\*\*\*\*\*

CONTROL INFORMATION

NUMBER OF BARRIER NODES = 39  
 NUMBER OF CONTROL NODES = 4  
 NUMBER OF NODE GENERATIONS = 3  
 NUMBER OF INTERFACES = 1  
 NUMBER OF MEMBERS = 57  
 NUMBER OF MEMBER GENERATIONS = 14  
 NUMBER OF DIFFERENT MEMBER SERIES = 2  
 NUMBER OF ADDITIONAL WEIGHT SETS = 0  
 BASIC TIME STEP (SEC) = .00250  
 LARGEST ALLOWABLE TIME STEP (SEC) = .00250  
 MAXIMUM TIME SPECIFIED (SEC) = .60000  
 MAX. NO. OF STEPS WITH NO CONTACT = 50  
 OVERSHOOT INDEX = 0  
 ROTATIONAL DAMPING MULTIPLIER = 1.00  
 STEP-BY-STEP INTEGRATION TYPE = 1

OUTPUT FREQUENCIES

AUTOMOBILE DATA = 5  
 BARRIER DEFLECTIONS = 5  
 BARRIER FORCES = 5

ENERGY BALANCE = 5

CONTACT INFORMATION = 5

PUNCHED JOINT DATA = 0

PUNCHED TRAJECTORY = 0

CONTROL NODE COORDINATES (IN)

NODE	X-ORD	Y-ORD
1	.00	.00
17	500.00	.00
31	802.50	.00
39	1150.50	.00

COORDINATE GENERATION COMMANDS

FIRST NODE	LAST NODE	NO. OF NODES	NODE DIFF	DISTANCE
---------------	--------------	-----------------	--------------	----------





YOUNGS MODULUS (KSI)										WEIGHT (LB/FT)										YIELD FORCE (K)										YIELD MOMENT (K.IN)										YIELD ACCURACY LIMIT																			
.300E+05										.300E+05										.300E+05										.300E+05										.300E+05																			
.692E+01										.692E+01										.207E+02										.730E+01										.820E+01										.900E+01									
.995E+02										.995E+02										.300E+03										.106E+03										.120E+03										.134E+03									
.685E+02										.685E+02										.280E+03										.650E+02										.750E+02										.785E+02									
.100E+00										.100E+00										.100E+00										.100E+00										.100E+00										.100E+00									
9 1 21.0										.0 15.0 11.0 50.0										315.0 231.0										.1 18.8										13.8 20.0										20.0									
10 2 21.0										.0 15.0 15.0 77.0										315.0 315.0										.1 18.8										18.8 20.0										20.0									
11 3 21.0										.0 18.0 18.0 121.0										378.0 378.0										.1 22.5										22.5 20.0										20.0									
12 4 21.0										.02955.02955.0200.0										2670.0 2670.0										.1 127.0										127.0 1.0										1.0									

1POSTS, 300 SERIES

TYPE NUMBER										HEIGHT OF NODE I (IN)										HEIGHT OF NODE J (IN)										A AXIS STIFFNESS (K/IN)										B AXIS STIFFNESS (K/IN)										EFFECTIVE WEIGHT (LB)										B AXIS YIELD MOMENT (K.IN)										A AXIS YIELD MOMENT (K.IN)										YIELD ACCURACY LIMIT										A SHEAR AT FAILURE (K)										B SHEAR AT FAILURE (K)										A DEFLN AT FAILURE (IN)										B DEFLN AT FAILURE (IN)									
1										2										3										4										5										6										7										8										9										10																																							
.210E+02										.210E+02										.210E+02										.210E+02										.210E+02										.210E+02										.210E+02										.210E+02										.210E+02										.210E+02																																							
.750E+02										.750E+02										.750E+02										.750E+02										.750E+02										.750E+02										.750E+02										.750E+02										.750E+02																																																	
.411E+04										.411E+04										.411E+04										.411E+04										.411E+04										.411E+04										.411E+04										.411E+04										.411E+04																																																	
.384E+04										.384E+04										.384E+04										.384E+04										.384E+04										.384E+04										.384E+04										.384E+04										.384E+04																																																	
.820E+01										.820E+01										.820E+01										.820E+01										.820E+01										.820E+01										.820E+01										.820E+01										.820E+01																																																	
.120E+03										.120E+03										.120E+03										.120E+03										.120E+03										.120E+03										.120E+03										.120E+03										.120E+03																																																	
.000E+00										.000E+00										.000E+00										.000E+00										.000E+00										.000E+00										.000E+00										.000E+00										.000E+00																																																	
.100E+00										.100E+00										.100E+00										.100E+00										.100E+00										.100E+00										.100E+00										.100E+00										.100E+00																																																	
.825E+02										.825E+02										.825E+02										.825E+02										.825E+02										.825E+02										.825E+02										.825E+02										.825E+02																																																	
.675E+02										.675E+02										.675E+02										.675E+02										.675E+02										.675E+02										.675E+02										.675E+02										.675E+02																																																	
.000E+00										.000E+00										.000E+00										.000E+00										.000E+00										.000E+00										.000E+00										.000E+00										.000E+00																																																	
.000E+00										.000E+00										.000E+00										.000E+00										.000E+00										.000E+00										.000E+00										.000E+00										.000E+00																																																	

1MEMBER GENERATION COMMANDS

FIRST MEMBER										NODE I										NODE J										LAST MEMBER										NODE DIFF										TYPE NO.										1										2										PRESTRESS DATA										3										4										5									
1										1										2										16										1										101										.000										.000										.000										.000										.000																			
17										17										18										1										102										.000										.000										.000										.000										.000																													
19										19										0										0										104										.000										.000										.000										.000										.000																													
20										20										0										0										105										.000										.000										.000										.000										.000																													
21										21										0										0										106										.000										.000										.000										.000										.000																													
22										22										0										0										107										.000										.000										.000										.000										.000																													
23										23										0										0										108										.000										.000										.000										.000										.000																													
31										31										32										1										103										.000										.000										.000										.000										.000																													
39										39										0										0										304										.000										.000										.000										.000										.000																													
40										40										0										0										301										.000										.000										.000										.000										.000																													
48										48										49										2										301										.000										.000										.000										.000										.000																													
50										50										0										0										302										.000										.000										.000										.000										.000																													
51										51										0										0										303										.000										.000										.000										.000										.000																													
53										53										0										0										304										.000										.000										.000										.000										.000																													

1COMPLETE MEMBER DATA

BEAMS, 100 SERIES										MEMBER										NODE I										NODE J										TYPE										FORCE										I-MOMENT										J-MOMENT									
1										1										2										101										.00										.00										.00																			
2										2										3										101										.00										.00										.00																			
3										3										4										101										.00										.00										.00																			
4										4										5										101										.00										.00										.00																			
5										5										6										101										.00										.00										.00																			
6										6										7										101										.00										.00										.00																			
7										7										8										101										.00										.00										.00																			
8										8										9										101										.00										.00										.00																			
9										9										10										101										.00										.00										.00																			
10										10										11										101										.00										.00										.00																			
11										11										12										101										.00										.00										.00																			
12										12										13										101										.00										.00										.00																			
13										13										14										101										.00										.00										.00																			
14										14										15										101										.00										.00										.00																			
15										15										16										101										.00										.00										.00																			

16	16	17	101	.00	.00	.00
17	17	18	102	.00	.00	.00
18	18	19	102	.00	.00	.00
19	19	20	104	.00	.00	.00
20	20	21	105	.00	.00	.00
21	21	22	106	.00	.00	.00
22	22	23	107	.00	.00	.00
23	23	24	103	.00	.00	.00
24	24	25	103	.00	.00	.00
25	25	26	103	.00	.00	.00
26	26	27	103	.00	.00	.00
27	27	28	103	.00	.00	.00
28	28	29	103	.00	.00	.00
29	29	30	103	.00	.00	.00
30	30	31	103	.00	.00	.00
31	31	32	108	.00	.00	.00
32	32	33	108	.00	.00	.00
33	33	34	108	.00	.00	.00
34	34	35	108	.00	.00	.00
35	35	36	108	.00	.00	.00
36	36	37	108	.00	.00	.00
37	37	38	108	.00	.00	.00
38	38	39	108	.00	.00	.00

## POSTS, 300 SERIES

MEMBER	NODE I	NODE J	TYPE	A-SHEAR	B-SHEAR	B-MOMENT	A-MOMENT	ANGLE
39	1	0	304	.00	.00	.00	.00	.00
40	3	0	301	.00	.00	.00	.00	.00
41	5	0	301	.00	.00	.00	.00	.00
42	7	0	301	.00	.00	.00	.00	.00
43	9	0	301	.00	.00	.00	.00	.00
44	11	0	301	.00	.00	.00	.00	.00
45	13	0	301	.00	.00	.00	.00	.00
46	15	0	301	.00	.00	.00	.00	.00
47	17	0	301	.00	.00	.00	.00	.00
48	19	0	301	.00	.00	.00	.00	.00
49	21	0	301	.00	.00	.00	.00	.00
50	23	0	302	.00	.00	.00	.00	.00
51	25	0	303	.00	.00	.00	.00	.00
52	27	0	303	.00	.00	.00	.00	.00
53	29	0	304	.00	.00	.00	.00	.00
54	33	0	304	.00	.00	.00	.00	.00
55	33	0	304	.00	.00	.00	.00	.00
56	37	0	304	.00	.00	.00	.00	.00
57	39	0	304	.00	.00	.00	.00	.00

## STIFFNESS MATRIX STORAGE

REQUIRED = 702  
 ALLOCATED = 6000  
 1AUTOMOBILE PROPERTIES

WEIGHT (LB) = 4100.0  
 MOMENT OF INERTIA (LB.IN.SEC2) = 40992.0  
 NO. OF CONTACT POINTS = 19  
 NO. OF UNIT STIFFNESSES = 2  
 NO. OF WHEELS = 4  
 BRAKE CODE (1=ON, 0=OFF) = 0  
 NO. OF OUTPUT POINTS = 1

## UNIT STIFFNESSES (K/IN/IN)

NO.	BEFORE BOTTOMING	AFTER BOTTOMING	UNLOADING	BOTTOMING DISTANCE
1	.040	.240	.330	15.00
2	1.000	2.000	1.500	10.00

## CONTACT POINT DATA

POINT	R COORD	S COORD	STIFFNESS NO.	TRIBUTARY LENGTH	INTERFACE CONTACTS			
1	96.00	15.50	1	12.00	1	0	0	0
2	96.00	25.50	1	12.00	1	0	0	0
3	96.00	37.50	1	12.00	1	0	0	0
4	84.00	37.50	1	12.00	1	0	0	0
5	72.00	37.50	1	12.00	1	0	0	0
6	60.00	37.50	1	12.00	1	0	0	0
7	48.00	37.50	1	12.00	1	0	0	0
8	36.00	37.50	1	12.00	1	0	0	0
9	-55.00	37.50	1	12.00	1	0	0	0
10	-67.00	37.50	1	12.00	1	0	0	0
11	-79.00	37.50	1	12.00	1	0	0	0
12	-91.00	37.50	1	12.00	1	0	0	0
13	-103.00	37.50	1	12.00	1	0	0	0
14	-115.00	37.50	1	12.00	1	0	0	0
15	-115.00	25.50	1	12.00	1	0	0	0
16	-115.00	-37.50	1	1.00	0	0	0	0
17	96.00	-37.50	1	1.00	0	0	0	0
18	56.00	33.00	2	1.00	1	0	0	0
19	-62.00	33.00	2	1.00	1	0	0	0

## OWHEEL COORDINATES (IN), STEER ANGLES (DEG), AND DRAG FORCES (LB)

POINT	R-ORD	S-ORD	STEER ANGLE	DRAG FORCE
1	56.00	31.00	.00	430.00
2	56.00	-31.00	.00	430.00
3	-62.00	31.00	.00	390.00
4	-62.00	-31.00	.00	390.00

## OUTPUT POINT COORDINATES (IN)

POINT	R-ORD	S-ORD
-------	-------	-------

1 .00 .00  
INITIAL POSITION AND VELOCITIES OF AUTO

## SPECIFIED BOUNDARY POINT

X ORDINATE OF POINT = 3  
Y ORDINATE OF POINT = 750.00  
= .00

ANGLE FROM X AXIS TO R AXIS (DEG) = 25.00  
VELOCITY IN R DIRECTION (M.P.H) = 60.00

VELOCITY IN S DIRECTION (M.P.H) = .00  
 ANGULAR VELOCITY (RAD/SEC) = .000  
 MINIMUM RESULTANT VELOCITY (M.P.H) = 10.00

TRANSLATIONAL KINETIC ENERGY (K.IN) = 5922.35  
 ROTATIONAL KINETIC ENERGY (K.IN) = .00  
 TOTAL INITIAL KINETIC ENERGY (K.IN) = 5922.35

# AUTO TRAJECTORY RESULTS

PT	X-DRD	Y-DRD	ANGLE	X-VEL	Y-VEL	R-VEL	S-VEL	T-VEL	ANGLE	X-ACC	Y-ACC	R-ACC	S-ACC	T-ACC	ANGLE
TIME = .0000 SECS															
1	678.8	-74.6	25.0	54.38	25.36	60.00	.00	60.00	25.0	.00	.00	.00	.00	.00	.0

# BARRIER DEFLECTIONS, TIME = .0000 SECS

NODE	X-DEFL	Y-DEFL	X-DRD	Y-DRD
1	.00	.00	.0	.0
2	.00	.00	37.5	.00
3	.00	.00	75.0	.00
4	.00	.00	112.5	.00
5	.00	.00	150.0	.00
6	.00	.00	187.5	.00
7	.00	.00	225.0	.00
8	.00	.00	262.5	.00
9	.00	.00	300.0	.00
10	.00	.00	337.5	.00
11	.00	.00	375.0	.00
12	.00	.00	412.5	.00
13	.00	.00	450.0	.00
14	.00	.00	487.5	.00
15	.00	.00	525.0	.00
16	.00	.00	562.5	.00
17	.00	.00	600.0	.00
18	.00	.00	618.8	.00
19	.00	.00	637.5	.00
20	.00	.00	656.3	.00
21	.00	.00	675.0	.00
22	.00	.00	693.8	.00
23	.00	.00	712.5	.00
24	.00	.00	731.3	.00
25	.00	.00	750.0	.00
26	.00	.00	768.8	.00
27	.00	.00	787.5	.00
28	.00	.00	806.2	.00
29	.00	.00	825.0	.00
30	.00	.00	843.7	.00
31	.00	.00	862.5	.00
32	.00	.00	898.5	.00
33	.00	.00	934.5	.00
34	.00	.00	970.5	.00
35	.00	.00	1006.5	.00
36	.00	.00	1042.5	.00
37	.00	.00	1076.5	.00

CRITICAL  
DESIGN LOADING  
FOR  
CONCRETE BRIDGERAIL

Impact Node . . . 28

ENERGY BALANCE, TIME = .0875 SECS

TYPE OF ENERGY PERCENT OF ORIG AUTO KE

TRANSLATIONAL K.E. OF AUTO = 60.2  
 ROTATIONAL K.E. OF AUTO = 2.4  
 BARRIER K.E. = .0

ELASTIC ENERGY IN MEMBERS

BE .0  
 : : : : : 101\ -ZN1E7B?

PO\*\*\*\*\*  
 : : : : : 10M\* ;HN2H7MS

INELASTIC WORK ON MEMBERS

BE .0  
 : : : : : 10Q5K)2N6ZX>N

PO\*\*\*\*\*  
 : : : : : 10K\U4EN0\$#.Z

ELASTIC ENERGY IN AUTO = 7.5  
 INELASTIC WORK ON AUTO = 6.9

DAMPING LOSSES = .1

AUTO-BARRIER FRICTION LOSS = 21.4  
 AUTO-PAVEMENT FRICTION LOSS = .3

SUM OF ALL CONTRIBUTIONS = 101.3

DATA ON AUTO-BARRIER CONTACT, TIME = .0875 SECS

AUTO POINT	CONTACT INTERFACE	CONTACT BETWEEN NODE AND NODE	X COORDINATE	Y COORDINATE	NORMAL FORCE	X FORCE	Y FORCE
1	1	32 31	892.06	.02	2.13	-.77	-2.12
2	1	32 31	877.61	.02	12.36	-4.81	-12.18
3	1	32 31	862.36	.05	46.19	-19.22	-45.01
4	1	31 30	858.61	.54	29.54	-12.27	-28.79
5	1	31 30	854.22	1.13	14.51	-6.01	-14.15
6	1	31 30	849.01	1.84	5.91	-2.44	-5.76
7	1	30 29	842.62	2.53	3.30	-1.34	-3.23
8	1	30 29	834.43	2.45	1.16	-.43	-1.15
18	1	31 30	850.69	1.61	6.69	-2.77	-6.53
						50.06 K	118.95 K

AUTO TRAJECTORY RESULTS

PT	X-ORD	Y-ORD	ANGLE	X-VEL	Y-VEL	R-VEL	S-VEL	T-VEL	ANGLE	X-ACC	Y-ACC	R-ACC	S-ACC	T-ACC	ANGLE
TIME = .1000 SECS															
1	825.4	-42.9	19.2	43.10	-2.11	40.00	-16.19	43.15	-2.8	-9.96	-23.94	-17.29	-19.32	25.93	-112.6

124

Data Documents



CRITICAL  
TRAFFIC BARRIER  
IMPACT LOCATION

TABLE —

(1/1)

# BARRIER VII SIMULATIONS

## NDR HP ER 86-2

Vehicle Weight ..... 4,100 lb.  
 Impact Speed ..... 60 mph  
 Impact Angle ..... 25 deg.  
 Barrier Transition ..... 12 Ga. Tubular Thrie Beam

X-Dir No.	Impact Node	Maximum Barrier Railing Deflections (in.)												Max. Veh. C.G. Decel. (G's)		Max. Veh. Forces (kips)		Veh. Exit Conditions		Veh. Hwy Angle (deg)
		Node (19)	Node 20	Node (21)	Node 22	Node (23)	Node 24	Node (25)	Node 26	Node (27)	Node 28	Node 29	Node 30	Long. (ft)	Lat. (ft)	X	Y	Speed (mph)	Angle (deg)	
	19																			
	20																			
2FF	21	0.63	1.64	2.80	6.08	8.79	10.13	9.77	7.85	5.62	4.33	2.93	1.48	12.09	11.36	27.94	63.24	40	-19	
2DD	22	0.19	0.50	1.00	3.23	5.71	8.16	8.88	8.41	6.26	4.69	3.10	1.50	12.31	11.99	27.99	65.36	41	-20	
2GG	23	0.05	0.16	0.35	1.21	2.21	4.98	7.50	8.30	7.10	4.68	2.32	11.20	11.74	25.99	61.93	41	-20	-1	
2CC	24	-0.06	-0.08	0.15	0.31	0.69	2.91	5.21	7.71	8.27	8.13	5.96	3.04	11.44	12.01	27.26	63.33	41	-23	
2EE	25	-0.04	-0.08	-0.11	0.16	0.45	2.01	3.66	5.51	7.23	7.56	3.94	14.76	14.04	39.27	74.4	39.0	-30	-33	
2AA	26	-0.04	-0.07	-0.11	-0.12	0.05	0.69	1.39	3.18	4.75	7.58	7.37	5.11	19.50	17.97	52.42	96.06	38.1	-38	45
2HH	27	-0.04	-0.11	-0.20	-0.27	-0.20	0.28	0.73	1.92	5.30	4.79	6.74	4.66	23.69	21.47	60.37	117.21	38	-42	-44
1BB	28	-0.03	-0.09	-0.18	-0.26	-0.22	-0.07	0.24	0.64	1.35	2.47	3.82	3.94	24.52	23.05	57.93	126.84	40	-31	-43
1II	29	-0.01	-0.01	-0.02	-0.02	-0.01	0.03	0.07	0.13	0.18	0.23	0.23	0.16	19.35	21.05	39.20	111.27	43	-30	-37
1JJ	30	0.00	0.00	0.00	0.00	0.00	0.00	0.01	0.02	0.03	0.04	0.0	0.02	19.10	21.06	38.55	110.26	44	-4	-39

Notes: (a) Circled node represents location of post (see Fig. — for numbering of Posts) —

TABLE —

(—/—)

## BARRIER VII SIMULATIONS

NDR HPFR 86-2

Vehicle Weight ..... 4,100 lb.  
 Impact Speed ..... 60 mph  
 Impact Angle ..... 25 deg.  
 Barrier Transition ..... 10 Ga. Tubular Thrie Beam

X-Dir Node No.	Imposed Node	Maximum Barrier Railing Deflections (in.)												Max. Veh. C.G. Decel. (G's)		Max. Veh. Forces (kips)		Veh. Exit Conditions		Veh. Heavy Angle (deg)
		Node (19)	Node 20	Node (21)	Node 22	Node (23)	Node 24	Node (25)	Node 26	Node (27)	Node 28	Node 29	Node 30	Long (R)	Lat. (S)	X	Y	Speed (mph)	Angle (deg)	
	19																			
	20																			
IFF	21	0.76	2.12	3.75	6.46	5.74	9.27	8.94	1.05	5.03	3.77	2.49	1.24	11.73	12.21	25.47	17.97	41	-20	
IDD	22	0.27	0.68	1.31	3.59	6.16	7.55	8.30	7.92	5.79	4.50	3.10	1.50	11.99	11.62	26.0	64.04	41	-20	
IGG	23	-0.12	0.16	0.49	1.44	2.66	4.82	6.82	6.85	5.40	3.62	1.73	11.75	12.20	24.27	65.83	41	-21		
ICC	24	-0.09	-0.11	0.12	0.35	0.82	2.88	5.01	7.19	6.93	4.76	2.39	11.43	11.95	27.82	65.97	41	-23		
IEE	25	-0.07	-0.11	-0.14	0.18	0.51	2.06	3.70	5.45	7.07	6.30	3.20	13.89	13.84	36.35	72.49	39.5	-29	-31.5	
IAA	26	0.07	0.14	0.24	0.32	0.22	1.1	2.1	3.6	5.3	7.2	6.4	3.70	19.1	17.4	48.5	94.9	39	-37	-43
IHH	27	-0.07	-0.15	-0.25	-0.33	-0.23	0.32	0.99	1.97	3.05	4.21	5.79	3.71	1.60	20.28	53.95	111.24	40	-40	-45
IBB	28	-0.04	-0.10	-0.18	-0.21	-0.21	0.08	0.26	0.60	1.20	1.87	2.56	2.64	21.98	22.25	50.06	118.95	41	-44	-42
III	29	-0.06	-0.01	-0.01	-0.01	-0.01	0.02	0.04	0.08	0.11	0.14	0.13	0.04	19.25	21.01	38.13	110.75	43	-27	-37
IJJ	30	0.00	0.00	0.00	0.00	0.00	-0.01	-0.01	-0.02	-0.03	-0.04	-0.04	-0.02	19.07	20.89	38.55	110.25	43	-27	-37

Notes: (a) Circled node represents location of post (see Fig. — for numbering of Posts) —

# IMPACT NODE 25

TYPE OF ENERGY PERCENT OF ORIG AUTO KE

TRANSLATIONAL K.E. OF AUTO = 71.0  
ROTATIONAL K.E. OF AUTO = 1.4  
BARRIER K.E. = .0

## ELASTIC ENERGY IN MEMBERS

BE .0  
: : : : : 00721#N41=:F

PD\*\*\*\*\*  
: : : : : 00,V9"N46?TS

## INELASTIC WORK ON MEMBERS

BE .0  
: : : : : 0P2(YMN5W0QQ

PD\*\*\*\*\*  
: : : : : 00=S8IN6U^CE

ELASTIC ENERGY IN AUTO = 2.2  
INELASTIC WORK ON AUTO = 3.9

DAMPING LOSSES = .3

AUTO-BARRIER FRICTION LOSS = 14.8  
AUTO-PAVEMENT FRICTION LOSS = .3

SUM OF ALL CONTRIBUTIONS = 99.9

## DATA ON AUTO-BARRIER CONTACT, TIME = .0875 SECS

AUTO POINT	CONTACT INTERFACE	CONTACT BETWEEN NODE AND NODE	X COORDINATE	Y COORDINATE	NORMAL FORCE	X FORCE	Y FORCE
1	1	30 29	838.03	3.69	3.33	-1.64	-3.13
2	1	30 29	826.10	5.49	7.26	-3.52	-6.84
3	1	29 28	812.56	7.24	27.24	-11.56	-26.44
4	1	29 28	808.34	7.78	13.11	-5.29	-12.84
5	1	28 27	802.93	7.87	4.96	-1.85	-4.92
6	1	28 27	796.37	7.59	4.02	-1.35	-4.04
7	1	28 27	788.79	7.27	1.83	-.53	-1.86
18	1	28 27	798.46	7.68	1.99	-.69	-2.00

## AUTO-TRAJECTORY RESULTS

PT	X-ORD	Y-ORD	ANGLE	X-VEL	Y-VEL	R-VEL	S-VEL	T-VEL	ANGLE	X-ACC	Y-ACC	R-ACC	S-ACC	T-ACC	ANGLE
TIME = .1000 SECS															
1	770.9	-39.8	20.2	47.16	7.05	46.69	-9.70	47.69	8.5	-8.14	-16.94	-13.49	-13.07	18.79	-115.7

BARRIER DEFLECTIONS, TIME = .1000 SECS

229

NODE	X-DEFL	Y-DEFL	X-ORD	Y-ORD
1	.02	.00	.0	.0
2	.05	.00	37.5	.0
3	.08	.00	75.1	.0
4	.11	.00	112.6	.0
5	.14	.00	150.1	.0
6	.17	.00	187.7	.0
7	.20	.00	225.2	.0
8	.24	.00	262.7	.0
9	.27	.00	300.3	.0
10	.31	.00	337.8	.0
11	.35	.00	375.3	.0
12	.39	.00	412.9	.0
13	.42	.00	450.4	.0
14	.47	.00	488.0	.0
15	.51	.00	525.5	.0
16	.56	.00	563.1	.0
17	.61	.00	600.6	.0
18	.64	.01	619.4	.0
19	.66	.02	638.2	.0
20	.82	.03	657.1	.0
21	.85	.02	675.8	.0
22	.87	.04	694.6	.0
23	.89	.20	713.4	.2
24	.86	1.59	732.1	1.6
25	.82	3.06	750.8	3.1
26	.74	5.02	769.5	5.0
27	.66	6.96	788.2	7.0
28	.63	8.61	806.9	8.6
29	.61	7.19	825.6	7.2
30	.30	3.62	844.4	3.6
31	.02	.02	863.1	.0
32	.01	.00	881.9	.0
33	.01	.00	900.6	.0
34	.01	.00	919.4	.0
35	.01	.00	938.1	.0
36	.00	.00	1006.5	.0
37	.00	.00	1042.5	.0
38	.00	.00	1078.5	.0
39	.00	.00	1114.5	.0
40	.00	.00	1150.5	.0

Max. Deflection

MEMBER FORCES, TIME = .1000 SECS

Anchor Force (approx.)

BEAMS, 100 SERIES	MEMBER	NODE I	NODE J	TYPE	FORCE	I-MOMENT	J-MOMENT	F-CODE	M-CODE
1	1	1	2	101	48.36	.00	.00	1	1
2	2	2	3	101	48.39	.00	.00	1	1
3	3	3	4	101	49.46	.00	.00	1	1
4	4	4	5	101	49.45	.00	.00	1	1
5	5	5	6	101	51.46	.00	.00	1	1
6	6	6	7	101	51.44	.00	.00	1	1
7	7	7	8	101	54.39	.00	.00	1	1
8	8	8	9	101	54.36	.00	.00	1	1
9	9	9	10	101	58.31	.00	.00	1	1
10	10	10	11	101	58.27	.00	.00	1	1
11	11	11	12	101	63.31	.00	.01	1	1
12	12	12	13	101	63.26	-.01	-.01	1	1
13	13	13	14	101	69.47	.01	-.03	1	1
14	14	14	15	101	69.42	.03	-.02	1	1
15	15	15	16	101	76.93	.02	.22	1	1
16	16	16	17	101	76.88	-.22	.80	1	1
17	17	17	18	102	85.85	-.80	.46	1	1

POSTS, 300 SERIES	MEMBER	NODE I	NODE J	TYPE	A-SHEAR	B-SHEAR	B-MOMENT	A-MOMENT	CODE
39	300	0	0	304	48.38	.00	1016.01	.00	1
40	300	0	0	301	1.16	.00	24.29	.00	1
41	300	0	0	301	2.09	.00	43.86	.00	1
42	300	0	0	301	3.06	.00	64.22	.00	1
43	300	0	0	301	4.08	.00	85.74	.00	1
44	300	0	0	301	5.18	.00	108.81	.01	1
45	300	0	0	301	6.37	.00	133.85	-.04	1
46	300	0	0	301	7.68	.00	161.33	.10	1
47	300	0	0	301	9.13	-.05	191.77	-1.11	1
48	300	0	0	301	9.94	-.25	208.75	-5.20	1
49	300	0	0	301	12.69	-.23	266.58	-4.78	1
50	300	0	0	302	13.42	3.06	281.82	64.34	1
51	300	0	0	303	14.78	6.83	310.46	143.46	1
52	300	0	0	303	11.95	14.37	251.02	301.69	1
53	300	0	0	304	-51.11	48.20	-1073.36	1012.16	1
54	300	0	0	304	-29.14	-4.44	-612.02	-93.24	1
55	300	0	0	304	-17.04	-.30	-357.77	6.40	1
56	300	0	0	304	-10.70	-.01	-224.75	-.18	1
57	300	0	0	304	-7.99	.00	-167.87	-.02	1

ENERGY BALANCE, TIME = .1000 SECS

TYPE OF ENERGY	PERCENT OF ORIG AUTO KE
----------------	-------------------------

TRANSLATIONAL K.E. OF AUTO = 63.2

ROTATIONAL K.E. OF AUTO = 2.4

BARRIER K.E. = .0

ELASTIC ENERGY IN MEMBERS

```

*** BE .0
      :::::00(P,IN4)\1\

```

```

*** PD*****
      :::::00=<">N4$-^+

```

INELASTIC WORK ON MEMBERS

## APPENDIX D

### METHOD TO DETERMINE OCCUPANT RISK

The time that a hypothetical unrestrained front seat passenger moved laterally a distance of 12 in. and struck the side of the vehicle door was determined by an analysis of the high-speed film from the overhead camera. During impact, it was assumed that the occupant maintained the same straight path and velocity of the vehicle just prior to impact as shown in Figure D1. When the distance between the C.G. path of the redirected vehicle and the straight path of the occupant was 12 in., the time was computed by multiplying the camera speed (fr/sec) by the number of frames from the instant of impact. Plotting the vehicle C.G. path, as shown in Figure D1, was very tedious work. A much simpler and faster method was later used which consisted of taping a straight-edge along the path of the vehicle before impact and then checking the distance between the front target on the vehicle roof (vehicle C.G.) and the straight-edge until a distance of 12 in. was obtained. It is important to note in Figure D1 that practically no change in vehicle direction occurred while crushing sheet metal until a time of about 35 msec. after impact. The instant when the vehicle became parallel to the centerline of traffic barrier was the time in which the lateral velocity component of the vehicle was equal to zero.

The time-velocity data obtained was then plotted as shown in Figure D2 to measure the impact velocity of the occupant striking the side door of the vehicle. The vehicle lateral velocity component was taken perpendicular to the centerline of the traffic barrier. The velocity was assumed to be constant for a time of 20 msec. After a time of 20 msec, the velocity was assumed to decrease



TEST NO. 4  
 SPEED 61 mph  
 TRANSITION Double Thrie Beam  
 DATA POINT INTERVAL 23 msec

△ VEHICLE IMPACT  
 □ VEHICLE EXIT

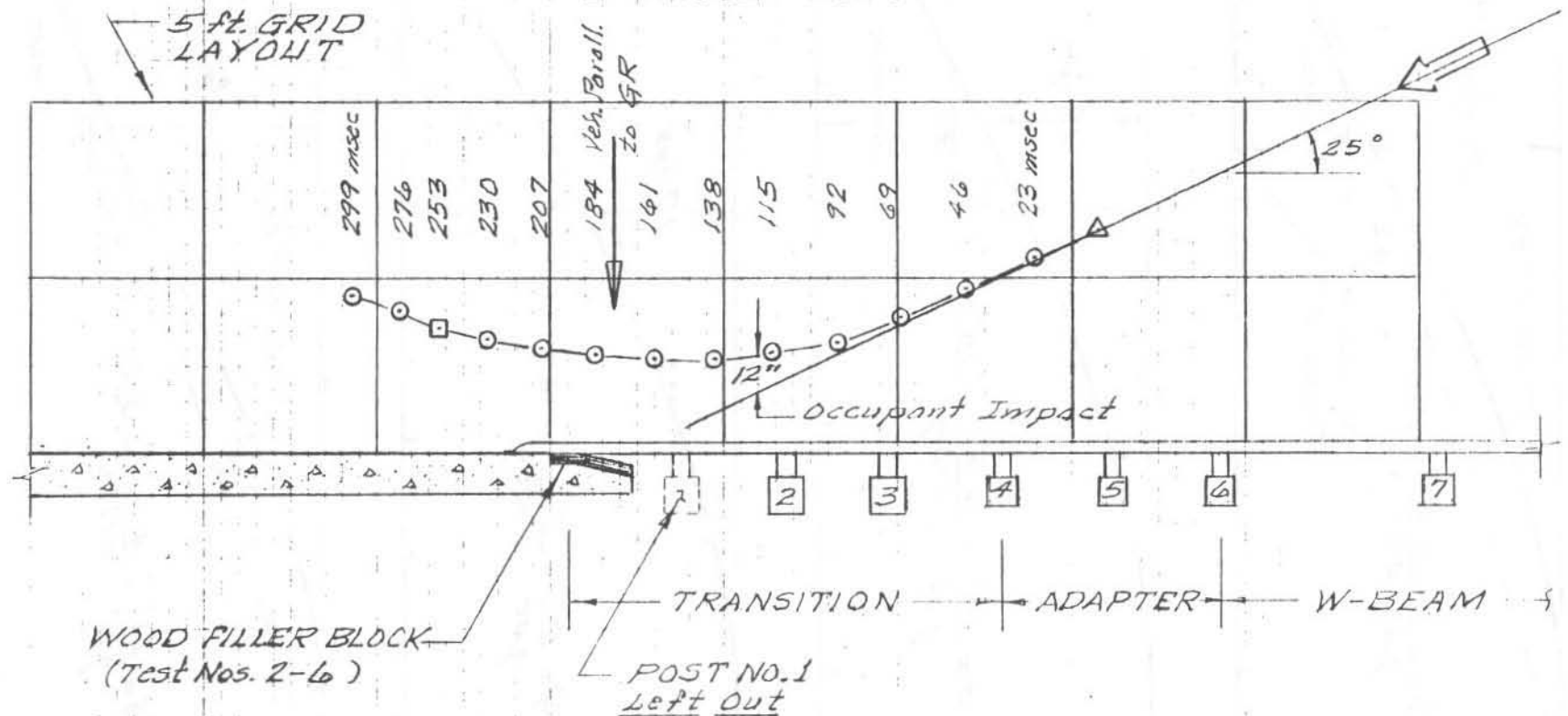


Figure D1  
 C.G. PATH OF VEHICLE

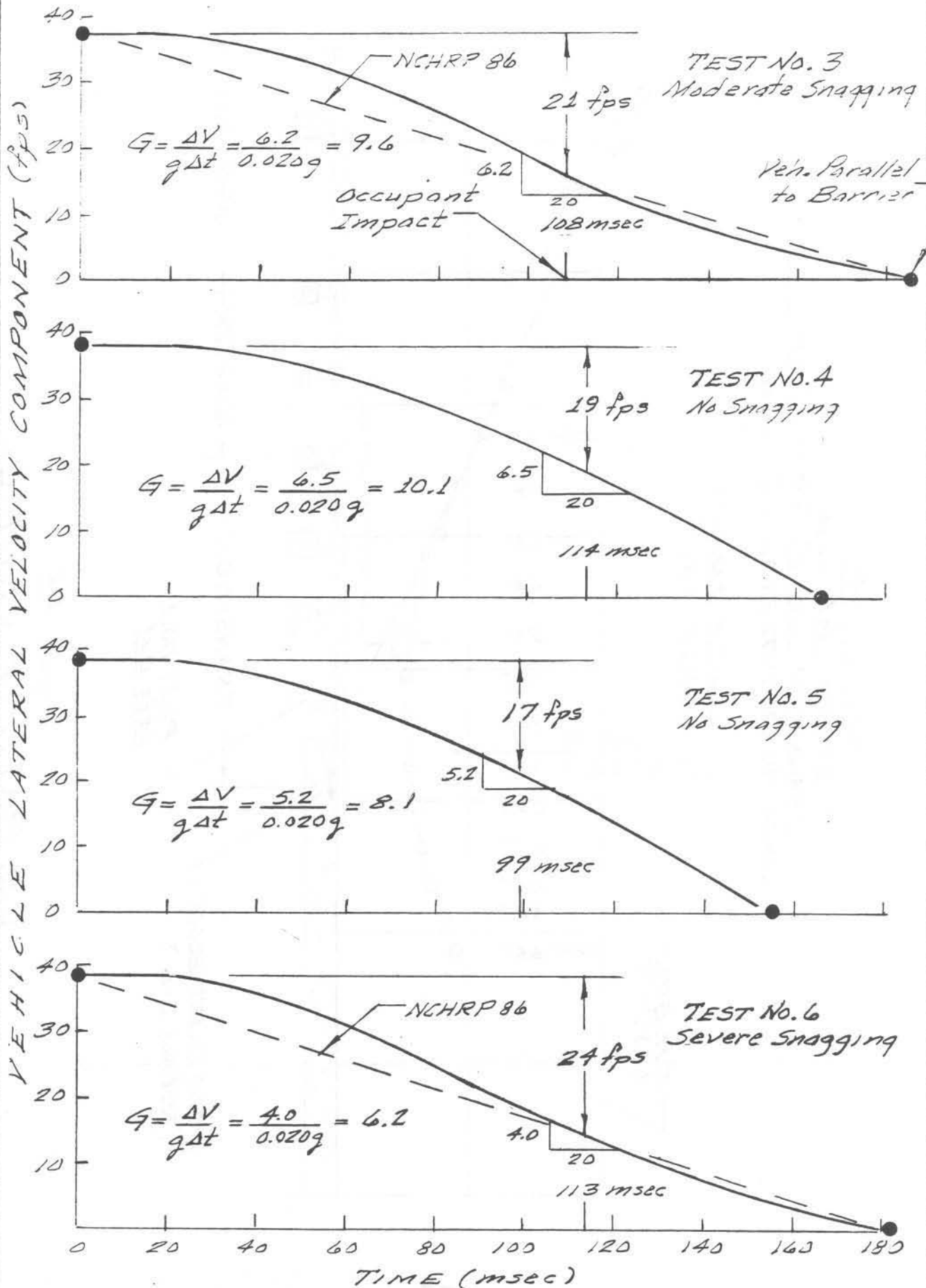


Figure D2

in a slightly non-linear manner to a value of zero when the vehicle became parallel to the centerline of the traffic barrier. The occupant impact velocity was measured by taking the difference between the impact lateral velocity component of the vehicle and the lateral velocity component of the vehicle when a hypothetical passenger had moved 12 in. laterally.

A similar method was presented in NCHRP 86 (8) for validating a mathematical model by assuming a linear straight line decrease in velocity from the instant of impact to that time when the vehicle became parallel to the barrier. The straight line method in NCHRP 86, with an accuracy of + 20%, seems to compare well with the non-linear plots in Test Nos. 3 and 5 in which snagging occurred.

APPENDIX E  
INJURY ACCIDENT PROBABILITY

NATIONAL COOPERATIVE HIGHWAY RESEARCH PROGRAM  
REPORT

**86**

## TENTATIVE SERVICE REQUIREMENTS FOR BRIDGE RAIL SYSTEMS

ROBERT M. OLSON, EDWARD R. POST,  
AND WILLIAM F. McFARLAND  
TEXAS A & M UNIVERSITY  
COLLEGE STATION, TEXAS

RESEARCH SPONSORED BY THE AMERICAN ASSOCIATION  
OF STATE HIGHWAY OFFICIALS IN COOPERATION  
WITH THE BUREAU OF PUBLIC ROADS

SUBJECT CLASSIFICATION:  
HIGHWAY DESIGN  
BRIDGE DESIGN  
HIGHWAY SAFETY

HIGHWAY RESEARCH BOARD  
DIVISION OF ENGINEERING      NATIONAL RESEARCH COUNCIL  
NATIONAL ACADEMY OF SCIENCES—NATIONAL ACADEMY OF ENGINEERING      1970

signs tested. Barrier rail systems that deflected laterally were effective, as noted by the lower transverse readings. It is interesting to note that there was no significant difference between the vertical readings for the New Jersey barrier, which has a lower sloping face, and the W-beam guardrail when tested under the same impact conditions. Also of interest, the longitudinal decelerations of the anthropomorphic dummy in the majority of tests were approximately or equal to one-half of the lateral decelerations. As shown in Appendix A, a similar relationship was found to exist between the average lateral and longitudinal decelerations of vehicles involved in full-scale dynamic tests.

Thus, an occupant restrained by a seat belt and shoulder harness would most likely experience decelerations similar to the vehicle compartment area, whereas an unrestrained occupant might experience decelerations completely different from that of the vehicle. In any event, the severity of damage to the vehicle would appear to be a good indication of the vehicle decelerations and incidence of injury to unrestrained occupants. Based on the work of Michalski (12) and employing the mathematical model discussed previously, this hypothesis has been confirmed.

From the results of a 1967 field study conducted in Oregon involving 951 vehicles in traffic accidents of which there were 184 personal injuries and 7 fatalities, Michalski demonstrated, as shown in Figure 6, that the proportion of damaged vehicles in which injuries occurred was proportional to the square of the severity of damage to a vehicle as rated on a 7-point photographic scale (17) by police officers and others at the scene of an accident. Michalski

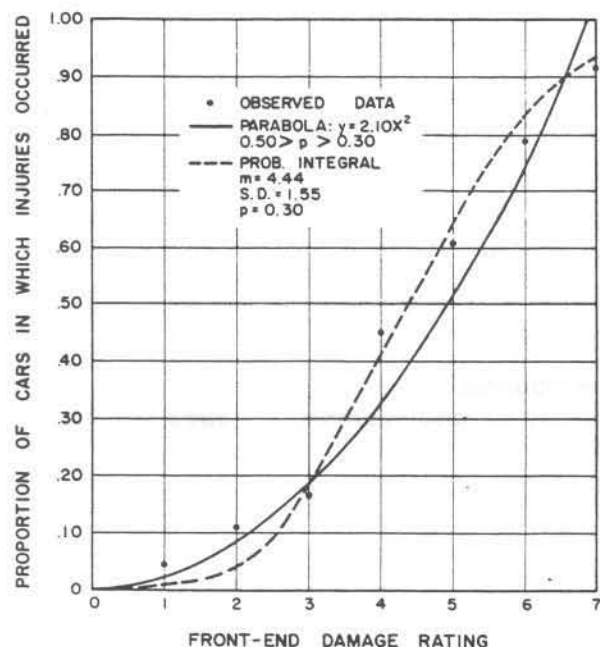


Figure 6. Occurrence of personal injuries in relation to front-end damage rating (12, p. 38).

indicates that the probability integral and parabolic curves in Figure 6 may be used with equal facility to predict incidence of injuries in relation to vehicle damage rating. Michalski has indicated verbally that less than 5 percent of the vehicle occupants were restrained by a seat belt and/or shoulder belt.

To apply and extend the work of Michalski to include average vehicle decelerations, vehicles damaged in full-scale dynamic tests by various research agencies were selected for evaluation. As shown in Figures 7 and 8, the results of this study, which are developed in depth in Appendix B, indicate that the average vehicle decelerations are directly proportional to: (1) the proportion of damaged vehicles involved in traffic accidents in which occupant injuries occurred, and (2) the square of the vehicle damage rating. In mathematical notation, this relationship would be represented by the equations:

Type Vehicle Impact	Mathematical Equation
Front	$G_{\text{long.}} = 0.280 R^2 = 13.7 P \quad (10)$
Angle	$G_{\text{lat.}} = 0.204 R^2 = 10.0 P \quad (11)$

in which

$G$  = average vehicle deceleration;

$R$  = vehicle damage rating; and

$P$  = proportion of vehicles in which injuries occurred.

It must be noted that the average lateral vehicle decelerations are based on the assumption that the vehicle is smoothly redirected by the barrier rail.

In addition to demonstrating that the proportion of vehicles in which personal injuries occurred in relation to damage rating was nearly parabolic in form, Michalski determined that at mean damage ratings\* of: (1) 1.99—vehicles are drivable, (2) 4.08—vehicles are non-drivable, (3) 4.45 and 4.73—injuries occurred in front-end and side vehicle impacts, respectively, and (4) 2.32 and 2.49—no injuries occurred in front-end and side vehicle impacts, respectively. Based on the mathematical relationship established, Eqs. 10 and 11, the average vehicle decelerations and the percent of vehicles involved in an accident in which injuries would occur that correspond to the conditions for which mean damage ratings were determined by Michalski are given in Table 9.

Before attempting to predict the severity of a barrier rail accident, a study of vehicle encroachments on a barrier rail must be made. From accident data on the Ohio Turnpike for a period of five months during the summer and fall of 1967, Garrett (13) reported vehicle speeds and the departure angles as given in Table 10. For purposes of this study, it is assumed that the mean departure angles for various speeds as reported by Garrett would also be representative for an out-of-control vehicle striking a barrier railing.

From injury accident data involving guardrail on two-lane highways and four-lane divided highways, it was possible to estimate from the graph presented by Deleys (2, p. 6) that approximately 85 to 90 percent of the accidents (excluding inappropriate data) occurred at an angle of 20° and less.

\* Unless noted, the mean damage ratings include all types of impacts.

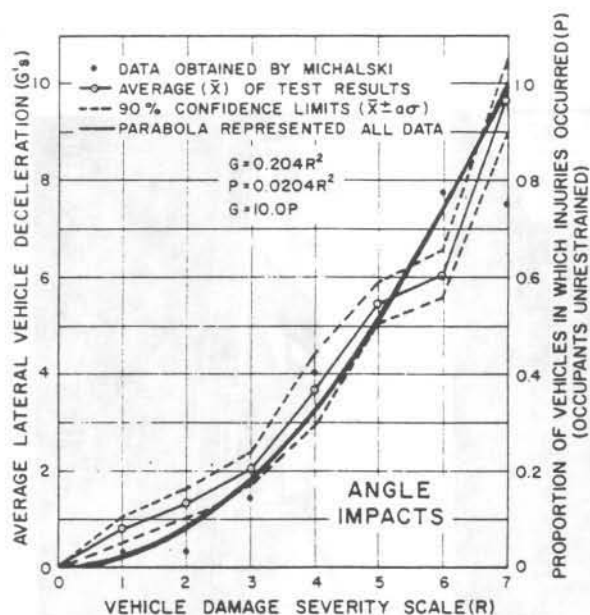


Figure 7. Curve relating lateral deceleration, proportion of injuries, and damage rating scale.

When the average lateral decelerations of the mathematical model, Eq. 5, are graphically plotted using the vehicle impact speed as the ordinate and the impact angle as the abscissa, it is evident as shown in Figure 9 that approximately 80 to 85 percent of the accident data reported by Deleys and the curve representing the information obtained by Garrett fall to the left (less than) of a 2-G level deceleration curve; whereas 85 to 90 percent of the accident data fall to the left of a 3-G deceleration curve.

Based on the information presented, and assuming that the hazardous conditions discussed in section "Accident Information" are eliminated, this agency-conducted study indicates that for approximately 85 percent of the accidents, a standard-size vehicle would be subjected to an average lateral deceleration (at the center of mass of the vehicle) of 3 G's or less for various combinations of impact speed and angle. At this deceleration level, this study also indicates that 85 percent of the accidents would be non-fatal, and 60 percent of the accidents would not produce injuries to unrestrained occupants. As is evident from Table 9, a 3-G average deceleration level for angle impacts would correspond to a slightly lower rating than that at which vehicles are non-drivable.

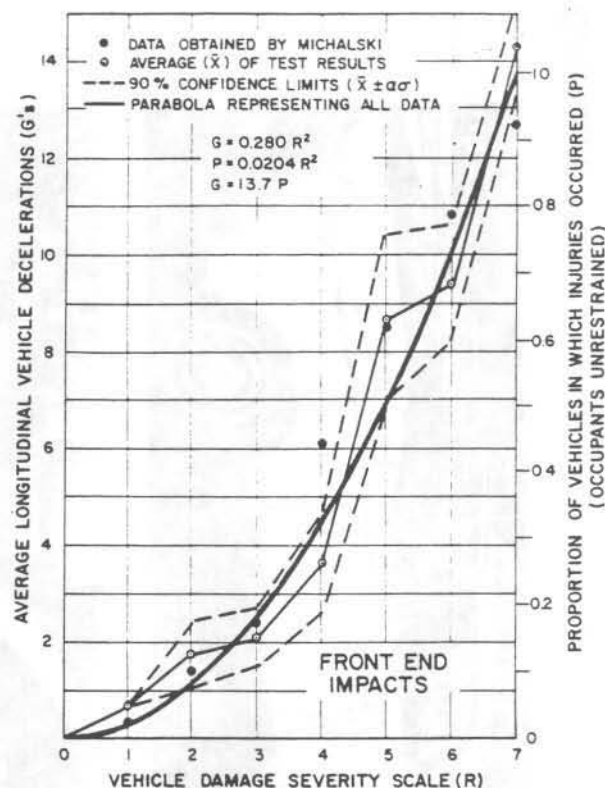


Figure 8. Curve relating longitudinal deceleration, proportion of injuries, and damage rating scale.

TABLE 9

AVERAGE VEHICLE DECELERATIONS  
AS FUNCTION OF NSC MEAN DAMAGE  
VEHICLE RATINGS AND INJURY LEVELS

CONDITIONS FOR WHICH MEAN DAMAGE RATINGS WERE DETERMINED BY MICHALSKI (12)	AVERAGE VEHICLE DECELERATIONS (G's)		% OF VEHICLES IN WHICH IN- JURIES WOULD OCCUR	
	FRONT IM- PACTS	ANGLE IM- PACTS	FRONT IM- PACTS	ANGLE IM- PACTS
Vehicles drivable	1.1	0.8	8	8
Vehicles non-drivable	4.7	3.4	34	34
No injuries	1.5	1.3	11	13
Injuries	5.5	4.6	40	46

TABLE 10

SPEED-MEAN DEPARTURE ANGLE

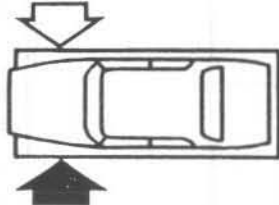
Speed range (mph)	10-19	20-29	30-39	40-49	50-59	60-69
Mean departure angle* (degrees)	48.5	8.8	7.9	7.1	2.0	3.7
No. of observations	2	5	8	30	78	126

\* Departure angle was defined as the angle of the path of the vehicle as it left the paved roadway.

# SEVERITY SCALE

## LFQ/RFQ

Front Quarter Damage  
Angular Impact



This scale is applicable to damage to the left or right front quarter of subject vehicle (ahead of passenger compartment) resulting from an angular impact, by another vehicle or object.

### Damage Rating

LFQ-1 or RFQ-1 ➡

LFQ-2 or RFQ-2 ➡

LFQ-3 or RFQ-3 ➡

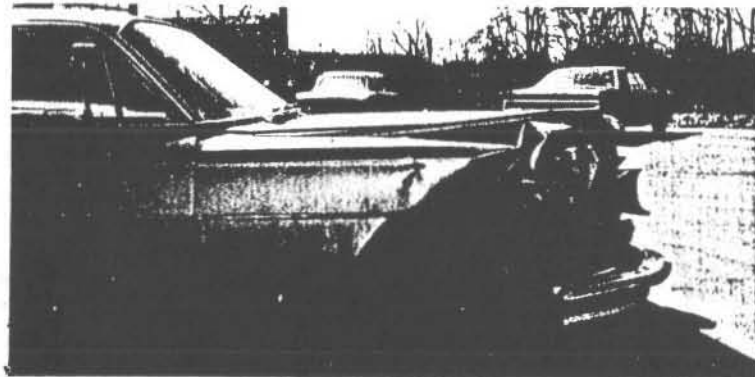
LFQ-4 or RFQ-4 ➡

LFQ-5 or RFQ-5 ➡

LFQ-6 or RFQ-6 ➡

LFQ-7 or RFQ-7 ➡

LFQ/RFQ



140